**The Thesis Committee for Roy George Eid**
**Certifies that this is the approved version of the following thesis:**

# Reverse Engineering Toolbox for Pedagogical Applications

**APPROVED BY**
**SUPERVISING COMMITTEE:**

**Supervisor:** Kristin Wood

**Co-Supervisor:** Richard Crawford

# Reverse Engineering Toolbox for Pedagogical Applications

**by**

**Roy George Eid, B.S.M.E.**

**Thesis**

Presented to the Faculty of the Graduate School of

The University of Texas at Austin

in Partial Fulfillment

of the Requirements

for the Degree of

**Master of Science in Engineering**

**The University of Texas at Austin**

**May 2012**

# Acknowledgements

First and foremost, I would like to thank my parents for always believing in me and for pushing me to strive for a bright future. Without their words of encouragement and their example, I would not have the mindset and ambition that I have today.

I would also like to thank my supervisors, Dr. Kristin Wood and Dr. Richard Crawford, for teaching me valuable lessons in engineering and design, and for having the patience in dealing with my extroverted and Thomas Edison-like methods to design and development.

Lastly, I would also like to thank my friends and loved ones who stuck beside me throughout the good and the bad.

# Abstract

## Reverse Engineering Toolbox for Pedagogical Applications

Roy George Eid, M.S.E

The University of Texas at Austin, 2012

Supervisors: Kristin Wood, Richard Crawford

Reverse engineering, the technique of using different tools and methodology to recreate an object or machine, is increasingly used in academia to solidify theoretical concepts as part of the Kolb learning cycle. This thesis aims to aid the use of reverse engineering as a pedagogical tool by developing a toolbox that can be used by students, and professionals alike, to properly reverse engineer a mechanical or electro-mechanical product.

The development begins with an analysis of House of Quality matrices, a design methodology tool used by the industry to relate customer needs to engineering metrics and specifications. After a consolidated list of metrics was developed, the appropriate tools to properly quantify said metrics were researched and documented. Finally, a toolbox was created, with set goals in mind, and applied in two case studies to analyze its performance.

Simultaneously, a portable dynamometer was developed, documented, and tested, with the goal of creating an inexpensive and accessible tool to measure the power output of fractional horsepower DC and AC motors.

# Table of Contents

# List of Tables

# List of Figures

# Chapter 1: Background

## 1.1 Introduction to Reverse Engineering

Reverse Engineering is a methodology that involves the use of analysis, measurement, and testing to reconstruct an object. It can be used in industry as a tool to recreate a part, or an entire machine, when the original designs and blueprints are unavailable. An example of this need would be for a company using legacy machines no longer supported by the industry. If a part breaks on such a machine, the only way to keep the machine from total obsolescence is to reverse engineer the broken part and create a new one. Another example, widely used by industry competitors, is to reverse engineer the competition's product to reveal secrets of the trade, as well as catch up on years of lengthy research and development (Wang, 2011).

Another use of reverse engineering, which will be the main focus of this thesis, is within the realms of academia. The use of reverse engineering as a pedagogical tool is cited as an essential tool for allowing students to work with a physical product instead of abstract theory and homework problems. The addition of reverse engineering to the mechanical engineer's course work is explored in Wood et al. (2001). In this paper, several benefits of hands-on teaching are mentioned, including completing Kolb's cycle of learning (Figure 1). Kolb's cycle is composed of concrete experience, observation and reflection, conceptualization and theory, and finally, active experimentation. Reverse engineering would then help fulfill this learning cycle by adding a more concrete physical experience and experimentation for students (Wood, Jensen, Bezdek, & Otto, 2001). Barr et al. (2000) describe the implementation of a freshman introductory course at the University of Texas at Austin that revolves around reverse engineering. This course

successfully exposes students to the first phase of the reverse engineering cycle (explained in more detail in Section 1.2), helping them get excited about engineering (Barr, Schmidt, Krueger, & Twu, 2000).

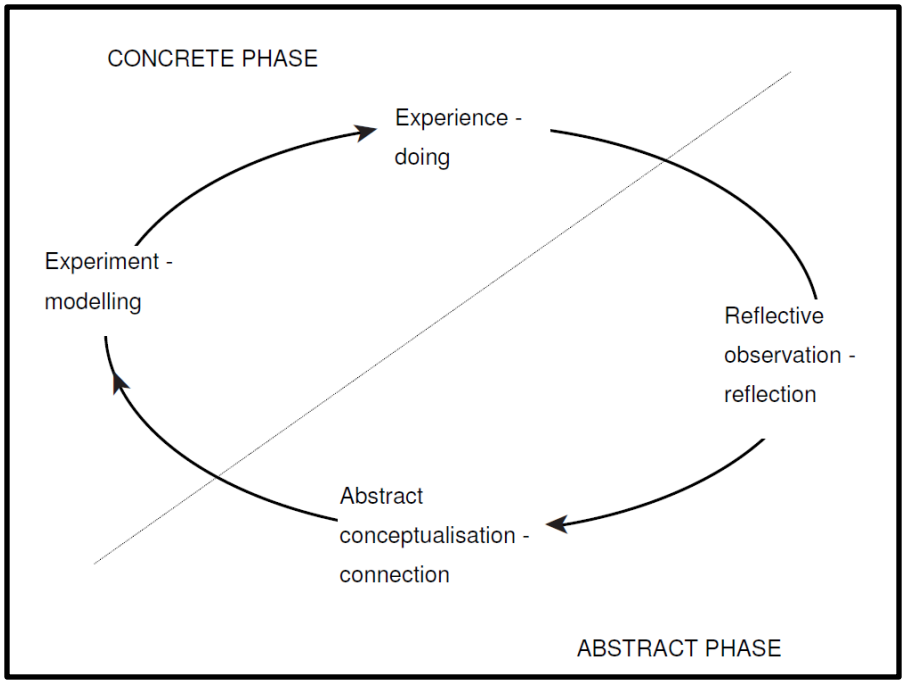


Figure 1 – Kolb's learning cycle (Bell & Morse, 2003, p. 144).

## 1.2 Reverse Engineering and Redesign

### 1.2.1 Steps of the Reverse Engineering and Redesign Process

Reverse engineering consists of several steps that an engineer will go through to effectively analyze and quantify an object. Even though the number of steps varies between authors and literature, the reverse engineering and redesign process can be broken down into three phases: product disassembly/product mapping (reverse engineering), modeling and analysis, and redesign (see Figure 2).

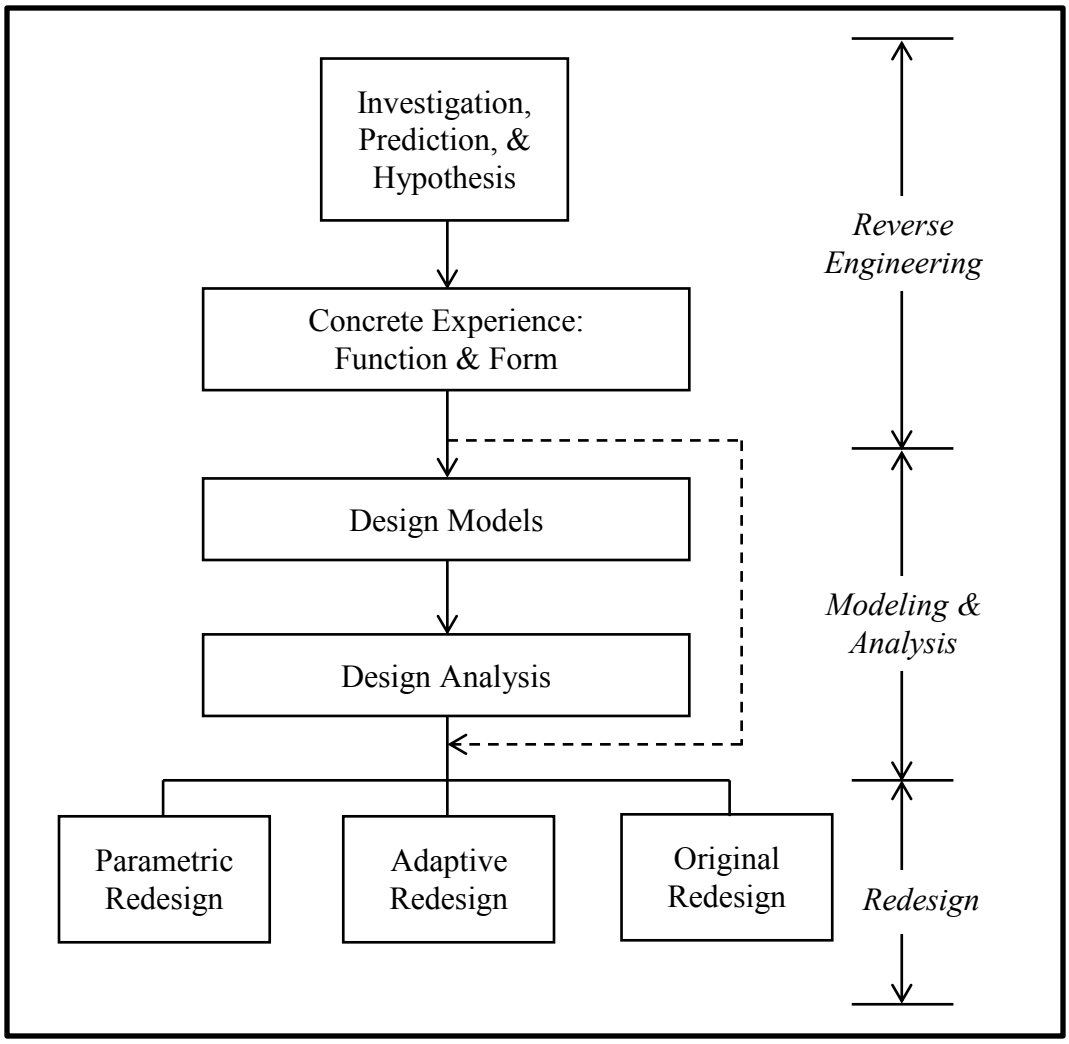


Figure 2 – General reverse engineering and redesign methodology (reproduced from Otto & Wood, 2001, p. 23).

According to Otto and Wood, the first step of the reverse engineering phase is for the engineer to use and experience the product and predict how the product functions. Various product modeling techniques can be used, including a black box diagram, activity diagram, and preliminary functional model. Then the engineer proceeds to disassemble the product, using various tools and techniques. After disassembly, an actual functional model is made to describe how the product's various subsystems function and exchange energy, material, and signals among each other. A bill of materials can also be

developed to facilitate the redesign process later. It is during this phase that all of the engineering specifications and metrics are developed and measured. This step will be explored in more detail in the following sections.

After the reverse engineering phase is completed, the modeling and analysis phase begins, where various parameters of the product can be modeled and studied to determine avenues for redesign. This can include anything from computer simulations to actual physical models and experimentation.

Finally the redesign process begins, where the product can be improved, augmented, or totally changed using the results from the modeling phase. A prototype can be built which will then lead to a final, marketable product.

### 1.2.2 Developing and Measuring Relevant Engineering Metrics

Since the focus of this thesis is the measurement of engineering metrics, it is worthwhile to expand and focus on this step of the reverse engineering process as described in Section 1.2.1. The development of engineering metrics stems from the gathering and analysis of customer needs pertaining to the specific product. Customer needs drive the inclusion of certain functions in the product and are thus important to consider when designing the final product.

The process of gathering customer needs begins with several techniques, including personal interviews, focus groups, and product analysis techniques (Franceschini, 2002, pp. 39-40). Personal interviews involve asking customers directly and individually about products they currently use or have used before, their likes and dislikes about the products, and what they would improve. Focus groups involve gathering six to eight customers to talk about what they would like in the product being developed. This is advantageous compared to personal interviews in that customers can

feed from one another to invoke needs that they would not have thought of on their own. Product analysis techniques involve the customer evaluating a product aloud as they use the product (Franceschini, 2002, pp. 39-40).

After the customer needs are gathered, they are grouped using several techniques, including the affinity diagram and customer sort method. They are then sorted according to importance using techniques such as the interview data method and questionnaire method (Otto & Wood, 2001, pp. 130-139).

The affinity diagram method involves writing the individual customer needs on Post-it® notes. These Post-it® notes are then arranged on a whiteboard and grouped according to similar needs. The groups are then counted to give the frequency. The customer sort method involves transferring the individual customer needs to index cards, which are then given to a select customer and sorted by them. The interview data method is used to determine the importance of the needs and involves recording the frequency that each need is mentioned, then weighting that need using a statement by the customer that classifies that need as a must, good, should, or nice. The questionnaire method involves sending out a questionnaire with the gathered needs, asking customers to rank them as they see fit (Otto & Wood, 2001, pp. 130-139).

After the customer needs are sorted and analyzed, they are then transformed to engineering metrics using a technique called the House of Quality, also known as Quality Function Deployment (Otto & Wood, 2001, p. 290). The House of Quality provides a way to correlate the customer needs gathered to measurable, quantifiable engineering metrics that designers can work with. The House of Quality technique is discussed in further detail in Chapter 2.

After all relevant engineering metrics are established, the measurement phase can be initiated. The measurements taken depend on the product being dissected (or a better

descriptor would be the product's domain); however, Wang provides general metrics that can be applied to the reverse engineering of many mechanical products. Wang identifies and provides techniques to determine an object's geometry, material and material properties, manufacturing process, and lifetime/durability, which are important considerations in the reverse engineering of many products (Wang, 2011).

## 1.3 Objective and Motivation

The objective of this thesis is to document and justify the development of a reverse engineering toolbox to be used to dissect and quantify consumer products across several domains. The toolbox will be developed from the analysis of engineering metrics across several domains of consumer products. The motivation for the development of this toolbox is the anticipation that it will be used as a pedagogical aid to help students during their reverse engineering courses. The goal of this toolbox is for it to be cost effective, made from readily available commercial off the shelf (COTS) products, and easy to use and manipulate. The toolbox will then be applied to several case studies to assess its performance in meeting the goals.

## 1.4 Thesis Organization

Chapter 2 – This chapter explores the transformation of customer needs to engineering metrics that can be measured using the Quality Function Deployment method. Also, the gathering of engineering metrics for the development of the toolbox is documented in this chapter as well.

Chapter 3 – This chapter discusses the current state of the art techniques and tools used to measure the engineering metrics found in Chapter 2.

Chapter 4 – This chapter discusses the development of the reverse engineering toolbox and describes its constituents in detail.

Chapter 5 – This chapter documents two case studies on consumer products to assess the usefulness of the reverse engineering toolbox in aiding students.

Chapter 6 – This chapter summarizes the results of the research with respect to the objective described above. Future work is also discussed for expanded research on this topic.

# Chapter 2: Gathering Engineering Metrics for the Development of a Reverse Engineering Toolbox

To develop a proper reverse engineering toolbox, the metrics and parameters that will be measured must be compiled. This step is necessary before selection of dissection tools to be included in the toolbox. Two methods were used to identify the dissection tools and engineering metrics: analysis of a pool of House of Quality matrices from previous students who took the reverse engineering course, including those currently enrolled presently in the course; as well as a direct survey documenting the students' experience during the dissection process.

## 2.1 Analysis of a Pool of House of Quality Matrices

As part of the Mechanical Engineering curriculum at The University of Texas at Austin, students take ME366J Mechanical Engineering Design Methodology, which is taught using reverse engineering as a tool to make the experience more concrete. The House of Quality matrices that are used for this analysis were taken from the final poster presentations of previous students who took this reverse engineering course, as well as the final reports of current students.

### 2.1.1 House of Quality (Quality Function Deployment)

Quality function deployment is a technique used to correlate one set of requirements to another. This methodology was created in 1972 by Mitsubishi Heavy Industries in Kobe, Japan, and diffused to the United State by Xerox Corporation in 1984 (Franceschini, 2002, pp. 21-22).

Quality function deployment is a set of matrices that cover the entire product development phase, from customer requirements to process and quality control.

However, the matrix that concerns this thesis is the first matrix of the set, one relating customer needs and product requirements (or engineering metrics). This particular matrix is called the House of Quality (Franceschini, 2002, p. 27).

According to Otto and Wood, the House of Quality (aptly named for its resemblance of a house) consists of seven main areas, as shown in Figure 3. The first, and important, constituent of the HoQ is the customer needs list in the leftmost area. This list includes all of the important customer needs that the product needs to address, derived from the techniques described in Section 1.2.2. The customer needs are then assigned importance ratings in the column to their right, the second part of the HoQ. These importance ratings are also derived from the abovementioned techniques. The next major area of the HoQ is the functional requirements or engineering metrics section. This is a list that spans from left to right and includes engineering metrics that measure the degree of satisfaction of the customer needs. On top of these metrics an arrow is placed, pointing either upwards or downwards; this arrow denotes if the metric should be maximized or minimized. On the opposite side of the engineering metrics list, on the bottom, is the target values area, which tabulates the values for the metrics the designers should strive for during the design process. The rightmost list is the competitor benchmark area, where several competitive products are ranked based on how well they meet each customer need.

The two areas left in the HoQ, the relationship and correlations matrices, are the most important areas and are the purpose of creating the HoQ. The relationship matrix tabulates the relationship between a specific customer need and an engineering metric on the top. Usually four relationships are used in HoQ: strong relationship, some relationship, weak relationship, and no relationship (matrix cell left blank). An ideal HoQ

would look like an identity matrix; one metric for each customer need. However, in practice, this is rarely the case.

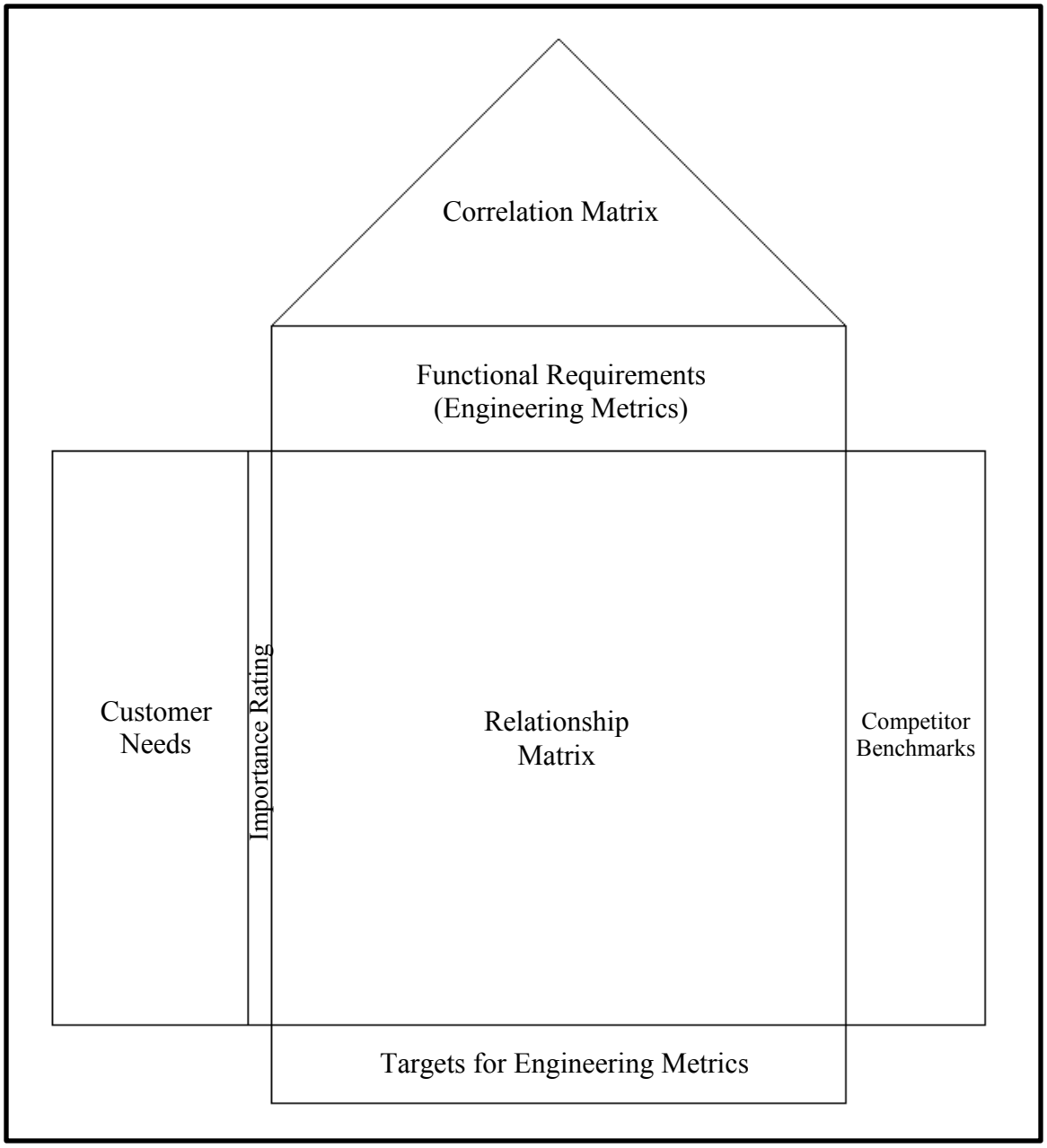


Figure 3 – Example template for House of Quality matrix (reproduced from Otto & Wood, 2001).

Finally, the correlation matrix on top is used to show the relationships between the different engineering metrics, either positive or negative. An example of a negative correlation is weight and strength; in the case of steel, making the part lighter means making it thinner, a sacrifice in strength. However, correlations like these open avenues for creativity and innovation; in the abovementioned example, an innovation would be a carbon fiber composite, which is both lightweight and strong.

The area that this thesis is concerned with is the functional requirements, or engineering metrics, area. Through a compilation and analysis of these requirements from various House of Quality matrices, a comprehensive list of metrics can be created. These metrics can then be translated into specific tools that need to be included in the toolbox.

### 2.1.2 Acquiring the House of Quality Matrices

The HoQ matrices were acquired by collecting all of the matrices on the previous students' poster presentations. These posters document the reverse engineering projects by previous students in the course, including the results of the methodology they used to document metrics, and any improvements they made or recommended. Since soft or hard copies of the matrices were not available for immediate use, the matrices were instead documented using a digital camera. A total of 24 posters included matrices that could be used for the analysis.

Matrices from current students were obtained from hard copies of the reports that were available for review. A total of 16 HoQ matrices were collected for analysis from these reports.

After the matrices were collected, a tallying procedure was performed to categorize all of the engineering metrics and record their frequency of occurrence. Some metrics were lumped together to make the results clearer for analysis (i.e. area and

volume were lumped into the category "Geometry"). These categories also included properties that can be derived from the measured metric. Table 1 lists the categories used in the tallying process.

| **Metric Category** | **Constituents** |
|---|---|
| Geometry | Area, Volume, Length, Width, Height, Diameter, Thickness, etc. |
| Time | Time to assemble, Time to dispense, etc. |
| Sound level | Noise level |
| Mass | Mass, Weight, Density |
| Temperature | Temperature, Heat produced, Heat Transferred |
| Elec. properties | Voltage, Current, Power, Resistance, Capacitance, etc. |
| Torque | Torque |
| Force | Linear force |
| Angular velocity | Angular velocity |
| Pressure | Pressure of air or liquid |
| Flow rate | Flow rate of air or liquid |
| Material property | Yield Strength, Tensile Strength, Hardness, etc. |
| Light intensity | Light Intensity, Screen brightness |
| Linear velocity | Linear Velocity |
| Vibration | Vibration amplitude, frequency |
| Friction | Friction between surfaces, either kinetic or static |

Table 1 – Categories used to tally engineering metrics and their constituents.

### 2.1.3 Results from HoQ Matrices Analysis

After tallying the metrics from the pool of HoQ matrices (Appendix B), a trend started to emerge from the random groupings of metrics measured by the students. Figure 4 shows a frequency chart for the different metrics.

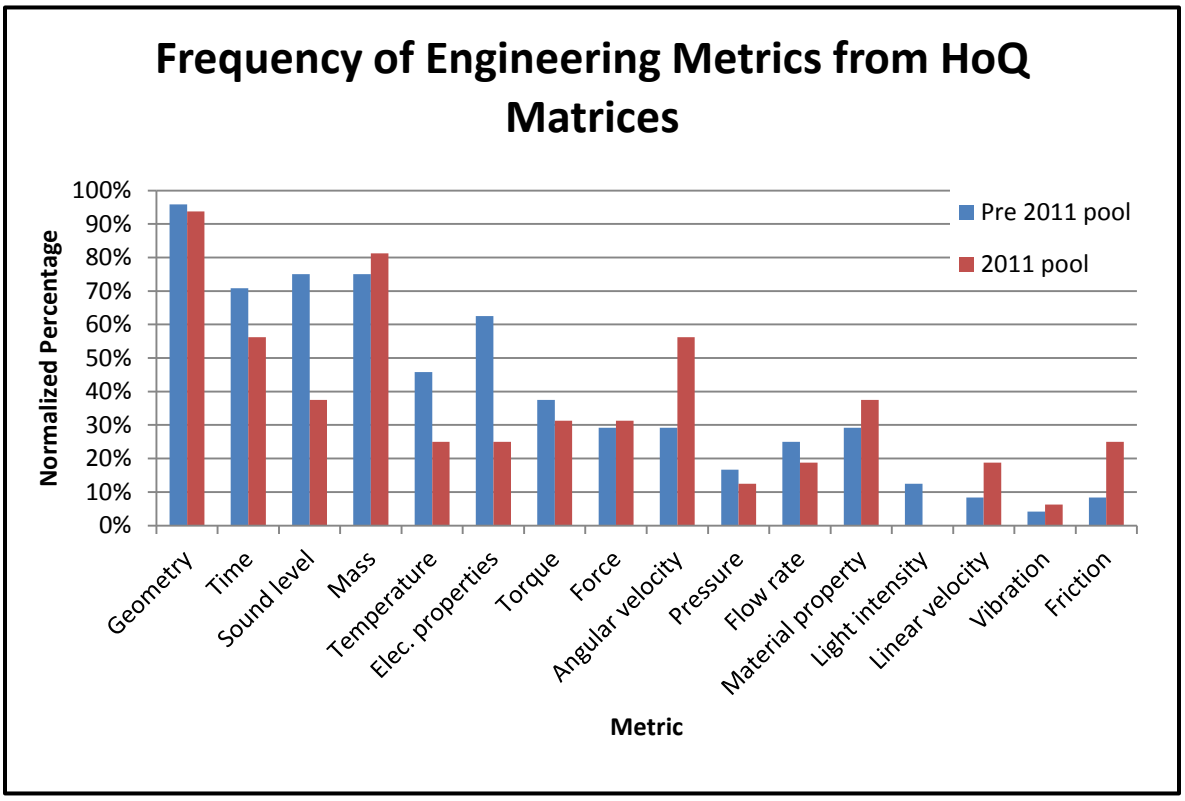


Figure 4 - Frequency chart of various engineering metrics.

From the chart, there are several dominating metrics, including Geometry, Time, Sound Level, Mass, Electrical Properties, and Angular Velocity. The most frequently cited category was Geometry. As noted in Table 1, Geometry encompasses all measurements of dimensions, including length, area, volume, diameter, etc. Since this is always the first metric an engineer needs to measure to replicate a product (or to model a product in CAD software), the high frequency of geometry is to be expected.

To distill the data, a threshold could be defined where the metrics underneath the threshold are deemed irrelevant to the experiment (for example, 15%). However, since there are not many metrics in the data set, all 16 metrics were considered in the final list.

## 2.2 Survey of Student Dissection Experience

### 2.2.1 Survey Deployment

The second method used to acquire engineering metrics and dissection tools for the reverse engineering toolbox is a survey. The survey was prepared online using SurveyMonkey® and sent out with the help of Dr. Mitchell Pryor, the instructor for the design methodology course at the time (fall of 2011). The survey asked general questions about the product, its domain, and difficulty of disassembly. The survey then asks more specific questions about the tools the students used, the metrics they measured, and the measuring devices they used. Please refer to Appendix A for a copy of the survey.

### 2.2.2 Results from Survey of Students

After the survey was sent out, the collection time continued until no new responses were recorded by the online server, which then prompted the survey to be closed. The results were then downloaded and analyzed for trends and patterns. Because of the nature of the reverse engineering class, there were duplicate responses in the survey since the students work in groups, with one product for each group. These

duplicates were manually removed from the survey results and the remaining responses were analyzed again. There was no significant difference in the distribution of the results between the original and modified results, and so for the remainder of this section, the modified data will be used. Both data sets can be found in Appendix C.

The survey yielded some valuable insight on the domain of products students chose to dissect and the actual dissection process itself, in addition to the engineering metrics that the students measured. According to the survey, all of the products dissected by the students are household products used to perform a simple function, i.e. sewing machine or potato peeler. The products' domain was distributed about 50% purely mechanical and about 50% electromechanical, which signifies the importance of having tools that accommodate electronic components. Refer to Table 2 for a list of products dissected by the students.

In addition to product domain information, information about the dissection procedure was also extracted from the survey. The results as a whole showed no major problems in opening and dissecting the products; using common tools such as screwdrivers and pliers was sufficient. By far the most used tool to dissect the products was a Phillips head screwdriver. The second most used tool was the flathead screwdriver, followed by pliers. Other tools cited are a drill, hex keys, craft knife, manual saw, open ended wrench, Torx screwdriver, soldering iron, and wire cutters. Since the toolbox developed in this research is targeted for use by students, the survey indicates that a simple assortment of hand and power tools is sufficient.

| |
|---|
| Lil' Sew and Sew hand sewing machine |
| Shark HH vacuum |
| A rotating tie rack |
| Traveling Tractor Sprinkler |
| The Claw (personal version of the claw arcade game) |
| Automatic Peeler |
| Automatic tennis ball launcher for dogs made by Go Dog Go |
| automatic hose reel (water powered) |
| iPong ping pong robot |
| NERF Vortex Gun |
| Garden Groom (hedge trimmer) |

Table 2 – List of products dissected by reverse engineering students (duplicates removed).

The final section of the survey inquires about the metrics measured by the students. This section is interesting to analyze, especially when referring back to the metrics gathered from the pool of HoQ matrices. This is helpful since it revealed any general inconsistencies between metrics from the HoQ matrices and metrics measured by students.

Analysis of the metrics measured by the students reveals a similar trend to the one from the HoQ matrices, with Geometry occurring most frequently, followed by Mass and Electrical Properties (Figure 5). However, there is also a surprising number of metrics missing from the chart. This discrepancy can be seen more clearly when the same group of students is analyzed, as shown in Figure 6:

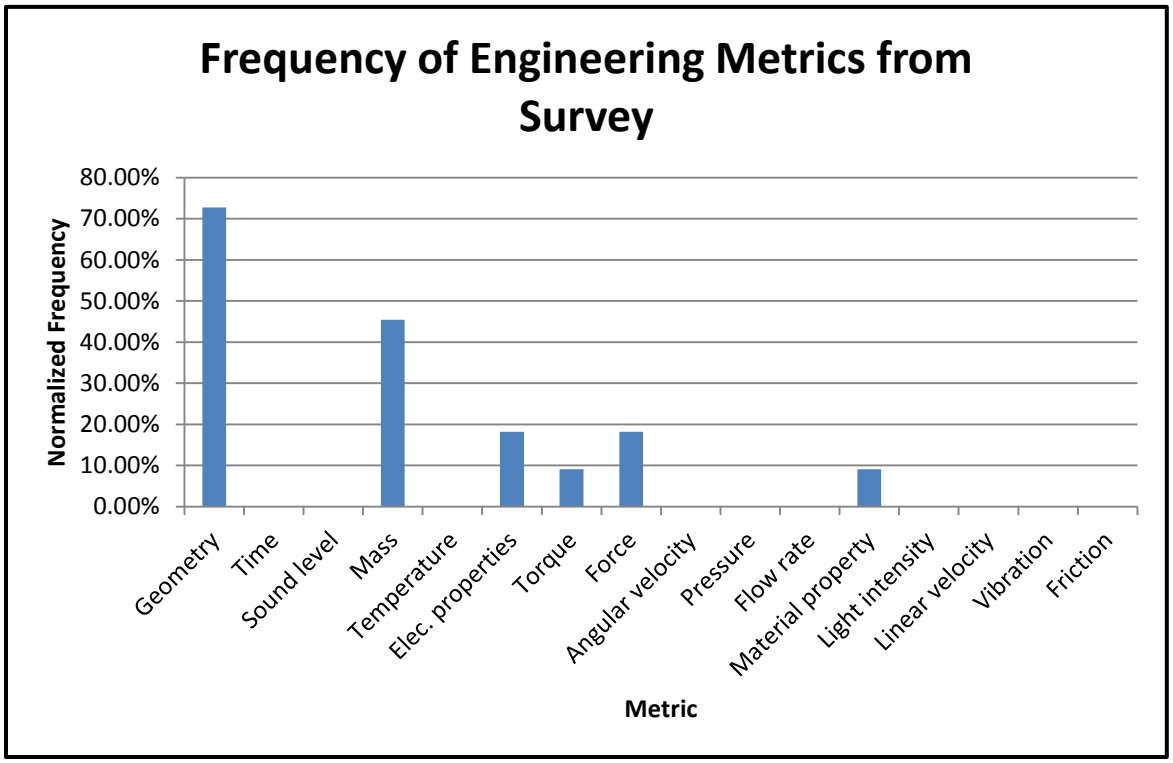


Figure 5 – Frequency chart of metrics measured by engineering students.

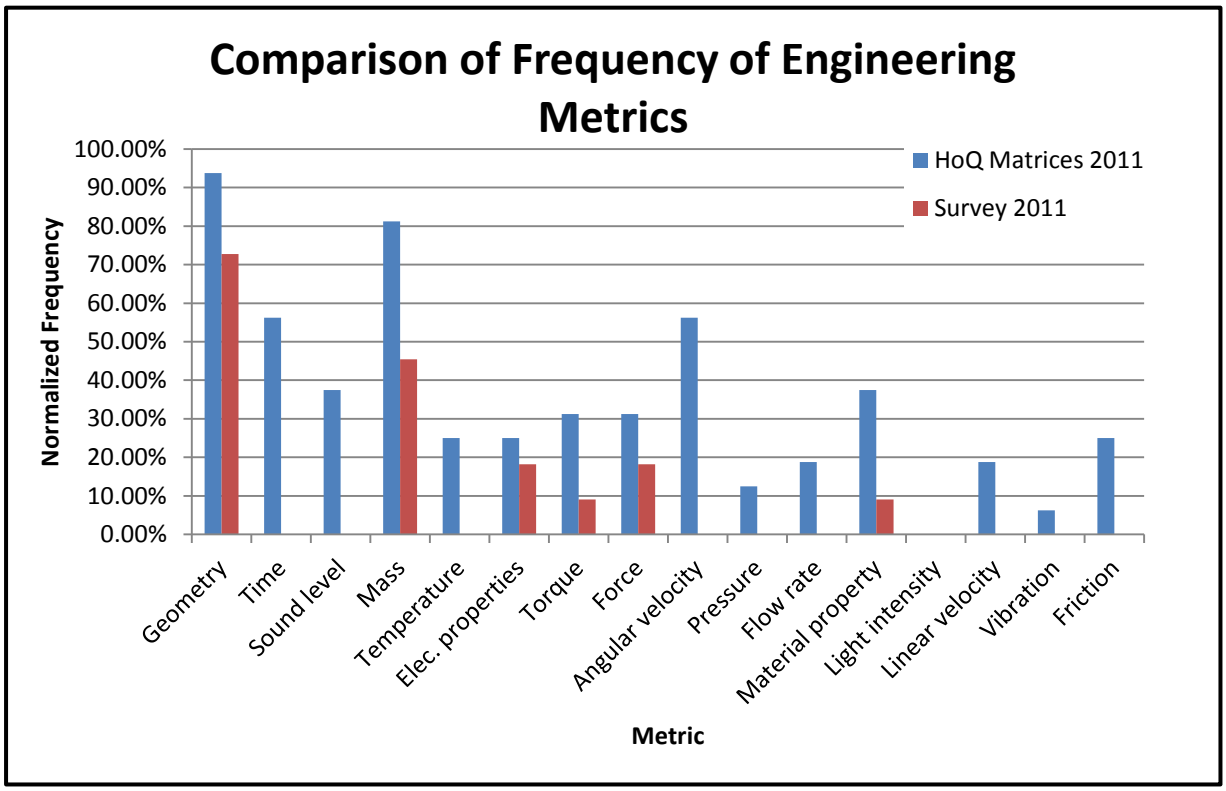


Figure 6 – Comparison of the frequency of engineering metrics from the survey and HoQ matrices for the same group of students.

The difference between the metrics the students deemed necessary for reverse engineering and the metrics the students measured can be attributed to many factors, one of which is tool accessibility; a problem the toolbox developed in this research aims to address.

### 2.3 Finalized Lists for Toolbox Development

After analyzing the results from the HoQ matrices and student surveys, finalized lists of engineering metrics and dissection tools were created. These lists consolidated all of the results into lists that can be referenced when creating the reverse engineering toolbox.

The consolidation process was not very complicated; no weighted average methods or complicated matrix calculations were performed. The lists simply included all of the metrics and tools obtained with a few modifications to account for duplicates and needs of the same category. The finalized lists are presented below.

### 2.3.1 Finalized Engineering Metrics List

| Geometry |
|---|
| Mass |
| Time |
| Sound level |
| Temperature |
| Force |
| Electrical properties |
| Torque |
| Angular velocity |
| Material properties |
| Flow rate |
| Light intensity |
| Linear velocity |
| Vibration |
| Friction |
| Pressure |

Table 3 – Finalized list of engineering metrics.

Table 3 above presents the finalized list of engineering metrics to be considered for the reverse engineering toolbox. The list was created by meshing the metrics acquired from the HoQ matrices with the metrics from the student survey. Duplicate metrics were then combined together to form a single metric on the list. The next step is to determine the tools necessary to measure the metrics, which is further explored in Chapter 3.

### 2.3.2 Finalized Dissection Tools List

The finalized dissection tools list is presented in Table 4. The tools listed here are the results from the survey, including the comments given by students. As stated earlier, the complexity of the products is fairly mild, and thus requires no special tools or equipment.

| |
|---|
| Phillips Head Screwdriver |
| Flat Head Screwdriver |
| Torx Screwdriver |
| Pliers |
| Drill |
| Hex Keys |
| Open Ended Wrench |
| Hack saw |
| Utility knife |
| Soldering Iron |
| Wire Strippers |

Table 4 – Finalized dissection tools list.

## 2.4 SUMMARY OF FINDINGS

As a result of the methodology in this chapter, a list of metrics was consolidated, which allows the development of the toolbox in later chapters by researching the tools necessary to measure those metrics. Along with the metrics, it was found that the tools required for dissection are relatively simple, and a finalized list of commonly found tools was then developed to be included in the toolbox.

# Chapter 3: Current State-of-the-Art Tools and Techniques for the Measurement of Engineering Metrics

## 3.1 Introduction

This chapter explores the current consumer and industrial tools and equipment for measuring and quantifying the engineering metrics found in Chapter 2. It is not feasible to plan on covering every choice available on the market; however, every attempt is made to paint an appropriate picture of what is required to measure the metric in question. It should be noted that the products/examples discussed in this chapter represent the state of the art; and as with every professional grade measuring tool on the market, they are fairly expensive. Since one of the goals of this research is to develop a low cost toolbox for academic use, the examples shown here are not necessarily appropriate for the development of the final reverse engineering toolbox, but should merely be viewed as "benchmarks" to which the final products are compared to.

## 3.2 Method of Research

The main avenue for researching tools and methods was through querying several search engines on the World Wide Web. Online versions of manufacturers' parts catalogues can be searched for specific tools, presenting a fast and effective way of finding the appropriate tools. This method has a very good chance of uncovering most of the available options on the market today, since it is the nature of websites that they are constantly updated (as opposed to print catalogues which can get outdated). When deemed necessary, experts in the appropriate field were consulted to facilitate the research process, including visits to brick and mortar stores.

Note: The author is in no way affiliated with any of the companies and vendors featured in this chapter.

## 3.3 TOOLS AND METHODS

### 3.3.1 Geometry

The Geometry group includes all metrics that comprise length measurements; mainly length, width, height, area, volume, diameter, etc. The most straightforward tool used for length measurements is the humble ruler. The ruler provides a quick and easy way to determine measurements when accuracy is not required. A good machinist's ruler, for example one made by Starrett, can provide accuracy to 0.020" (0.5 mm) (Starrett, 2011). However, a ruler is unable to provide the accuracy needed for really small parts and tight tolerances, and cannot be used effectively for inside dimensions (for example, inside of a small hollow shaft). For more accurate measurements and versatility, engineers often turn to calipers. Several types of calipers exist on the market, including dial, digital, and Vernier. A dial caliper uses a pointer on a dial to show the measurement, while a digital caliper uses a digital readout instead. A Vernier caliper uses a special sliding scale to show the measurement instead (Tresna, 2008). An example of a high quality digital caliper is one made by Mitutoyo, shown in Figure 7. This particular caliper boasts accuracy down to 0.001 inch, with versatile jaws that can measure inside and outside dimensions, as well as a depth gauge made by the lower sliding half, the tang (Mitutoyo America Corporation, 2011).

It is also worth mentioning micrometers as a length measurement tool. Micrometers, similar to calipers, have a sliding scale and can be used to measure. The advantage over calipers is that their accuracy can be higher for some models; for example, one made by Mitutoyo claims an accuracy of 0.00005 inch (Mitutoyo America Corporation, 2011). The disadvantage of micrometers is their lack of versatility. Whereas a caliper can measure outside and inside diameters and depth, a different micrometer is required for every type of measurement.

For measurements on a larger scale, a standard tape measure or laser range finder can be used, both providing accuracies of about 1/16 of an inch (Bosch, n.d.). However, since the scope of this research is concerned about common household products dissected by students, the majority of measurements will be short range and can be fulfilled by a ruler and calipers.

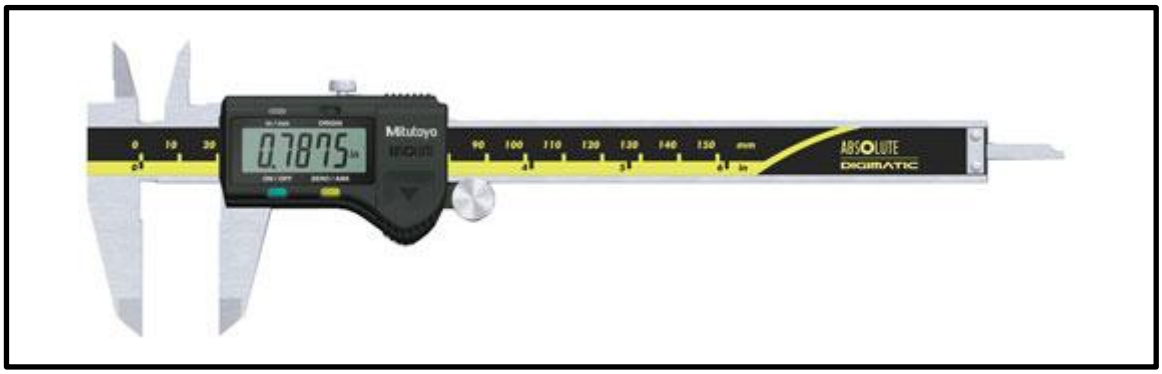


Figure 7 – Example of digital caliper (Mitutoyo America Corporation, 2011).

Another tool that quantifies geometry is a 3D point scanner. Relatively more complex (and more expensive) than regular hand tools, a 3D point scanner is an apparatus that can scan a 3D object in space and record its dimensions through software. Two types of 3D point scanners will be discussed: a laser scanner, and a Coordinate Measuring Machine (CMM).

A 3D laser scanner uses the principle of triangulation to find the coordinate of a point on the object in space. It does this by projecting a laser beam onto the object, then reading the reflected beam using an optical sensor. The time of flight (the time it takes the laser beam to bounce back) is measured and the distance is determined (since the speed of light is constant). The laser is scanned across the whole object in this same manner by means of a mirror rotated by a galvanometer, creating a 3D representation of

the object in software (3D digital corp, 2010). An example of a 3D laser scanner is one made by Konica Minolta, the Vivid 9i (Figure 8). This laser scanner boasts a resolution of 50 micrometers and only 2.5 seconds per scan (Konica Minolta, 2012).

A CMM uses a different principle to create a 3D image of an object. Instead of a laser beam, it uses a miniature probe attached to a robotic arm (see Figure 9). To make a measurement, the user touches the probe to a specific point of interest on the object, and the software records the angles of the joints of the robotic arm. From these angles, and some forward kinematics equations, the software can locate exactly where the probe's tip is in space. Claimed resolution is around 0.024 mm (Faro, 2012).


Figure 8 – Konica Minolta Vivid 9i laser scanner (Konica Minolta, 2012).


Figure 9 – Faro's Fusion Arm (Faro, 2012).

The last aspect of geometry to be discussed the measurement of angular displacement, and angles in general. The simplest tool to measure angles (and therefore, angular displacement), is the humble protractor. Available in all colors and sizes, the protractor is a circular (either half or full) gauge with marks for the angles (usually in degrees). A more complicated model, the bevel protractor, incorporates a Vernier scale and a clever mechanism to measure both acute and obtuse angles, to an accuracy of 1/12° (5 minutes) (TFT Tools, Inc., n.d.). This type of protractor is usually used in machining operations where the measurement of angles is critical.

### 3.3.2 Mass

Measuring the mass of an object is very important when trying to categorize material properties. This is essential when calculating how objects will behave in response to external stresses. Also of importance is the accurate tallying of a product's weight; often, a design is driven by the need for a lightweight product, and an accurate way to measure weight is crucial.

Perhaps the most widely used tool for weighing an object is the humble balance, an apparatus that can trace its roots to ancient civilizations. The first documented use of the balance can be seen in archeological evidence of pre-dynastic Egypt, where a balance beam made of limestone was used with calibrated stones (Petruso, 1981, p. 45). However, the use of balances has given way to the convenience of a spring scale, which have evolved to become electronic standalone models, with no need for an external counterweight. A spring scale differs from a balance in that it uses spring tension instead of a counterweight to "balance" the load, allowing a more compact form factor.

To look for precision and accuracy, it is helpful to look at laboratory settings, where all the equipment used is of high quality and as close to perfect calibration as possible. Searching online catalogues of companies who sell laboratory grade equipment yielded several examples of precision digital scales. An example is a model made by Sartorius, the AZ series (Figure 8). Depending on the user's needs, these scales can measure up to 220 grams with 0.1 mg accuracy, or up to 6200 grams with 10 mg accuracy. This model also boasts internal calibration (no need for an external calibrated weight) and a draft shield to prevent ambient air currents from compromising the readings (*M-Pact Precision Analytical*, n.d.). Another example scale is the Ohaus EX series, boasting up to 320 grams with 0.1 mg accuracy, and up to 10,200 grams with 10 mg accuracy. This model

also comes with internal calibration and a draft shield, but also adds a detachable touch screen (*Explorer® Analytical and Precision*, 2012).

For less accurate measurements, one can use a simpler spring scale similar to those fishermen use to weigh their catch. Figure 11 shows an example of a spring scale made by Ohaus. The accuracy of such a scale depends on the range, anywhere from 10 grams to 200 grams (*Spring Mechanical Scales*, 2012).


Figure 10 – Sartorius AZ series scale with draft shield (Sartorius *AZ124, M-POWER*, 2012).

Figure 11 – Example of spring scale made by Ohaus (*Spring Mechanical Scales*, 2012).

### 3.3.3 Time

Since a lot of the units of measurement that engineers deal with every day have a time aspect to them (velocity, frequency, etc), measuring time is essential to reverse engineering. However, since measuring time is in itself a broad term, for the purposes of the toolbox, it will be defined as the need to measure the time passed between two marks initiated by a human operator.

The obvious first choice is a run of the mill wrist watch or wall clock. These devices use a quartz crystal, a piezoelectric material that resonates at a constant frequency, to keep time (Dwyer, 2012). However, the average clock or wristwatch only provides accuracy to one second. For more accurate time, the standard stopwatch can be used.

A stopwatch, either analog or digital, allows the user to trigger the start and stop points and indicates how much time has elapsed (See Figure 12). Even though analog stopwatches have been around for a long time, digital stopwatches offer much higher resolutions, able to measure time to 1/100 of a second (*Traceable Stopwatch*, 2012). While this resolution might not be suitable for quantum physics and such, it is more than ample for timing the set up time of a product, how much time a machine needs to warm up, etc. This makes the digital stopwatch a suitable component for a reverse engineering situation.


Figure 12 – Traceable® digital stopwatch (*Traceable Stopwatch*, 2012).

### 3.3.4 Sound Level

The ability to measure sound level is important to reverse engineering by enabling the engineer to quantify acoustic properties of the product, such as the noise made by a motor, or the loudness of a coffee maker's beep. Sound level is quantified by measuring the Sound Pressure Level (SPL), measured in decibels.

SPL is a measure of how intense a sound wave is at a given distance away from the source. It is measured in decibels (dB), a unit which in itself is relative to a reference sound pressure. This reference sound pressure is taken at the limit of human hearing, 0.02 mPa, and is designated as 0 dB. However, the human ear does not perceive equal loudness of a certain decibel level across all frequencies. In other words, a sound at 50 dB will not sound as loud across all frequencies; instead, the human ear is much more sensitive to sounds in the 1-4 kHz range than above or below. This difference can be compensated for by using what is referred to as an "A weighting filter." When a sound level meter is outfitted with an A-filter, the decibel readings will change to mimic how the human ear perceives that particular sound, and the units of measurement change to dBA. However, since the human ear is much more complex than any electronics, the A-filter is only an approximation (Wolfe, n.d.).

To measure the SPL, many different models of sound level meters exist. Their accuracy is categorized by type, ranging from Type 0 to Type 2. Type 2 is the most common meter on the market, with an accuracy of ±2 dB. An example of a high end Type 2 meter is the SDL600 by Extech (Figure 13). As can be seen in the figure, on top of the meter is the microphone, covered by a windscreen. This model has a 100 dB range, and also has built in data logging and a PC interface for advanced data management.

A Type 1 meter has an accuracy of ±1 dB, and is usually used in laboratory settings. An example of a high end Type 1 meter is the SVAN 979 by Svantek (Figure 13). This meter boasts a 155 dB range, data logging, several filters, and an OLED color screen.


Figure 13 – Extech Type 2 meter (left) (Extech, 2012) and Svantek Type 1 meter (Right) (Svantek, n.d.).

### 3.3.5 Temperature

A major concern of mechanical engineering involves quantification and analysis of heat transfer and thermodynamics, and one of the most important variables needed for such quantification is temperature. Measuring temperature allows the engineer to calculate how much heat a machine produces, how cold an ice cream machine gets, and how much energy is lost through bearing friction. There are many avenues for measuring temperature, and thus, many types of thermometers exist. However, for the sake of

simplification, they will be split into three categories: contact non-electronic, contact electronic, and non-contact.

Contact, non-electronic temperature measuring instruments refer to conventional thermometers that measure the temperature by means of making contact with the subject, while employing nonelectric transduction means. Examples of these thermometers include the standard glass thermometer, the bi-metallic meat thermometer, and thermochromic color changing strips (which also gained popularity a while ago as mood rings).

The glass thermometer has been in use for a long time, usually in the medical field, with the liquid inside being mercury. It uses the principle of thermal expansion of a liquid to measure the temperature with reference to a certain point (usually the freezing point of water). Since mercury is hazardous to both the environment and humans, it has now been replaced by spirits. These thermometers typically have a resolution of 1°C/F, read by matching the level of the liquid inside to the lines on the graduated scale printed or etched on the glass. An example of such a thermometer is one made by Palmer, shown in Figure 14 (Palmer Wahl, 2012). However, some of the drawbacks that prevent the glass thermometer from being a good candidate for a reverse engineering toolbox are its size, inflexibility, and fragile nature.

The bimetallic thermometer uses the principle of thermal expansion as well; however, it uses a metal strip instead of a liquid. As the name suggests; two dissimilar metal strips are joined together into one strip. When subjected to heat, one metal expands faster than the other metal. However, since they are joined together, this imbalance of forces created a twisting motion, and if the strip is coiled, this twisting can be measured using a simple dial indicator correlated with a temperature scale (Brain, n.d.).

Finally, thermochromic materials are materials that change state depending on the ambient temperature. Two types of thermochromic materials are discussed: liquid crystals and leucodyes. Thermochromic liquid crystals (TLCs) have small particles suspended in a liquid, aligned longitudinally. When light hits the crystals, the reflected beam is color shifted depending on the spacing of the particles. This spacing itself is what differs depending on the temperature. TLCs are advantageous in that they are fairly accurate in a small temperature range, and provide a quick way to find the temperature of an object. A practical application would be to stick a TLC strip onto a transformer and quickly know if it is overheating (Woodford, 2011).

Leucodyes are organic materials that change transparency depending on a preset temperature. Unlike TLCs, they exhibit an "on/off" behavior, rather than a slow change over a temperature change, and are thus useful for a quick check for whether a certain temperature has been achieved (Woodford, 2011).

Contact electronic thermometers are thermometers that have to make contact with the subject, and are electronic in nature. The three types that are explored in this category are resistance temperature detectors (RTD), thermistors, and thermocouples.

RTDs are, in effect, resistors that change resistance in response to a temperature change. A RTD is made of a length of fine wire wrapped around a ceramic or glass insulator, and is fairly fragile if not mounted inside a protective sheath. The accuracy of RTDs varies with temperature, anywhere from ±0.3°C at 0°C and ±4.3°C at 850°C. The advantage of RTDs is that they are immune to electromagnetic radiation, and can be used around rotating machinery and electromagnetic appliances to measure, for example, the temperature of an AC generator (thin film sensors are even made to be placed on a surface) (Omega, 2012.).

Thermistors, like RTDs, are resistors that change resistance in response to a temperature change. However, unlike RTDs, they are made of semiconductor material. They usually have a negative temperature coefficient, which means that resistance drops as the temperature increases. Thermistors differ from RTDs in that they are more accurate over a smaller range of temperatures, and are among the most accurate temperature sensors. Typical accuracy is ±0.1°C and the range is about 0-100°C (Omega, 2012).

Finally, thermocouples use a different principle from RTDs and thermistors, instead relying on the Seebeck effect. The Seebeck effect states that two dissimilar metals joined together, and then subjected to a temperature gradient will exhibit a voltage potential ("Seebeck Effect," 2012). Thusly, a thermocouple is made from two dissimilar metals joined together at a junction. Several types of thermocouples exist, designated by letters. The most common types are J, K, T, E, and all exhibit different ranges (Omega, 2012). Table 5 presents the properties of the different junction types.

| Common Thermocouple Temperature Ranges | | | |
|---|---|---|---|
| Calibration | Temp Range | Std. limits of Error | Spec. Limits of Error |
| J | 0ºC to 750ºC (32ºF to 1382ºF) | Greater of 2.2ºC or 0.75% | Greater of 1.1ºC or 0.4% |
| K | -200ºC to 1250ºC (-328ºF to 2282ºF) | Greater of 2.2ºC or 0.75% | Greater of 1.1ºC or 0.4% |
| E | -200ºC to 900ºC (-328ºF to 1652ºF) | Greater of 1.7ºC or 0.5% | Greater of 1.0ºC or 0.4% |
| T | -250ºC to 350ºC (-328ºF to 662ºF) | Greater of 1.0ºC or 0.75% | Greater of 0.5ºC or 0.4% |

Table 5 – Properties of different thermocouple types (reproduced from Omega, 2012).

Non-contact electronic thermometers are devices that can measure the temperature of an object remotely, without making contact with the object. This is helpful if there is danger associated with close contact (i.e. a pot of molten steel), or if proximity of the probe/user affects the readings.

The main effect measured for most the non-contact thermometers is infrared electromagnetic radiation. Every object in existence that is above zero Kelvin, the absolute zero point, emits heat in the form of radiation, which varies with the temperature of the object. The infrared thermometer can focus this emitted radiation and convert it to an electrical signal using sensitive sensors. However, since different objects have different surfaces and properties, to accurately acquire a measurement, a compensation for emissivity must be made. Emissivity is the ratio of how much radiation the object is emitting to the radiation that a perfect black body at the same temperature emits. This emissivity can range from 0.0 to 1.0, with 1.0 being a perfect black body (Omega, 2012).

Most infrared thermometers on the market have a feature to change the emissivity. An example of an infrared thermometer is the Fluke 574 (Figure 14). This meter has a range from -25°C to 900°C with 0.75% accuracy, and features an adjustable emissivity in 0.01 increments (Fluke Corporation, 2012).


Figure 14 – Fluke's 574 infrared non-contact thermometer (Fluke Corporation, 2012a).

### 3.3.6 Force

Measuring force, precisely, linear force, is an essential tool for the reverse engineering toolbox. Measuring the cutting force of a jig saw and the trigger load of a paintball gun are both examples of the importance of quantifying linear force.

Research uncovered many ways to measure linear force, with companies offering both mechanical and digital force gauges that work on a plethora of principles. Most force gauges measure force by means of displacement. This method is directly related to Hooke's law, which states that the force needed to deflect an object (whether it be a beam, spring, etc.) is related by a spring constant, *k*, as follows:

$$F = kx,$$

where *F* is the measured force, *k* is the spring constant, and *x* is the displacement.

Having a defined relationship between the two variables then allows the indirect measurement of force using an apparatus that has some form of spring constant. The simplest example of a force gauge that uses Hooke's law is the spring scale shown in Figure 11 in section 3.3.2. The spring constant is provided by a regular tension spring,

and the deflection is then measured using the vertical scale on either side of the pointer. Conversely, a simple example of a force gauge that measures compression is the standard scale shown in Figure 10 in section 3.3.2.

Another way to provide a spring constant is through a cantilever beam. An example of such an apparatus is a deflection beam design made by Dillon called the Model X (shown in Figure 15). This force gauge is shaped like a "D," with the top half acting as a cantilever beam. The force is applied to the top, in either tension or compression, and the deflection of the beam is transferred to the dial indicator by means of the wedge on the right side (Dillon, 2012, p. 2).


Figure 15 – Dillon Model X (Dillon, 2012, p. 2).

These examples are mechanical variants of a force gauge. To employ a digital version, a load cell is then used to convert mechanical displacement into a digital signal. Simply put, a load cell is a transducer, and can be based on many mechanical principles, including pneumatic, hydraulic, and piezoelectric. However, by far the most popular type of load cell is one based on a strain gauge.

A strain gauge is composed of a grid of very fine wire that is bonded to a backing material. When the gauge is placed under stress, the wire is either elongated or compressed, depending on the direction of the force. The wire has a finite volume, and so the cross section of the wire also shrinks and grows with the strain. Since electrical resistance is a function of the cross sectional area of the conductor, it too changes with strain. To measure the resistance, a Wheatstone bridge is used in conjunction with a voltmeter (Omega, 2012).

To create a load cell, the strain gauge is placed on a calibrated beam, which can take on several sizes and shapes. When a force is placed on the beam, the strain gauge measures the deformation of the beam, thus correlating a voltage with the force measured. Many digital force gauges are based on the strain gauge load cell; an example is the Series 5 digital force gauge by Mark-10 (Figure 16). This force gauge claims an accuracy of 0.1% over the full range of 0.12 – 100 lb (0.5 – 5000 N) in tension and compression, and also includes a myriad of features, including data logging, maximum and minimum values, and a graphical display.


Figure 16 – Digital force gauge by Mark-10 (*Mark-10 Force Gauge*, n.d.).

### 3.3.7 Electrical Properties

Measuring electrical properties is crucial for reverse engineering mechatronic products. Electrical properties such as voltage, current, resistance, and power provide insight into how the product works, how much energy it uses, and where the key components are. There are products dedicated to measuring every one of the abovementioned properties only; however, for the purpose of this thesis, multimeters – devices that can measure a myriad of electrical properties – are the focus of the discussion, since they are more convenient for the purposes of a toolbox.

Multimeters are available in both analog and digital flavors; however, the majority of multimeters in use today are digital, since they provide more resolution and more features. Digital multimeters work by using different circuits to measure the different properties, selectable by the user. For example, to measure resistance, the meter provides a small, constant current source to the element being tested, and then measures

the voltage drop generated by that current. Since electrical properties are governed by Ohm's law:

$$V = I * R$$

where *V* is the voltage, *I* is the current, and R is the resistance.

The resistance can then be calculated using the known quantities voltage and current. To measure current, the meter feeds the current to an integrated circuit designed to convert current to voltage. This voltage is then fed to an analog to digital converter and displayed on the screen. Similarly, to measure voltage, it is fed straight to the analog to digital converter and displayed on the screen (Vidyasagar, 2011).

An example of a portable handheld multimeter is a model 289 made by Fluke (Figure 17). This model is one of the premier industrial tools available, with built in data logging and a big screen. Some of the properties this meter can measure are DC voltage, AC voltage, DC current, AC current, resistance, capacitance, frequency, and even temperature. The accuracy for the measured properties ranges from 0.025% for DC voltage to 1% for temperature.


Figure 17 – Fluke 289 Digital Multimeter (Fluke Corporation, 2012b).

Another example of a multimeter is the bench top version. These meters are more suited for a laboratory setting instead of portable, on-the-go convenience. However, these meters provide the most accurate readings for precise measurements. An example of a high quality bench top multimeter is the Agilent 3458A (Figure 18). This meter boasts 8.5 digits of resolution and a sensitivity of 10 nV, with an accuracy of 0.0004% (Agilent Technologies, 2012).

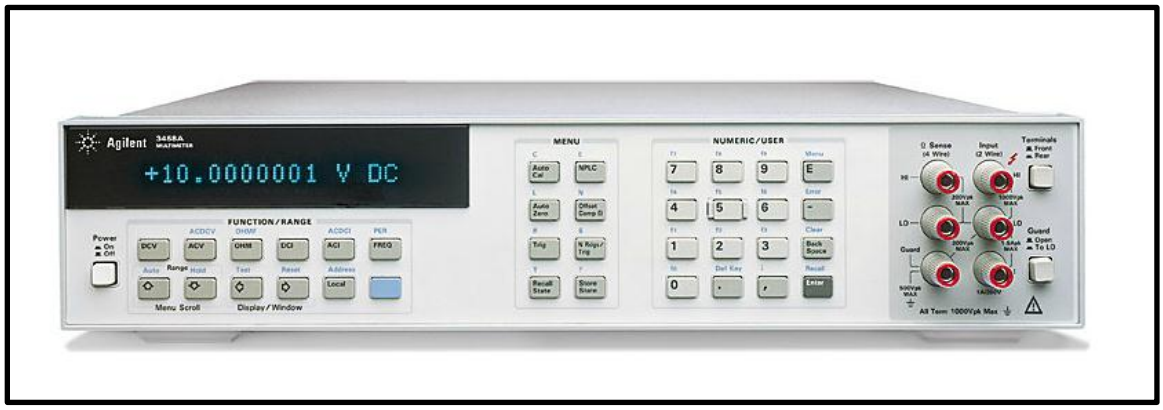


Figure 18 – Agilent's 3458A bench top multimeter (Agilent Technologies, 2012).

Measuring electrical power provides valuable data about how much energy an electrical or mechatronic device consumes. This can be a starting point in a calculation of energy transfer, for example, inside a heater, allowing the engineering to calculate the heat output and conversion losses.

Power, in general, is measured in units of Watts. Even though it is possible to measure electrical power using a multimeter and taking several measurements of electrical properties, a simpler solution exists on the market, the Watt meter. The way it is designed allows the user to simply plug the appliance to be tested into the meter, and plug the meter into the outlet. The meter's display then shows the instantaneous power consumption.

An example of this type of meter is the popular "Kill A Watt" power consumption meter made by P3 International (Figure 19). This meter can measure many metrics associated with energy consumption, including volts, current, watts, frequency, power factor, VA, and cumulated kWh within 0.2% accuracy (P3 International, 2012). This meter comes in handy if an engineer wants to quantify how much power a coffee machine uses when making a cup of cappuccino, for example.


Figure 19 – P3 International Kill A Watt meter (P3 International, 2012).

### 3.3.8 Torque

Measuring torque is essential when trying to quantify any forces that involve a twisting motion. This comes in handy, for example, when measuring the torque output of a hand drill, how much torque a bolt needs to break loose, or how much torque the cap on a water bottle needs to close.

As with most other meters, there are both analog and digital means of measuring torque. The simplest analog method is the torque wrench, most commonly used in the automotive industry for precisely tightening bolts. Several types of torque wrenches exist (even digital ones based on strain gauges). However, the most basic type is the beam torque wrench (Figure 20). This wrench is special in that it not only shows tightening torque, but also loosening torque. The wrench works by simply measuring the deflection of the wrench itself in relation to a pointer that always stays straight. Torque is related to a linear force by the equation:

$$T(torque) = F(force) * r(radius)$$

The amount of force deflecting the beam can be translated into a torque being applied to the bolt.

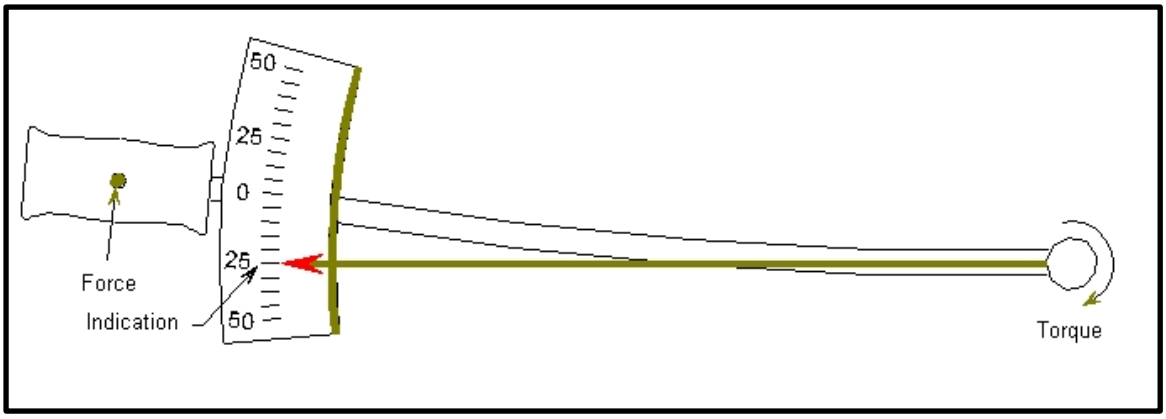


Figure 20 – Illustration of how a beam torque wrench works (Dille, n.d.).

A digital torque meter works on the same principle as a digital force gauge (Section 3.3.6); however, the strain gauges are oriented in a way that measures torque more effectively. The strain gauges are placed on a beam that twists with the applied torque, and then measure that twist (Omega, 2012). An example of a torque meter that uses strain gauges is the Tohnichi BTGE handheld torque gauge (Figure 21). This gauge is designed to be placed on the item to be measured, and then twisted by hand (ideal for measuring screw driver torque, or torque to open a soda bottle). The range for this gauge is 0.2 – 18 in lb with 2% accuracy (Tohnichi America Corp., 2012).


Figure 21 – Tohnichi handheld torque gauge used for low torque applications (Tohnichi America Corp., 2012).

Finally, for a more sophisticated method of measuring torque, such as for measuring the torque output of a DC motor, a dynamometer is used. Dynamometers are usually used for large gasoline and electric engines; however, miniature dynamometers have been developed. Magtrol offers a complete package to measure the torque-speed curve of miniature motors, called the Micro Dyne (Figure 22). The Micro Dyne can measure torque up to 4 mN·m and speeds up to 100,000 rpm, with a computer software interface that can plot the characteristics for the user to see (Magtrol Inc, 2012).

The concept behind this dynamometer is the dissipation of energy using a hysteresis brake (also known as an electromagnetic brake), and the torque imparted by the brake is then plotted against the speed to produce the torque-speed curve.

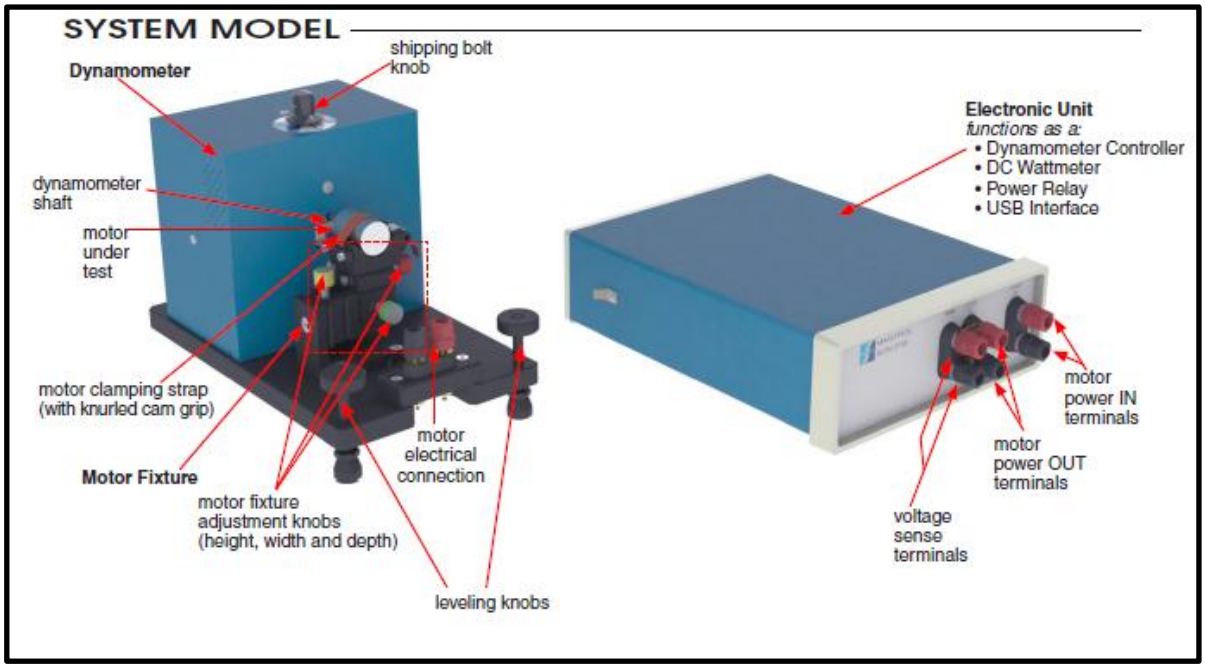


Figure 22 – Magtrol's Micro Dyne system with component labels (Magtrol Inc, 2012).

### 3.3.9 Angular Velocity

Measuring angular velocity quantifies the speed of rotating objects, including DC motors, ceiling fans, and impellers on a baseball pitching machines. To measure angular velocity, a device known as a tachometer is used. This can be either handheld for portability, or permanently mounted, as in an automobile. For the purposes of the toolbox, handheld models were explored. Tachometers, like thermometers, are available in both non-contact and contact forms.

Non-contact tachometers can work using several principles, including magnetism and induction. However, the most popular non-contact tachometer in use is the optical digital tachometer. These handheld tachometers work by using a light source (either infrared or visible laser) aimed at a rotating disk. The disk has a reflective marker attached to it, and when the marker reaches the light beam, it reflects the light back to the

tachometer, where a detector registers a pulse. The tachometer then measures the time between pulses and calculates the angular velocity, usually expressed in RPM (Morris, 2011, pp. 549-551).

Another non-contact tachometer that uses light is the stroboscope. The stroboscope has been in use in the automotive industry for a long time to set the spark timing on a gasoline engine. The stroboscope works by pulsing a bright light at a user determined frequency at the object being measured. The user then adjusts the frequency until the object seems to stand still, which means that the frequency of the light matches that of the rotating body (Morris, 2011, p. 552).

Contact tachometers can work on many principles, either through a small DC generator, which produces a DC voltage in relation to how fast it is spinning; through hall effect sensors, which vary their voltage depending on the strength of a magnetic field, and through a gated optical sensor, which has a rotating slot that allows a light source to hit a receiver every revolution (Morris, 2011, pp. 549-551). It is important, whatever method is used, that it not apply an artificial load on the rotating body and alter the results.

An example of a combination contact and non-contact optical tachometer is one made by Extech, model 461895, shown in Figure 23. This tachometer can take remote optical measurements using a laser, and also using a contact wheel on the opposite side. The accuracy of the meter is 0.05% for a range from 5 to 99,999 RPM (Extech, 2012b).


Figure 23 - Combination contact and non-contact optical tachometer by Extech (Extech, 2012b).

### 3.3.10 Material Properties

The measurement and quantification of material properties is a science in its own. Many methods and tools exist, and to document them all in their entirety in this thesis is intractable. Instead, this section focuses on three main qualities a reverse engineering student might need to measure: tensile and compressive strength, impact toughness, and hardness.

Tensile/compressive strength is an important factor in the material selection process. Typically, when testing a specimen to determine its tensile or compressive strength, it is placed under a steadily increasing force, either in tension or compression. The change in size of the specimen is then recorded against the applied force at the moment, creating a stress/strain diagram (an example is shown in Figure 24). Often, the

value of interest is the ultimate tensile strength, defined as the maximum stress a specimen experiences before failure (marked on the figure as UTS) (Instron, 2012a).

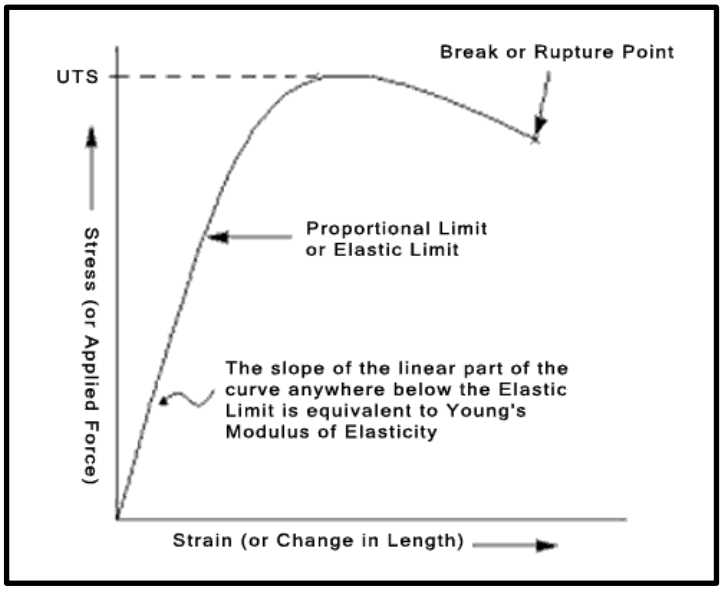


Figure 24 – Example of stress/strain diagram showing points of interest (Instron, 2012a).

Tensile and compressive testing is usually done using big, industrial sized, laboratory grade equipment. An example of a tension/compression tester is one made by Instron, model 5985. This machine can apply over 56,000 lb of force in either tension or compression using two big screw drives. Its bigger brother the 5989, measuring 10 feet tall and 5 feet wide, can apply up to 135,000 lb of force. Computer software then plots the force vs. displacement measurements, creating the stress/strain diagram for the engineer to study (Instron, 2012b).

However, a portable tensile tester is available on the market for testing smaller specimens. An example is one made by Sun-Tec called the PT Portable Tensile Tester (Figure 25). This tensile tester is a lot simpler than the laboratory grade Instron; it features a hand cranked screw drive on the right, and a dial force gauge on the left. The maximum specimen size that can be tested is six inches long (Sun-Tec Corporation, n.d.).

Figure 25 – PT portable tensile tester (Sun-Tec Corporation, n.d.).

Characterizing impact toughness is important when trying to determine, for example, the maximum height from which a TV remote can be dropped before the shell cracks, or how safe those safety glasses actually are. Impact toughness is usually measured in Joules, the unit of energy.

An impact tester most commonly uses a swinging pendulum to strike the sample to be tested. Such a pendulum can be set at a predetermined starting height, thus imparting a set amount of energy. To measure the impact energy, the ending height of the pendulum is measured, and the difference between the starting height and the ending height (and therefore the starting potential energy and ending potential energy) is the energy lost to fracturing the specimen. Depending on the type of impact testing, the specimen is shaped a certain way to keep uniformity between different tests. Figure 26 shows an example of a pendulum impact tester from Instron. The pendulum is capable of imparting from 33 to 406 Joules. It is also compatible with software that calculates the impact energy for the engineer, saving time and effort (Instron, 2012c).

Figure 26 – Example impact tester from Instron (Instron, 2012b).

Finally, the last material property discussed in this section is material hardness. Hardness is the resistance of a material to penetration; this is another useful property when trying to quantify the behavior of a material. For example, hardness testing will show whether a sleeve bearing will wear out before or after the axle shaft, or if a certain tool is appropriate to cut a certain metal or if it is too soft. It should be noted that hardness scales are relative, and do not represent an absolute property of the material.

There are many types of hardness tests used in the industry, but the most popular and easiest to use in the U.S. is the Rockwell hardness test. The Rockwell test consists of either a diamond tipped or ball tipped indenter mounted on the bottom of a plunger. First, a minor load is applied to the indenter, 10kg of force, and the position of the indenter is established as the datum. Afterwards, a major load is applied, which can be 60, 100, or

150 kg of force. The additional distance that the indenter travels is then recorded and compared to a scale (Wilson Hardness, 2012a).

An example of a hardness testing machine is the Rockwell 2000 Series tester by Wilson Hardness. This tester is a fully automated machine that can test any material according to the Rockwell testing method described above (Wilson Hardness, 2012b).

As with tensile testing, a portable version of the hardness tester is available that uses a different principle than Rockwell; called the Leeb Rebound Hardness Test. The Leeb Rebound test fires a small projectile at the target material, and then measures how much energy is left in the projectile after impact (during the rebound phase). The energy lost by making a small indentation in the material is proportional to the hardness of the material, and thus can be correlated to a hardness value (Kompatscher, 2004). This type of tester is much more portable than a lab sized Rockwell tester, and can be used in the field or on the production line for quality testing. An example of such a tester is shown in Figure 27. Both the projectile and sensor are enclosed in a small, pen-like probe shown on the right side of the figure.

An even simpler hardness test method, which also happens to be the least expensive, is the use of hardness testing files. This method consists of using these files, which are each made of a material with a different, known hardness, to try to scratch the surface of the test material. Working down from the highest hardness, the highest file that does not mark the surface determines the lower bound of the hardness value. Even though this method is not as accurate and repeatable as other methods, it offers a quick and inexpensive way to determine the range of hardness values of a test material (Fred V. Fowler Company, Inc., n.d.).

Figure 27 –Leeb rebound hardness tester (Kern-Sohn, 2009).

### 3.3.11 Flow Rate

Flow rate refers to the amount of a material moving across a point in space in a given amount of time. For the purposes of the tool box, the two types of materials that are of interest are gases and liquids. Flow rate is a helpful metric to measure since it allows the engineer to quantify the output of fluid based system (e.g., the amount of air a desk fan pushes, or how much coolant circulates within a computer's liquid cooling system).

Flow rate can be measured directly, using chambers with known volumes, or indirectly, using the speed of the moving fluid and some simple geometric data and formulas. To measure the speed of a moving gas, or specifically air, several tools exist on the market. The first tool to be discussed is the hot wire anemometer. The hot wire anemometer is a probe-like tool used to measure the flow of a moving gas (and in some cases, a liquid as well). The probe has a tip which holds a very thin wire, about 1 mm long. This wire is usually made of tungsten or platinum, and at 5µm in diameter, is 17

times thinner than a human hair. The wire is heated using an electrical current to keep it at a constant temperature, using a Wheatstone bridge to detect the resistance of the wire. When the speed of the moving fluid around the wire changes, heat is lost due to convection, cooling it down. The electronics then detect this cooling and increase the current to keep the wire at the predetermined temperature. This change in current is then measured and correlated with a velocity (Lomas, 2011, pp. 1-3).

An example of a hot wire anemometer is one made by Omega, model HHF42 (Figure 28). This anemometer is designed for low fluid velocities, and can measure a range from 0.2-20 m/s with 0.1 m/s accuracy (Omega, 2012b).

Another tool to measure the velocity of air is the rotating vane anemometer. This type of anemometer uses a small fan-like impeller mounted in a protective, ducted housing, similar in concept to the wind turbines used in renewable energy farms or a pinwheel toy. The impeller is then held in the flow, and the velocity of the air causes it to spin. The speed of the rotations is then measured, and correlated with a flow rate.


Figure 28 – Hot wire anemometer from Omega (Omega, 2012b).

An example of a rotating vane anemometer is shown in Figure 29. On the left side of the figure, the rotating vane can be seen inside a circular duct. This anemometer can measure air speeds from 0.3 to 40 m/s in 0.1 m/s increments, with a 0.75% accuracy (Omega, 2012d).


Figure 29 – Example of rotating vane anemometer by Omega (Omega, 2012d).

To measure the flow rate of a liquid, many options exist on the market, with a plethora of different technologies and configurations. Each different tool presents its own advantages and disadvantages; but for the purposes of the toolbox, a liquid flow meter was chosen because it easily integrates into the flow of an existing system and is portable.

Reviewing all of the technologies found on Omega's technical reference site (summarized in Table 6), one technology that seemed to fit the criteria is the turbine flow meter. This type of flow meter contains an impeller mounted on an axis of rotation, and a method to count the rotations of the impeller. The fluid enters the meter and spins the impeller, while the counter registers the rotations and sends them as electrical impulses.

| Flowmeter element | Recommended Service | Rangeability | Pressure Loss | Typical Accuracy, percent | Required Upstream pipe, diameters | Viscosity effect | Relative Cost |
|---|---|---|---|---|---|---|---|
| Orifice | Clean, dirty liquids; some slurries | 4 to 1 | Medium | ±2 to ±4 of full scale. | 10 to 30 | High | Low |
| Wedge | Slurries and Viscous liquids | 3 to 1 | Low to medium | ±0.5 to ±2 of full scale | 10 to 30 | Low | High |
| Venturi tube | Clean, dirty and viscous liquids; some slurries | 4 to 1 | Low | ±1 of full scale | 5 to 20 | High | Medium |
| Flow nozzle | Clean and dirty liquids | 4 to 1 | Medium | ±1 to ±2 of full scale | 10 to 30 | High | Medium |
| Pitot tube | Clean liquids | 3 to 1 | Very low | ±3 to ±5 of full scale | 20 to 30 | Low | Low |
| Elbow meter | Clean, dirty liquids; some slurries | 3 to 1 | Very low | ±5 to ±10 of full scale | 30 | Low | Low |
| Target meter | Clean, dirty viscous liquids; some slurries | 10 to 1 | Medium | ±1 to ±5 of full scale | 10 to 30 | Medium | Medium |
| Variable area | Clean, dirty viscous liquids | 10 to 1 | Medium | ±1 to ±10 of full scale | None | Medium | Low |
| Positive Displacement | Clean, viscous liquids | 10 to 1 | High | ±0.5 of rate [3] | None | High | Medium |
| Turbine | Clean, viscous liquids | 20 to 1 | High | ±0.25 of rate | 5 to 10 | High | High |
| Vortex | CLean, dirty liquids | 10 to 1 | Medium | ±1 of rate | 10 to 20 | Medium | High |
| Electromagnetic | Clean, dirty viscous con-ductive liquids and slurries | 40 to 1 | None | ±0.5 of rate | 5 | None | High |
| Ultrasonic (Doppler) | Dirty, viscous liquids and slurries | 10 to 1 | None | ±5 of full scale | 5 to 30 | None | High |
| Ultrasonic (Time-of-travel) | Clean, viscous liquids | 20 to 1 | None | ±1 to ±5 of full scale | 5 to 30 | None | High |
| Mass (Coriolis) | Clean, dirty viscous liquids; some slurries | 10 to 1 | Low | ±0.4 of rate | None | None | High |
| Mass (Thermal) | Clean, dirty viscous liquids; some slurries | 10 to 1 | Low | ±1 of full scale | None | None | High |
| Weir (V-notch) | Clean, dirty liquids | 100 to 1 | Very low | ±2 to ±5 of full scale | None | Very Low | Medium |
| Flume (Parshall) | Clean, dirty liquids | 50 to 1 | Very low | ±2 to ±5 of full scale | None | Very low | Medium |

Table 6 – Table of available flow rate measurement technology (Omega, 2012).

The number of rotations per set time period can then be correlated to the flow rate of the liquid (Omega, 2012).

An example of a turbine flow meter is the FTB600B from Omega, shown in Figure 30. This flow meter offers a compact, inline package that can be inserted anywhere in the flow loop of a system. The rotations of the impeller are measured using an infrared LED transmitter and receiver pair, and the output is sent as a square wave. Depending on the model, this flow meter can measure anywhere from 0.1 to 120 liters per minute (Omega, 2012c).

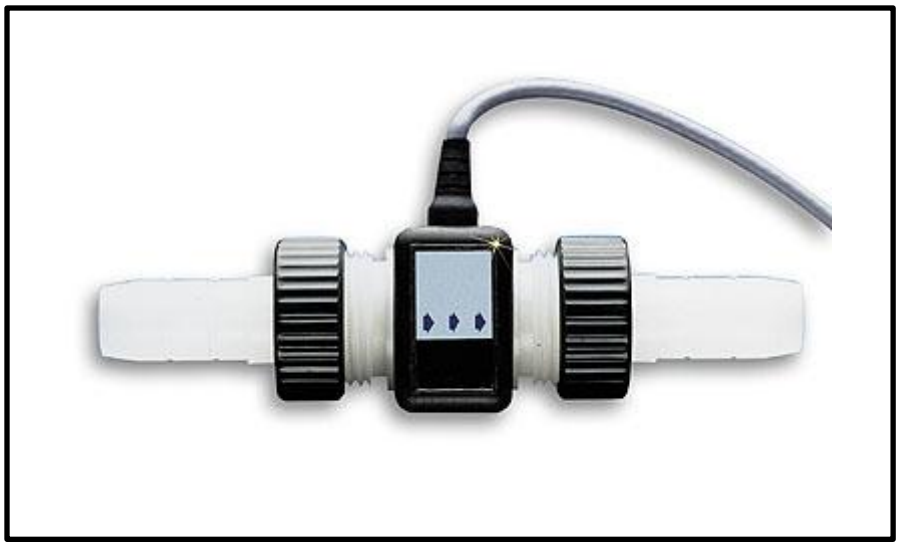

Figure 30 – Omega's FTB600B inline turbine type flow meter (Omega, 2012c).

### 3.3.12 Light Intensity

The ability to quantify the intensity of a light source is helpful when reverse engineering products that rely on light signals to perform a function. For example, an engineer can measure how bright the display on a coffee machine is, how bright an indicator light needs to be to show in sunlight, or how powerful that flashlight really is.

Measuring light intensity is not straightforward. Similar to measuring sound intensity, light intensity depends on many factors, including distance, area, and the perception of human vision. The unit for measuring the power of light is the candela, roughly equivalent to one candle. That same unit, when adjusted for the sensitivity of the human eye, results in the unit of lumen. Finally, lux is the measure of light flux, or in other words, lumens per unit area (Virdi, 2012, p. 446).

Light meters use this lux unit as a basis for their measurements, dubbed "lux meters." Lux meters are used extensively in photography to determine the exposure times, and also in work environments to prevent worker fatigue from insufficient lighting. Lux meters work by utilizing a photocell that converts incident light into a small electric current (Virdi, 2012, p. 478).

Photocells are the basis for solar energy, and they can be found anywhere from automatic night lights to alarm sensors. They are composed of a semiconductor material, that when struck by photons, releases electrons, thus creating an electrical current (Knier, 2002). This electrical current is proportional to the intensity of the light source, and thus a lux meter can correlate that current with a lux value.

An example of a high quality lux meter is one made by Gossen called the Mavolux 5032C (Figure 31). This meter can measure lux with a range from 0.01 – 199,999, and also comes with a spectral filter that mimics the frequency response of the human eye. For more precise measurements, it can be outfitted with a lens that narrows its field of vision down to about 1° (Gossen, 2011)


Figure 31 – Gossen's Mavolux lux meter (Gossen, 2011).

### 3.3.13 Linear Velocity/Speed

Linear velocity is helpful in characterizing products that might involve a projectile of some kind, such as a baseball pitching machine or a foam-dart toy gun. Measuring exit velocity can indicate how much force and acceleration those projectiles are experiencing, proving valuable when calculating the dynamics of the system.

Perhaps the most common method of measuring speed involves electromagnetic waves. This is popularly known as the "radar gun," and is the weapon of choice for police officers looking to catch innocent speedsters. Radar guns work by using the Doppler effect as applied to a radio wave sent out from the radar gun. When the radio wave hits a moving target, it experiences a frequency shift according to how fast the target is moving. After the reflected radio wave is received by the radar gun, the speed is calculated from this frequency shift (RadarGuns, 2012).

However, radar waves are not the only medium used to measure speed; LIDAR (Light Detection and Ranging) uses light waves to measure speed instead. LIDAR works on the principle of time-of-flight: a laser pulse is sent out to the target, then the detector waits for the reflected pulse to be received. The time it takes the laser pulse to travel to the target and back is recorded. Since the speed of light is constant, the distance to the target can then be calculated using a simple formula. To be used a speed sensor, multiple, consecutive pulses are sent out every second, and the change in distance between each reading can be calculated to produce a speed (Optech, 2006).

An example of a radar gun used for baseball pitches is shown in Figure 32. This radar gun, made by Stalker, features a 300 foot range and measurements up to 150 mph with 0.1 mph accuracy (Stalker Radar, 2012).

Another tool for measuring speed, common in laboratory settings and among gun shooters, is the optical chronograph. The optical chronograph works by using two optical "curtains," made by a light emitter/receiver pair (for example, IR LED and Photodiode). When the projectile breaks the beam of the first curtain, a timer starts until the projectile breaks the other curtain. Since the curtains are set at a known distance, speed can then be calculated using the recorded time elapsed (Paulter & Larson, 2009).


Figure 32 – Stalker's Sport 2 Baseball radar gun (Stalker Radar, 2012).

An example of an optical chronograph is one made by Oehler, the Model 35, shown in Figure 33. This model uses three curtains instead of two (v-shaped structures in figure), to provide "proof" that the chronograph is producing consistent measurements. Accuracy depends on the speed of the projectile and how far the curtains are from each other, but it is in the range of 0.1% (Oehler Research, Inc., 2012).

Figure 33 – Oehler's Model 35 optical chronograph (Oehler Research, Inc., 2012).

In situations where speed measurements are needed, but none of the other tools are appropriate (for example, the speed of a linkage in a machine), a high speed camera can be used. Simply put, a high speed camera is a camera that takes pictures at a high frame rate. To measure speed using such a camera, a video of the object can be recorded, with a suitable distance scale included in the background (or foreground). The video can then be uploaded to a suitable playback device and watched in slow motion, or even frame by frame. By recording the time between frames, and how far the object traveled using the scale, a speed can be calculated using simple formulas.

### 3.3.14 Vibration

Vibration can result from many things that an engineer might encounter on a daily basis. These vibrations can be either desirable (for example, an electric toothbrush), or undesirable (such as the vibrations arising from a misaligned drive shaft or unbalanced rotating disk). In either case, it is important to characterize the frequency and amplitude of the vibration. Since a discussion of the theory and mathematics of the different types of vibrations and how they are caused is beyond the scope of this thesis, this section instead focuses on how to measure general vibrations.

The main component of any vibration meter on the market is the accelerometer. An accelerometer is a sensor that measures acceleration imparted to it by an external force. There are several different types of accelerometers; however, they all contain some kind of mass suspended inside of the sensor. When this mass experiences a force, it shifts position proportional to the amplitude of the vibration. This position can then be measured using several different techniques.

The most popular type is the piezoelectric accelerometer, which uses a piezoelectric crystal to measure the deflection of the mass (Omega, 2012). Piezoelectric

crystals are ceramic materials that produce electric potential when deformed (and also deform when subjected to electric potential). If a mass is suspended using a piezoelectric ceramic, then the change in position of the mass deforms the crystal, thus producing an electric potential proportional to the acceleration (Fox Electronics, 2008).

Among the traits important in determining the type of accelerometer to use are frequency response and dynamic range. Frequency response refers to the range of frequencies the accelerometer can measure before it starts to attenuate the signal. Dynamic range is the amplitude of the vibration that the accelerometer can measure before it saturates the sensors and starts to distort/clip the signal (Omega, 2012).

An example of a relatively simpler vibration meter is the Balmac Model 200 (Figure 34). This meter has a handheld display with a remote accelerometer that is attached to the object of interest. The dynamic range is 0.001 to 199g (where g is 9.81 $m/s^2$) and the frequency response is 3 to 2000 Hz, with an accuracy of 5% (Balmac, n.d.).

A relatively more complicated meter is the PCE-VT 3000 from PCE Instruments (Figure 35). This meter also has a handheld display with a remote accelerometer; however, the display is capable of displaying a frequency spectrum of all of the vibration modes currently being measured, a helpful tool when trying to analyze different harmonics. This meter's dynamic range is 0.01 to 40g, with a frequency response of 10 to 10,000 Hz. The accuracy is 5% as well (PCE Instruments, n.d.).


Figure 34 – Balmac Model 200 vibration meter (Balmac, n.d.).


Figure 35 – PCE Instruments PCE-VT 3000 (PCE Instruments, n.d.).

### 3.3.15 Friction

Even though friction (or precisely, the friction coefficient $\mu$) cannot be measured directly, a simple method to indirectly measure static and kinetic friction is presented in this section. This method relies on the relationship between the normal force acting on an object and the frictional force resulting from the friction coefficient:

$$F_f = F_n \cdot \mu$$

where $F_f$ = friction force and $F_n$ = normal force.

An example is discussed to explain the method. Suppose a team is reverse engineering a rolling office chair, and the engineer needs to measure the friction coefficient of the wheels on the bottom. As with any statics or dynamics problem, a free body diagram is developed, as shown in Figure 36:

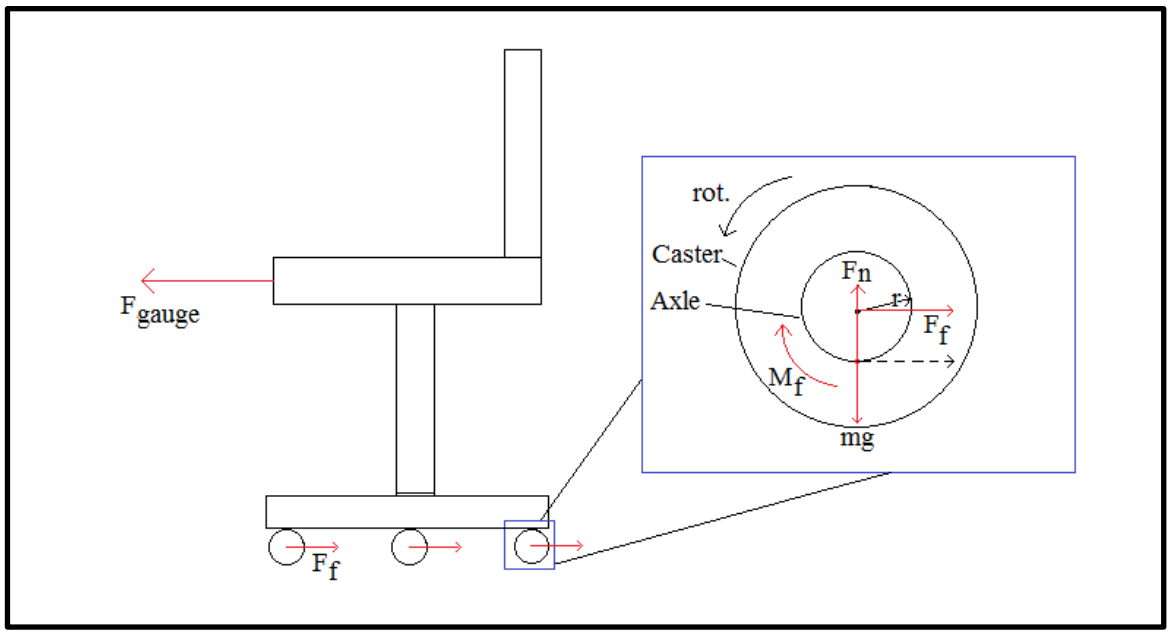


Figure 36 – Free body diagram of rolling chair with close up of caster wheels.

Given the counterclockwise rotation of the caster wheels, the friction force created by the axle rubbing against the wheel creates a friction force, $F_f$. This force is

equal but opposite on both the surfaces of the wheel and axle. The direction of the friction force shown in the diagram (dashed black line) is the force that acts on the axle for the rotation direction shown. To facilitate calculations, $F_f$ can be moved to the center of rotation, as long as the moment created by the force is also taken into account. $F_f$ creates a counterclockwise moment that induces an equal but opposite moment on the wheel surface, shown in the diagram as $M_f$. This moment resists the motion of the wheel.

Since $F_f$ is at the center of rotation acting on the axle, the total force acting upon the chair can be calculated by summing the number of wheels the chair has (assumed three in the diagram). Shown in equation form:

$$F_f = F_n \cdot \mu$$

Or:

$$\mu = \frac{F_f}{F_n}$$

The individual terms can be found by:

$$F_f = \frac{F_{gauge}}{3}$$

$$F_n = mg$$

Thus:

$$\boxed{\mu = \frac{F_{gauge}}{3mg}}$$

To measure $F_{gauge}$, any of the force gauges described in Section 3.3.6 can be used. And to measure weight, any of the scales described in Section 3.3.2 can be used.

The force measured will most likely peak right before the chair starts to roll, at which point it will decrease to a steady value. The peak force is the static friction, while the lower, steady value is the kinetic friction. This method can be used with any object, either rolling or sliding, and can be also adapted to rotating mechanisms.

### 3.3.16 Pressure

The measurement of pressure is an important tool to include in a reverse engineering toolbox. This can be helpful when quantifying the performance of products that output a fluid, or use a fluid in order to work. Examples of products include a pump-up water gun, an air compressor for a bicycle, and an espresso machine making steam for frothing milk.

Pressure measurements can be of three types: absolute, where they are compared to a perfect vacuum; gauge, where they are compared to atmospheric pressure; and differential, the difference between two absolute pressures. The most popular type of pressure measurement encountered daily is gauge pressure, which is used in applications from inflating tires to monitoring fire extinguishers

Pressure can be measured in a variety of ways, some similar to the measurement of force and torque. The three methods discussed in this section include a U-tube manometer, a Bourdon tube, and electronic pressure transducers based on diaphragms.

U-tube monometers are among simplest of pressure measurement devices in terms of operation and construction. A U-tube manometer consists of a vertically oriented, U-shaped tube filled with a liquid inside, usually water (See Figure 37). The two ends of the tube are subjected to two different pressures, and the difference in pressures can be read

by observing the difference in height of the two liquid columns (Morris, 2011, p 405). The height of the liquid is a function of the density of the liquid, the acceleration of gravity, and the pressure applied to the end of the tube:

$$P = \rho g h$$

where $P$ = pressure difference between ends of tube, $g$ = acceleration of gravity, h = difference in height of liquid column, and $\rho$ = density of liquid.

Usually, the U-tube manometer is used with one end open to the atmosphere, which then allows it to measure gauge pressure. The advantages of a U-tube manometer are the ease of construction and use; one can simply create one using a ruler and a length of small diameter vinyl tubing. However, it does have several drawbacks, one being the accuracy of the measurement. Also, depending on the density of the liquid used inside, it must be relatively long to show a range of pressures.

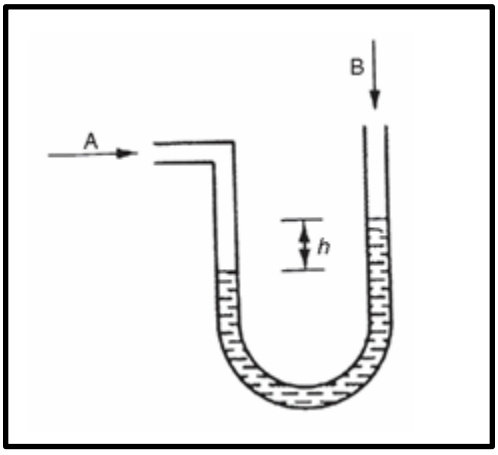


Figure 37 – Illustration of U-tube manometer (Morris, 2011, p. 406).

The second type of pressure measurement device is the Bourdon tube, the most common principle of operation for the analog pressure gauges. The Bourdon tube consists of a flexible metal tube with an oval cross section that is arranged in a circular arc, spiral, or helix. One end of the tube is free to move and sealed, and the other is open

and fixed. When a pressure is applied to the open end, the force applied to the inside of the tube changes the cross section of the tube, thus causing the free end to move from its original position. This change in position is then measured using a plethora of methods, and correlated with a measured pressure (Morris, 2011, pp.405-405).

An example of a Bourdon tube pressure gauge is shown in Figure 38, made by Wika Instruments. This gauge has an accuracy of 1% over the entire measurement range of 0 to 600 psi (Wika Instruments, Inc, 2010).


Figure 38 – Bourdon tube pressure gauge by Wika Instruments (Wika Instruments, Inc, 2010).

The last method discussed in this section is the electronic pressure transducer. This type of pressure transducer consists of a diaphragm mounted inside a housing. When a pressure is applied to either side of the diaphragm, it deflects in accordance to the magnitude of the pressure. The other side of the diaphragm can be open to the atmosphere, to measure gauge pressure, or evacuated and in a vacuum, to measure absolute pressure (Morris, 2011). The deformation of the diaphragm is most commonly

measured with a strain gauge, wired in a Wheatstone bridge configuration (Omega, 2012).

An example of an electronic pressure transducer is a screw-on model by Omega, shown in Figure 39. These transducers are capable of measuring a range from 0-10,000 psi with 0.2% accuracy (Omega, 2012e).

Figure 39 – External screw-on transducer by Omega (Omega, 2012e).

### 3.4 SUMMARY OF METRICS AND TOOLS

Table 7 is a summary of all of the metrics and tools researched in this chapter. This table acts as an aid for readers of this thesis interested in creating their own version of the toolbox with a unique combination of tools. It should be noted that this list is in no way comprehensive; however, it provides a starting point to developing a functional toolbox for reverse engineering.

| **Geometry** | **Torque** |
|---|---|
| Machinist Ruler | Beam Torque Wrench |
| Digital or Analog Calipers | Digital Strain Gauge Torque Meter |
| Micrometers | Dynamometer |
| Tape Measure | **Angular Velocity** |
| 3D Laser Scanner | Contact Tachometer |
| Coordinate Measuring Machine | Non-contact Tachometer |
| Protractor | **Material Properties** |
| **Mass** | Tension/Compression Tester |
| Digital or Analog Table Spring Scale | Impact Tester |
| Digital or Analog Hanging Spring scale | Hardness Tester (Rockwell, Vickers, Etc.) |
| **Time** | Hardness Files |
| Stopwatch | **Flow Rate** |
| **Sound Level** | Hot Wire Anemometer |
| Sound Level meter | Rotating Vane Anemometer |
| **Temperature** | Turbine Flow Meter |
| Glass Thermometer | **Light Intensity** |
| Bi-metallic Thermometer | Light Meter |
| Thermo-chromic materials | **Linear Velocity** |
| Resistance Temperature Detector (RTD) | Radar/LIDAR gun |
| Thermistors | Optical Chronograph |
| Thermocouples | High Speed Camera |
| Infrared Thermometer | **Vibration** |
| Infrared Camera | Vibration Meter (Standalone) |
| **Force** | Accelerometer with DAQ |
| Cantilever Analog Force Gauge | **Pressure** |
| Digital Force Gauge (Strain Gauge Based) | U-tube Monometer |
| **Electrical Properties** | Bourdon Tube Gauge |
| Digital or Analog Multi-meter | Electric Pressure Transducer |
| Watt Meter | |

Table 7 – Summary of the tools for each metric.

# Chapter 4: Developing the Reverse Engineering Toolbox

## 4.1 Introduction

After the development of a list of engineering metrics, and researching the tools necessary to measure those metrics, the next step is to add the tools necessary for the dissection of products. The dissection tools comprise the first part of the toolbox, and the quantification tools comprise the second part. The finalized lists of recommended tools are then presented to enable any engineer or professor desiring a reverse engineering laboratory to properly outfit their facilities.

## 4.2 Tools for Product Dissection

After analysis of the survey, it was determined that the complexity of the tools that students use to dissect their products was not extreme. Since the toolbox is mainly targeted towards academic use by reverse engineering students, there is no need for any specialized tools for special fasteners and such. As a result, all the tools needed are available from popular hardware stores locally and online. A list of the dissection tools is presented in Table 8, as well as example models and prices. All the tools were researched through Sears, Roebuck and Co., a popular retail store that produces quality tools under the brand name Craftsman® (Sears, 2012).

| Tool (Description) | Example | Price |
|---|---|---|
| **Phillips / Flathead / Torx Screwdriver** | | |
| To remove Phillips, flat head, and Torx fasteners (regular sizes) | Craftsman 29 pc. Screwdriver Assortment #41029 | $41.99 |
| To remove Phillips and flat head fasteners (miniature sizes) | Craftsman 5 pc. Screwdriver Set, Precision #4107 | $6.99 |
| **Pliers** | | |
| Various shapes and sizes, including needle nose and slip joint | Craftsman 8 pc. Pliers Set # 45399 | $64.99 |
| **Drill + Accessories** | | |
| To drill out fasteners | Craftsman NEXTEC 12.0V Lithium-Ion Drill/Driver #17586 | $49.99 |
| Drill bits for drill | Craftsman 21 pc. Drill Bit Set, Black Oxide #66020 | $14.99 |
| To remove stripped fasteners | Craftsman 3 pc. Deck-out Screw and Bolt Remover #52151 | $24.99 |
| **Hex Keys** | | |
| hex socket fasteners (Standard) | Craftsman 13 pc. Standard Ball End Hex Key Set #46754 | $19.99 |
| hex socket fasteners (Metric) | Craftsman 13pc Hex Key Set, Ball End Metric #46755 | $19.99 |
| **Combination Box / Open end Wrench Set** | | |
| Remove hex bolts and nuts, pipe fittings, etc. (Standard) | Craftsman 12 pc. Standard 6 pt. Combination Wrench Set #47236 | $29.99 |
| Remove hex bolts and nuts, pipe fittings, etc. (Metric) | Craftsman 12 pc. Metric 6 pt. Combination Wrench Set #47237 | $29.99 |
| **Hack Saw** | | |
| To cut enclosures, press fitted parts, etc. | Craftsman Adjustable/Tubular Frame Hacksaw #E0101673 | $8.99 |
| **Rotary Tool** | | |
| For general cutting of parts | Craftsman 4.8-volt Cordless Rotary Tool #61078 | 34.99 |
| **Utility Knife** | | |
| Cut adhesives, thin plastic tabs, blister packs, etc | Craftsman Utility Knife #94832 | $5.00 |
| **Soldering Iron** | | |
| Remove and re-solder electrical joints | Craftsman Solder Iron, 30 watt #54041 | $7.50 |
| **Wire Strippers/Cutters** | | |
| Cut and strip wires for attaching measurement equipment | Craftsman Electricians Tool #82563 | $15.99 |
| | **Total:** | $376.37 |

Table 8 – List of dissection tools, the first part of the toolbox.

## 4.3 TOOLS FOR MEASUREMENT AND QUANTIFICATION

Chapter 3 explored all of the state of the art tools available on the market today. These tools are industrial grade and used by professionals. However, since one of the goals of this research was to create a low cost toolbox for academia, less expensive versions of those tools are considered in the final list. Also, several choices were presented for each metric on the list, and for the final toolbox, only one alternative is chosen in the case where multiple devices perform the same function. It is expected that some compromises will be made; however, the tools selected are still accurate and reliable enough for good engineering practice.

### 4.3.1 Consumer off the Shelf Tools

Most of the metrics presented in Chapter 3 can be measured using relatively inexpensive, off-the-shelf tools found online and in hardware stores. An engineer can quickly furnish these tools to create the second part of the toolbox. Table 8 lists the available off-the-shelf solutions, as well as an example model and price. The prices shown are representative values from popular vendors, and do not necessarily represent the Manufacturer's Suggested Retail Price (MSRP).

The tools presented in Table 9 are compared to an existing toolbox uncovered during the research phase, marketed by Vernier Software and Technology, LLC (Vernier Software & Technology, 2012). This system is essentially a handheld data logging and processing module that accepts input from a plethora of available sensors for sale. Vernier's toolbox is targeted towards academia as well, and serves as an excellent benchmark for comparison of the final toolbox developed in this section.

| Metric (tool) | Example Model/Manufacturer | Specifications | Price |
|---|---|---|---|
| **Geometry** | | | |
| Machinist Ruler | Pro-Value Satin-Chrome Steel Precision Rule # 2042A73 (McMaster Carr, n.d.,b) | 12 in, +/- 0.005 in | $17.00 |
| Protractor | Staedtler Protractor 6" 360 Degrees Model 56880-15BK (Amazon.com, Inc., 2012b) | Full 360 degrees, 1 degree res. | $3.50 |
| Digital Caliper | Neiko Stanless Steel 6-Inch Digital Caliper Model 01407A (Amazon.com, Inc., 2012c) | 0-6 in, +/- 0.001 in | $16.00 |
| Tape Measure | Komelon Self Lock Speed Mark Model SL2925 (Komelon USA Corporation, 2011) | 25 ft | $11.00 |
| **Mass** | | | |
| Digital Table Scale | Ohaus CS Portable Balances Model CS2000 (Ohaus, 2012) | 2000 g, +/- 1 g | $85.00 |
| Digital Hanging Scale (Large range) | American Weigh Industrial Hanging Scale Model TL-330 (American Weigh, 2011a) | 0-150 kg, 0.1 kg res. | $60.00 |
| Digital Hanging Scale (Small range) | American Weigh Digital Hanging Scale Model SR-1KG (American Weigh, 2011b) | 0-1000 g, 1 g res. | $12.00 |
| **Force** | | | |
| Digital Hanging Scale (Large range) | American Weigh Industrial Hanging Scale Model TL-330 (American Weigh, 2011a) | 0-150 kg, 0.1 kg res. | ------- |
| Digital Hanging Scale (Small range) | American Weigh Digital Hanging Scale Model SR-1KG (American Weigh, 2011b) | 0-1000 g, 1 g res. | ------- |
| **Torque** | | | |
| Digital Hanging Scale (Large range) | American Weigh Industrial Hanging Scale Model TL-330 (American Weigh, 2011a) | 0-150 kg, 0.1 kg res. | ------- |
| Digital Hanging Scale (Small range) | American Weigh Digital Hanging Scale Model SR-1KG (American Weigh, 2011b) | 0-1000 g, 1 g res. | ------- |

Table 9 – List of metric quantification tools, the second part of the toolbox.

| | | | |
|---|---|---|---|
| **Pressure** | | | |
| Monometer | Dwyer Manometer, U-Tube, Model 1221-12-W/M (Dwyer Instruments, Inc., 2012) | 6" scale on both sides, 0.1" res. | $28.00 |
| Bourdon Tube Gauge | McMaster Carr Item # 38545K162 (McMaster-Carr, n.d.) | -100 - 100 kPa, +/- 1% | $22.20 |
| **Time** | | | |
| Digital Stopwatch | Extech Stopwatch/Clock Model 365510 (Extech, 2012d) | 0.001s resolution, +/- 3s per day | $20.00 |
| **Sound Level** | | | |
| Sound Pressure Meter | Pyle Digital Handheld Sound Level Meter Model PSPL25 (Pyle Audio, 2012) | 0-100 dB, +/- 1.5dB | $47.50 |
| **Temperature** | | | |
| Thermocouple (w/ Multimeter) | Extech Multimeter (w/ K type thermocouple) Model EX330 (Extech, 2012c) | -20 to 750ºC | ------- |
| **Electrical Properties** | | | |
| Watt meter | P3 International Kill A Watt Model P4400 (P3 International, 2012) | 0.2% accuracy | $19.99 |
| Multimeter | Extech Multimeter (w/ K type thermocouple) Model EX330 (Extech, 2012c) | 10A max, 600V max, +/- 0.5% | $59.99 |
| **Angular Velocity** | | | |
| Optical Tachometer | Neiko Laser Photo Non-Contact Tachometer Model 20713A (Amazon.com, Inc., 2012a) | 2.5-99,999 RPM, +/-0.05% | $25.00 |

Table 9 – List of metric quantification tools, the second part of the toolbox (cont).

| | | | |
|---|---|---|---|
| **Flow Rate** | | | |
| Anemometer | La Crosse Handheld Anemometer Model EA-3010U (La Crosse Technology, n.d.) | 0.2-30 m/s | $32.00 |
| Turbine Flow meter (w/ DAQ) | Koolance Coolant Flow Meter Model INS-FM17N (Koolance, 2012) | 1-15 Lpm | $19.99 |
| **Light Intensity** | | | |
| Light Meter | Mastech Digital Illuminance/Light Meter Model LX1330B Amazon.com, Inc., 2012b) | 0-200,000 lux, +/- 5% | $30.00 |
| **Linear Velocity** | | | |
| Digital Camera (w/Computer processing) | GoPro HERO2 (Woodman Labs, Inc., 2011) | 848 x 480 pixels, 120 frames/s | $299.99 |
| Optical Chronograph | Shooting Chrony F1 (Shooting Chrony, 2011) | 30 to 7000 ft/s | $94.00 |
| Accelerometer (w/ DAQ) | Analog Devices Model ADXL335 (Analog Devices, Inc., 2010) | +/- 3g range, 0-1600 Hz response | $10.00 |
| **Material Properties** | | | |
| Hardness Files | Flexbar Hardness Testing File Set (Flexbar Machine Corporation, 2012) | 40 - 65 HRc hardness scale | $85.00 |
| **Vibration** | | | |
| Accelerometer (w/ DAQ) | Analog Devices Model ADXL335 (Analog Devices, Inc., 2010) | +/- 3g range, 0-1600 Hz response | ------- |
| **DAQ card** | | | |
| For sensor input | NI MyDAQ (National Instruments Corporation, 2012) | 2 analog and 8 digital I/O ports | $175.00 |
| | | **Total:** | $1173.16 |

Table 9 – List of metric quantification tools, the second part of the toolbox (cont).

The tools presented above give an engineer the ability to measure the majority of the metrics found in Chapter 2, Table 3. They are not necessarily the top of the line tools; however, they are a good balance between cost and capability.

Some of the tools are used for dual purposes; this is done to keep costs down and also to improve portability by reducing the tool count. The first instance is measuring force/torque. Since the measurement of weight is just a specialized form of measuring force, a digital hanging scale can be used for both weight and force measurements. The procedure is as follows:

For Tension: Attach one end of the scale to the object to which to apply the force. Apply the tensile force on the other end of the scale, pulling *parallel* to the object. Read the force indicated.

For compression: Attach one end of the scale to the object to which to apply the force. Apply a tensile force in the direction of the compression force desired; in other words, pull in the *opposite* direction of the force in the tensile case to apply a compressive force on the object.

For torque: Attach one end of the scale to the object to which to apply the torque. Apply tensile force on the other end of the scale, pulling *perpendicular* to the moment arm. Read the force indicated then multiply by the length of the moment arm. This procedure only works for static torque, and an alternative for rotating motors is discussed in the Section 4.3.2.

Another instance where the same tool is used for multiple metrics is the accelerometer. The obvious use is for vibration, where the amplitude and frequency of the acceleration is used for quantifying vibration. However, by mathematically integrating the acceleration data, the accelerometer can also be used to measure the velocity of an object. This can come in handy when measuring the velocity of a fast

moving, reciprocating part; for example, inside a jigsaw. The integration can be performed by computer data gathering software in conjunction with the Data Acquisition (DAQ) card.

Most of the tools in the toolbox are standalone, requiring only a portable power source to operate. This is advantageous in that it allows multiple metrics to be gathered at the same time, without the need to depend on one data acquisition module. However, as mentioned above, some of the tools do indeed depend on a separate module, a data acquisition card. The example shown in Table 9 is the myDAQ, made by National Instruments. This DAQ system interfaces with a computer running National Instrument's LabVIEW® software to gather analog and digital data from a plethora of sensors. Using LabVIEW, the user can build a Virtual Instrument (VI) to manipulate the data and display it in a user friendly way. From the toolbox, the sensors requiring the DAQ card and/or LabVIEW are the accelerometer, turbine flow meter, and webcam (used in conjunction with a motion capture VI).

Now that the toolbox has been established, it is helpful to compare it to the closest competitor on the market, the toolbox available from Vernier. It was found, however, that Vernier did not offer tools to measure all of the metrics from Table 3, and thus the comparison will only include the metrics that are available. Table 10 lists the metrics from Vernier, and Table 11 shows a comparison between the two toolboxes.

| Metric (tool) | Specifications | Price |
|---|---|---|
| **Mass** | | |
| Digital Scale (made by Ohaus®) | 400 g, +/- 0.01g | $429.00 |
| **Force** | | |
| Digital gauge | 0-50 N, +/- 1% of reading | $109.00 |
| **Sound Level** | | |
| Sound Pressure Meter | 35-130 dB, +/- 1.5 dB | $165.00 |
| **Temperature** | | |
| Thermocouple | 0-1400 ºC | $59.00 |
| **Electrical Properties** | | |
| Current Probe | 10 A max | $79.00 |
| Voltage Probe | 30 V max | $39.00 |
| Watt meter (made by Watts Up®) | +/- 1.5% | $145.00 |
| **Flow Rate** | | |
| Anemometer | 0.5-30 m/s | $89.00 |
| Turbine Flow meter | 0-4 m/s, +/- 1% of reading | $129.00 |
| **Light Intensity** | | |
| Light Meter | 0-150000 lux | $55.00 |
| **Vibration** | | |
| Accelerometer | 0-25g, +/- 0.25g | $92.00 |
| **DAQ card** | | |
| LabQuest 2 | ---- | $329.00 |
| | | $1,719.00 |

Table 10 – List of metric quantification tools by Vernier (Vernier Software & Technology, 2012).

| Developed Toolbox | | | Vernier's Toolbox | | |
|---|---|---|---|---|---|
| **Metric (tool)** | **Specifications** | **Price** | **Metric (tool)** | **Specifications** | **Price** |
| **Mass** | | | **Mass** | | |
| Digital Table Scale | 2000 g, +/- 1 g | $85.00 | Digital Scale | 400 g, +/- 0.01g | $429.00 |
| **Force** | | | **Force** | | |
| Digital Hanging Scale (Large range) | 0 - 1471 N, 1 N res. | $60.00 | Digital gauge | 0-50 N, +/- 1% of reading | $109.00 |
| Digital Hanging Scale (Small range) | 0 - 9.81 N, 0.01 N res. | $12.00 | | | |
| **Sound Level** | | | **Sound Level** | | |
| Sound Pressure Meter | 0-100 dB, +/- 1.5dB | $47.50 | Sound Pressure Meter | 35-130 dB, +/- 1.5 dB | $165.00 |
| **Temperature** | | | **Temperature** | | |
| Thermocouple (comes with Multimeter) | -20 to 750ºC | ------- | Thermocouple | 0-1400 ºC | $59.00 |
| **Electrical Properties** | | | **Electrical Properties** | | |
| Watt meter | 0.2% accuracy | $19.99 | Current Probe | 10 A max | $79.00 |
| Multimeter | 10A max, 600V max, +/- 0.5% | $59.99 | Voltage Probe | 30 V max | $39.00 |
| | | | Watt meter | +/- 1.5% | $145.00 |
| **Flow Rate** | | | **Flow Rate** | | |
| Anemometer | 0.2-30 m/s | $32.00 | Anemometer | 0.5-30 m/s | $89.00 |
| Turbine Flow meter (w/ DAQ) | 1-15 Lpm | $19.99 | Turbine Flow meter | 0-4 m/s, +/- 1% of reading | $129.00 |
| **Light Intensity** | | | **Light Intensity** | | |
| Light Meter | 0-200,000 lux, +/- 5% | $30.00 | Light Meter | 0-150,000 lux | $55.00 |
| **Vibration** | | | **Vibration** | | |
| Accelerometer (w/ DAQ) | +/- 3g range, 0-1600 Hz response | $10.00 | Accelerometer | 0-25g, +/- 0.25g | $92.00 |
| **DAQ card** | | | **DAQ card** | | |
| For sensor input | 2 analog and 8 digital I/O ports | $175.00 | LabQuest 2 | ---- | $329.00 |
| | **Total:** | $346.97 | | **Total:** | $1,719.00 |

Table 11 – Comparison of developed toolbox and Vernier's toolbox.

The tools in general are comparable in performance and specifications. The only big difference is the accelerometer: the one chosen for the developed toolbox has a smaller range. However, the biggest advantage of the developed toolbox is the cost, with the Vernier toolbox costing over $1300 more. This fact, along with the missing metrics from the Vernier toolbox, places the developed toolbox in a respectable position in terms of fulfilling its development goals. Further analysis of these goals is presented in Chapter 6.

### 4.3.2 Development of the TorkBlock Portable Dynamometer

The goal for developing a portable dynamometer is to provide a method to characterize fractional horsepower motors. Since this toolbox is targeted towards the dissection of consumer products, many small DC and AC motors can be encountered in, for example, power tools, kitchen appliances, and garden tools. Several goals were set for the development of the dynamometer, including: 1) Accuracy, 2) Ease of Use, 3) Low Cost, 4) Portability, and 5) Robustness.

#### *4.3.2.1 Concept Generation Phase*

To choose a principle for developing the dynamometer, two major types were considered: inertial and absorbing. Inertial dynamometers measure power output by attaching a fixed, known mass to the motor under test. The motor is then used to accelerate the load to full speed, and the acceleration is measured throughout the ramp-up process (Dortch, 2012). Torque can then be calculated from acceleration using equations of motion as follows:

$$\tau = I * \alpha$$

where $I$ = mass moment of inertia and $\alpha$ = angular acceleration. The torque can then be plotted against angular speed to create a torque-speed curve.

Absorbing dynamometers, as the name implies, employ methods to apply a torque to the motor under test, "absorbing" power and enabling the user to observe the behavior of the motor under a specific load (see example shown in Figure 40). If the load on the motor is gradually increased until the motor stalls, a torque-speed curve can then be created. Many methods can be used to apply the load onto the motor; some examples include a friction brake, water brake, and an electromagnetic brake (Dortch, 2012).

The benefit of an inertial dynamometer is its simplicity, since the only major system is the mass attached to the motor. The disadvantage of the inertial dynamometer is the lack of control over the loading condition; the user is unable to hold a specific angular speed or test at a fixed load. On the contrary, an absorbing dynamometer is more complex in nature, the degree of complexity depending on the method used to provide the braking force. However, it offers the advantage of fixed load testing, which allows the flexibility of tuning an engine to operate at a specified speed, as well as repeated testing in a specific range (Dortch, 2012).

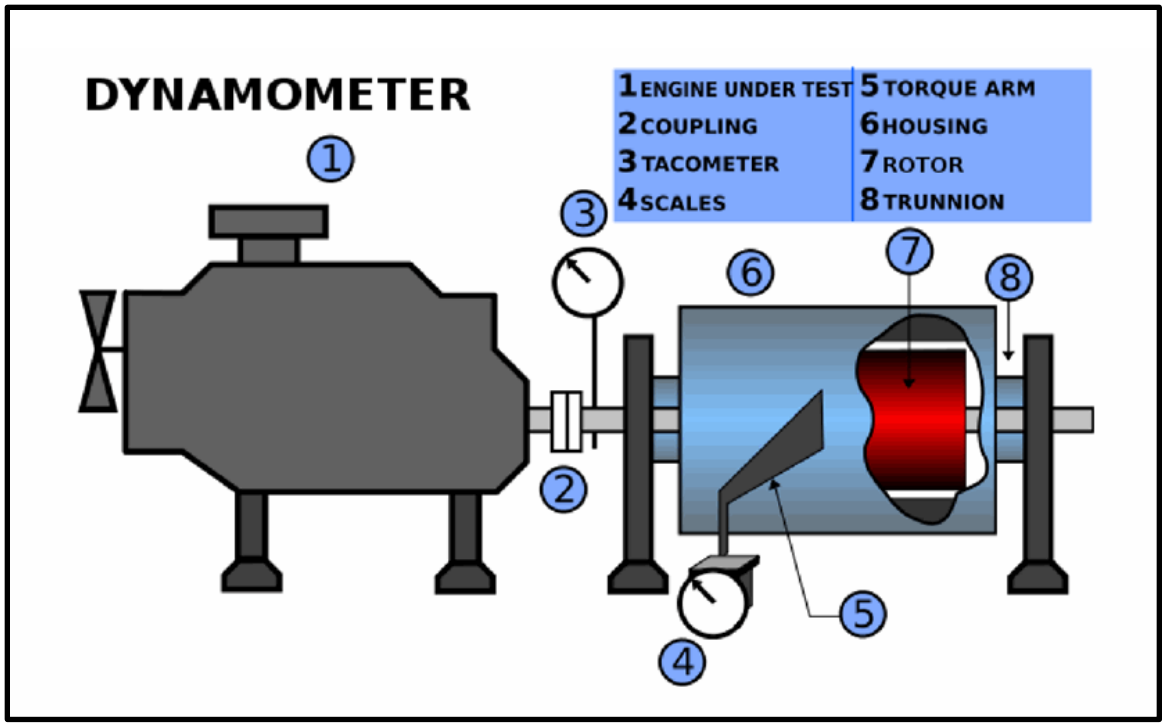


Figure 40 – Example of absorption dynamometer layout (Dortch, 2012).

Before concept generation was performed, it was decided that a dynamometer based on the inertial type would be pursued. This decision was based on some of the

abovementioned goals for the dynamometer, which include low cost and robustness. Even though an absorption dynamometer offers more flexibility, and has the potential of being more accurate, the complexity of the design required to supply those features increases both cost and sources of failure/errors.

Concept generation began with a brainstorming/mind mapping phase in order to develop some concepts for the dynamometer. The dynamometer was broken down into subfunctions, which allowed a greater breadth of concepts than if the system was considered as a whole. The mind map is shown in Figure 41.

After the mind map was created, concept sketches were created to detail system and subsystem level components, using different combinations of the concepts on the mind map. After the concepts were presented and discussed with faculty, one concept was chosen using several criteria, including projected cost, ease of manufacturing, robustness, and susceptibility to outside errors. The finalized concept was then recreated in SolidWorks® in order to design all of the details and tolerances, as well as position and package the components precisely.

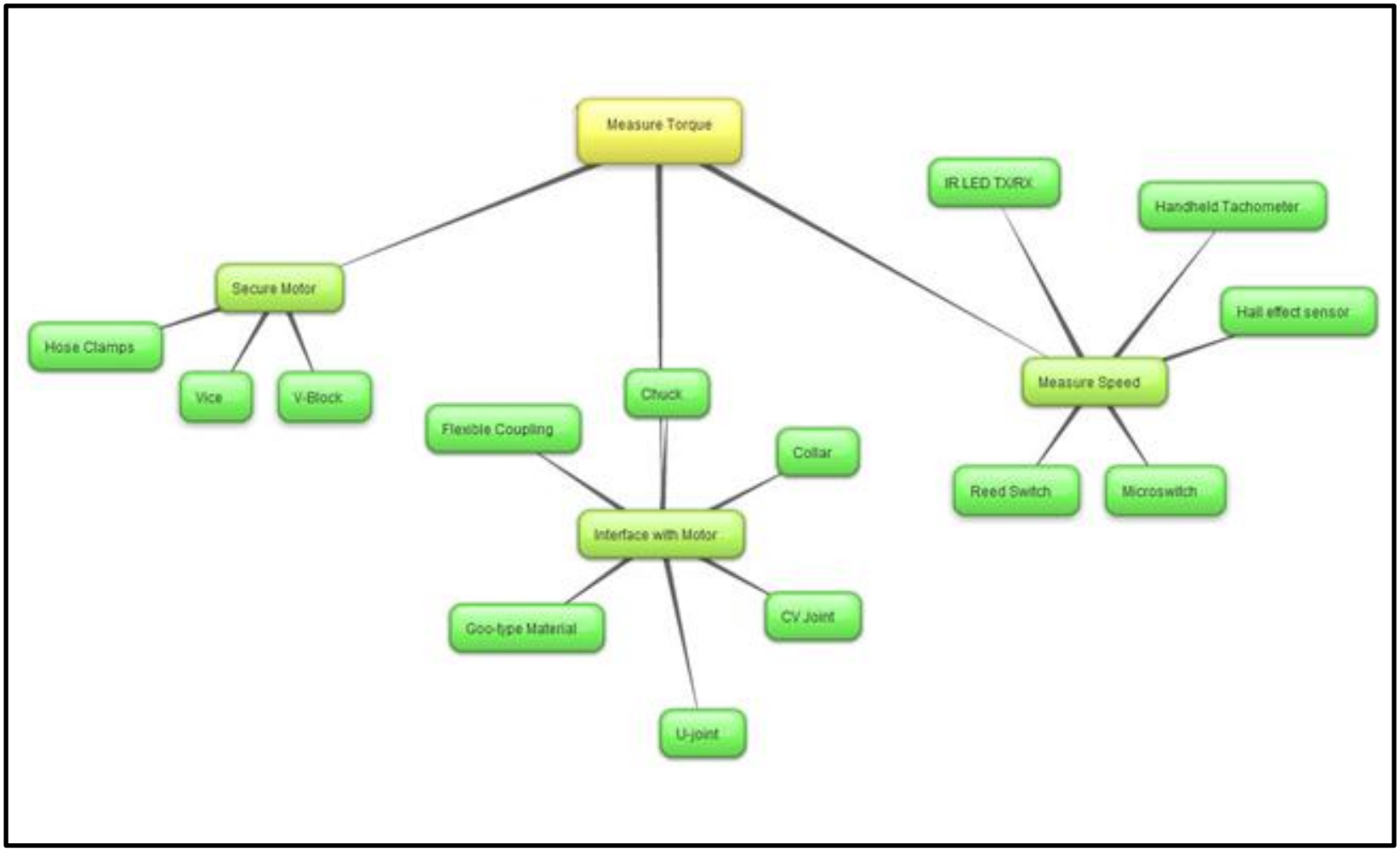


Figure 41 – Mind Map for dynamometer.

#### *4.3.2.2 Finalized Dynamometer Design*

The final design can be seen in Figure 42, and an exploded view with part numbers can be seen in Figure 43. First, the motor is secured to a mount and attached to the apparatus using the miniature chuck on the front (1). After the motor is attached, it is used to spin the disk (12) up to full speed through the drive shaft (6). The instantaneous speed of the disk is measured using an infrared tachometer (14) with an index wheel (13) that creates a pulse every revolution. The instantaneous speed is used to calculate the acceleration of the motor, and thus, the torque. The speed and torque data points are then logged, along with the instantaneous power produced by the motor. The measurement and logging are performed by an electronic control interface. The controller interfaces with the sensors in the dynamometer using a standard Ethernet port (9).

The device is housed in an aluminum structure consisting of five plates that surround the disk: a front plate (4), a rear plate (15), a bottom plate (7), and two side plates (5 and 8). To properly ensure that the drive shaft is aligned and centered between the two bearings (3), internally threaded spacers (10) are used that pass through the side plates. The drive shaft is secured by shaft collars (16) to prevent lateral movement.

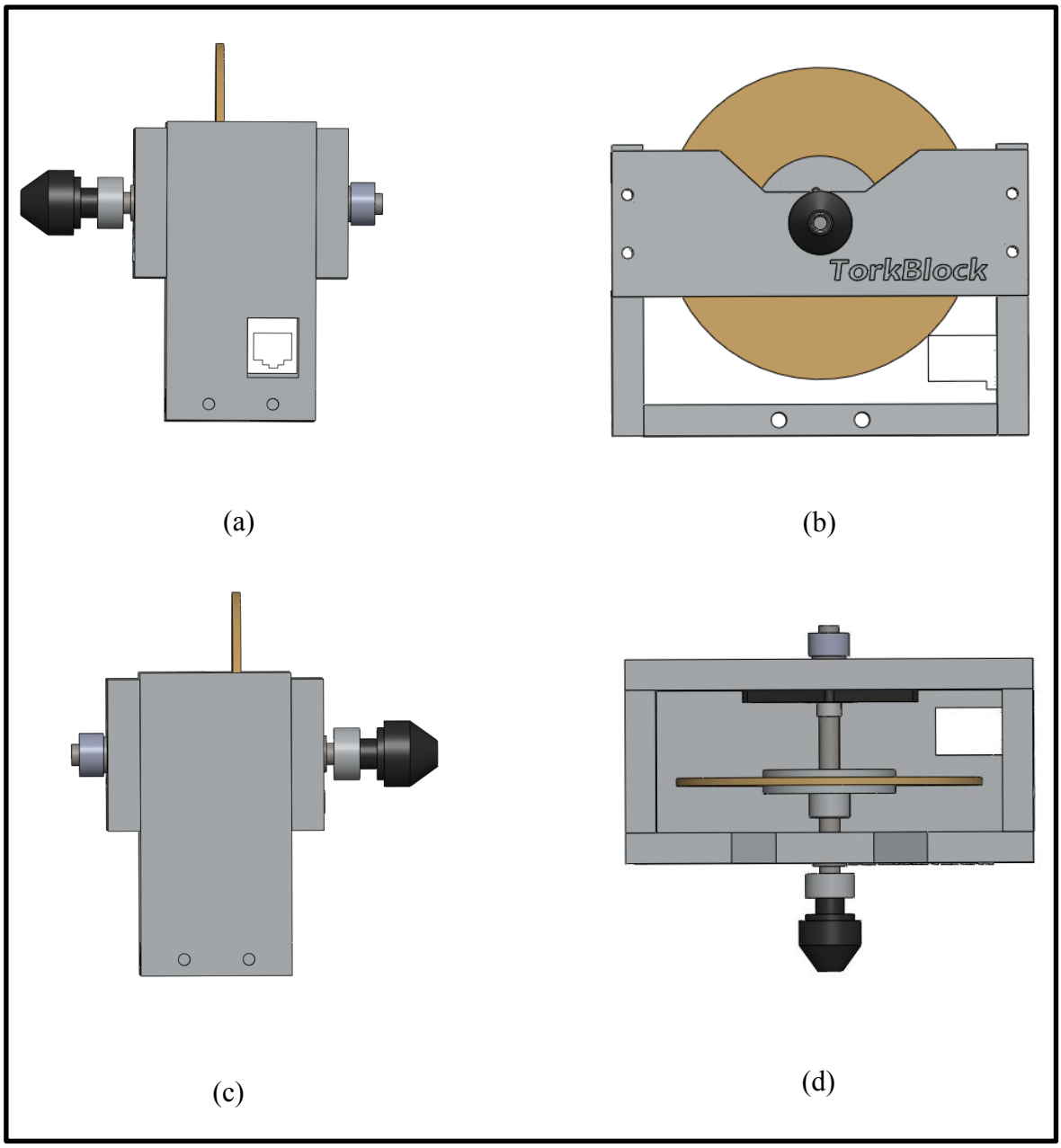


Figure 42 – Final dynamometer design: (a) right view (b) front view (c) left view (d) top view. Created using SolidWorks®.

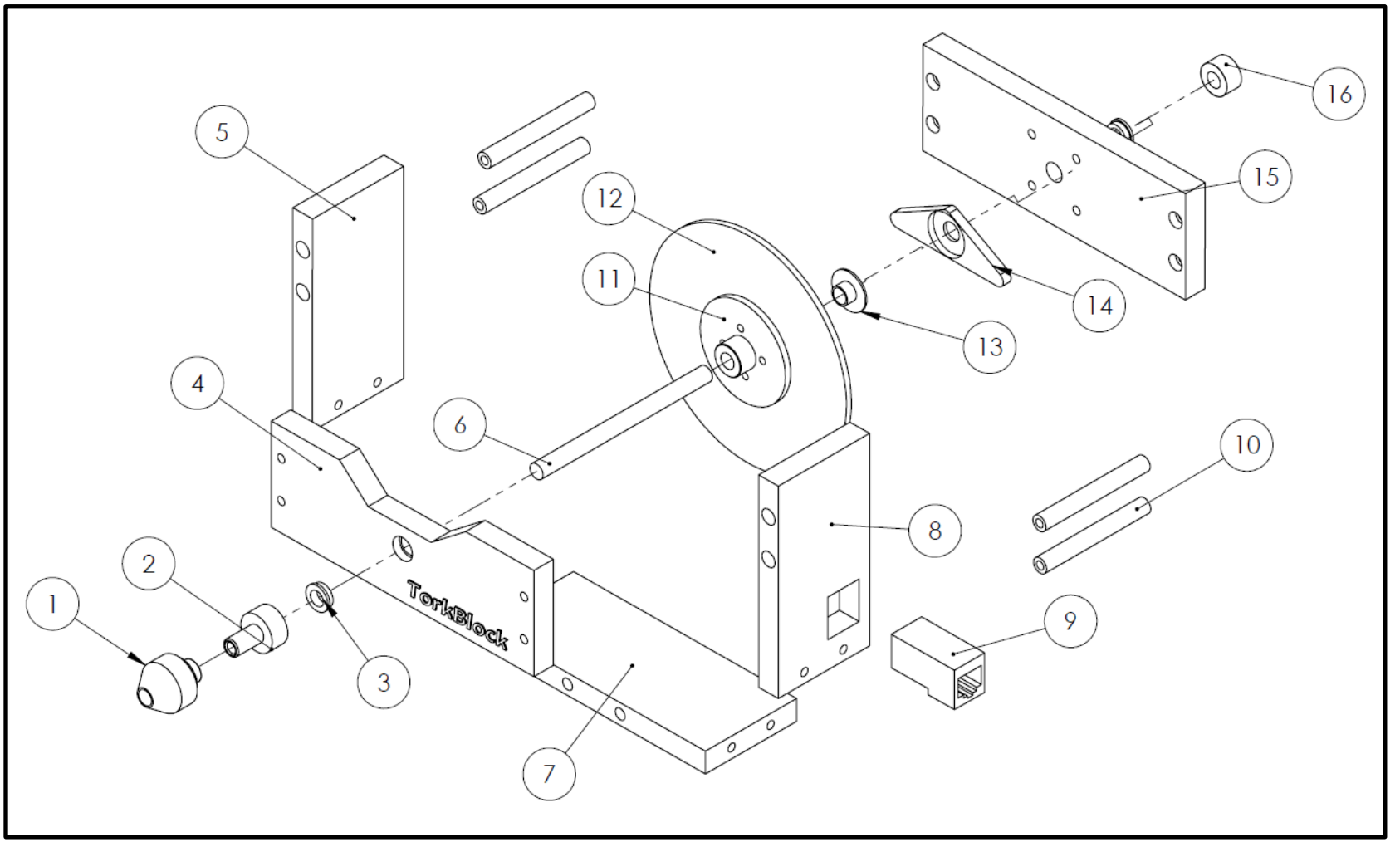


Figure 43 – Exploded view of final dynamometer design with part numbers.

The dynamometer's specifications are as follows:

- Dimensions: 5" (L) x 4.5" (W) x 4.25" (H)
- Maximum Design Motor Speed: 10,000 RPM
- Theoretical Torque Range (based on 4 Hz sampling rate): 0 – 837 mN-m

#### *4.3.2.3 Engineering Calculations*

As with all products engineered for use by others, a responsible engineer must use his or her knowledge and skills in order to ensure that the product will not fail in a matter that is catastrophic and harmful to the user under normal use. Since the dynamometer is designed for a maximum motor speed of up to 10,000 RPM, there is a risk of failure due to stresses and resonance at high angular speeds.

1) Resonance: To calculate the resonant speed of the rotating assembly, Dunkerley's method was used, as outlined in Shigley's Mechanical Engineering Design book (Budynas & Nisbett, 2008, p. 372). The calculations begin by representing the driveshaft as a simply supported beam with two loads on it; the mass of the shaft at the center (m), and the mass of the disk offset from the center (F) (Figure 44):

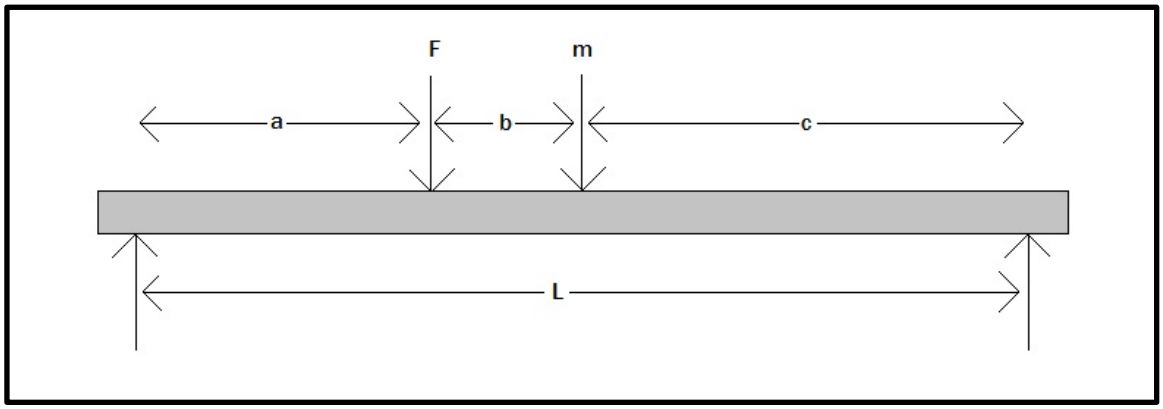


Figure 44 – Driveshaft with loads and reactions.

Afterwards, the influence coefficient δ is calculated for every load on the beam:

$$\delta_{ij} = \frac{b_j x_i}{6EIl}\left(l^2 - b_j^2 - x_j^2\right) \qquad x_i \leq a_i$$

where $b$ = distance from right end to load,

$x$ = distance from left end to load,

$l$ = length of shaft,

$E$ = young's modulus, and

$I$ = moment of inertia.

After the influence coefficients are found, the critical speed due to each load is then calculated:

$$\omega_i = \frac{g}{w_i \delta_{ii}}$$

where $g$ = acceleration of gravity,

$w$ = load at position $i$, and

$\delta$ = influence coefficient.

Finally, the resulting critical speed is calculated:

$$\frac{1}{\omega_c} = \sum \frac{1}{\omega_{ii}^2}$$

where $\omega_{ii}$ = speed due to load *i*.

For the drive shaft used in the dynamometer, the following properties are extracted:

*m* = 0.0273 kg (stainless steel)

*l* = 0.056 m

*F* = 0.722 N (extracted from SolidWorks mass data on aluminum disk)

*a* = 0.019 m

*b* = 0.009 m

*c* = 0.028 m

*d* = 0.00635 m

*E* = 200 GPa (for stainless steel)

*I* = $7.98 \times 10^{-11}$ $m^4$ (for round shaft)

Calculations were then performed following the method outlined above:

$$\delta_{11} = 2.29x10^{-7}\frac{m}{N}$$

$$\delta_{22} = 1.84x10^{-7}\frac{m}{N}$$

$$\omega_{11} = 12666\frac{rad}{s}$$

$$\omega_{22} = 8593\frac{rad}{s}$$

$$\frac{1}{\omega_c^2} = 1.977x10^{-8}$$

$$\omega_c = 7110\frac{rad}{s} = \boxed{67{,}895\ RPM}$$

Since the design speed is 30,000 RPM, the dynamometer has a safety factor of 6.78 against resonance.

2) Rotational stresses on the disk: To calculate the stresses that the disk will experience during high speed rotation, equations outlined in Shigley were used (Budynas & Nisbett, 2008, p. 110). There are two equations; one for tangential stress, the other for radial stress:

$$\sigma_t = \rho\omega^2\left(\frac{3+v}{8}\right)\left(r_i^2 + r_o^2 + \frac{r_i^2 r_o^2}{r^2} - \frac{1+3v}{3+v}r^2\right)$$

$$\sigma_r = \rho\omega^2\left(\frac{3+v}{8}\right)\left(r_i^2 + r_o^2 - \frac{r_i^2 r_o^2}{r^2} - r^2\right)$$

where $\rho$ = density,

$\omega$ = angular speed,

$\nu$ = Piosson's ratio,

$r_i$ = inner radius,

$r_o$ = outer radius, and

$r$ = radius at point of interest.

Applying the metrics from the aluminum disk used in the final design:

$\rho$ = 2700 kg/m$^3$

$\omega$ = 10,000 RPM = 1047.9 rad/s

$\nu$ = 0.33

$r_i = 0.00317$ m

$r_o = 0.0508$ m

$S_{ut} = 300$ MPa

$S_y = 276$ MPa

Microsoft Excel was used to compute the stresses on the various radii on the disk in 0.001 m increments. Figure 45 presents the results and shows a safety factor of 43 against yielding and 47 against fracture.

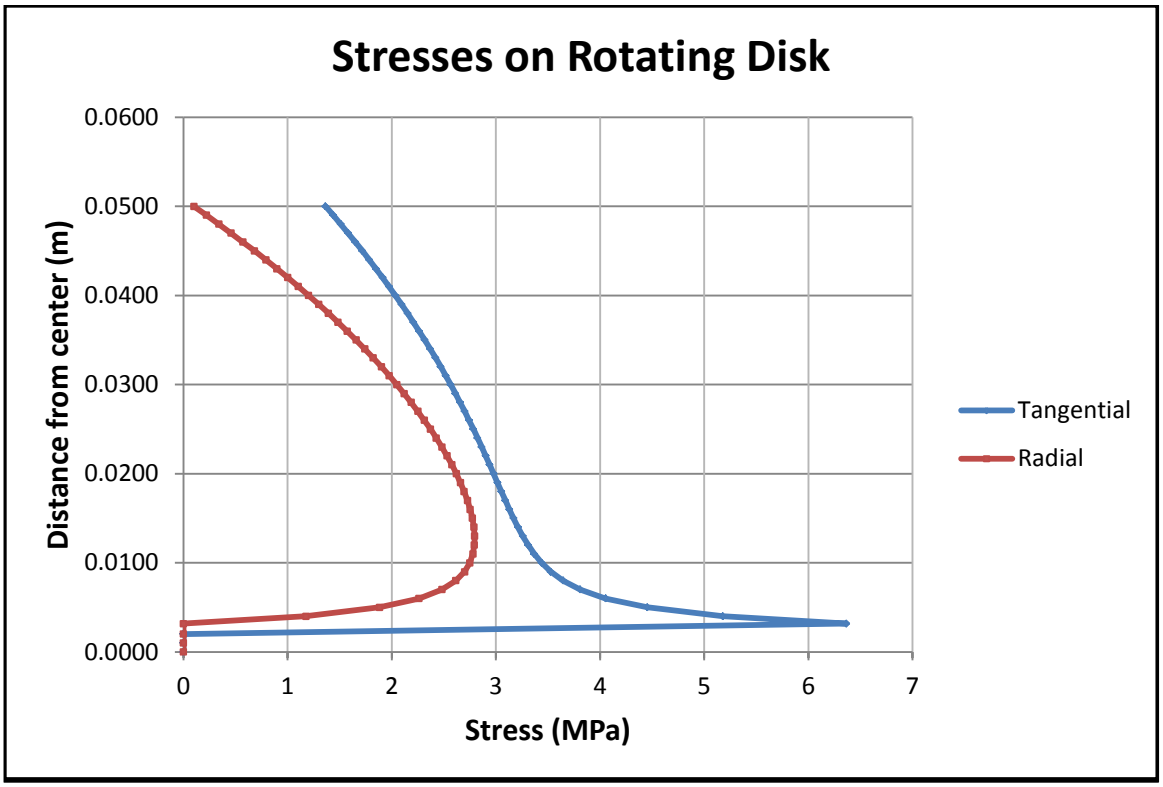


Figure 45 – Tangential and Radial stresses on the rotating disk.

3) Driveshaft fatigue failure: since the drive shaft has a constant downwards facing load applied to it, it will experience cyclic loading throughout its lifetime. And as with any type of cyclic loading, there is a chance of failure from fatigue of the material. To calculate the safety factor against such failure, the endurance limit was found using the method outlined in Shigley (Budynas & Nisbett, 2008, p. 278). Afterwards, the maximum stresses on the shaft were found, which allowed the use of the Distortion Energy Goodman and Soderberg criteria to calculate the safety factors (Budynas & Nisbett, 2008, p. 357).

The endurance limit can be calculated using the following equations:

$$S_e = k_a k_b k_c k_d k_e k_f S'_e$$

$$S'_e = 0.5 S_{ut} \qquad S_{ut} \leq 1400\ MPa$$

All of the *k* terms account for different factors that affect the endurance limit, as shown below. All tables and page numbers refer to *Shigley's Mechanical Engineering Design* (Budynas & Nisbett, 2008):

$k_a$= Surface finish modifier; table 6-2, pg. 337

$k_b$= Size modifier, eq. 6-20, pg. 337

$k_c$= Loading modifier, eq. 6-26, pg. 337

$k_d$= Temperature modifier, eq. 6-27, pg. 337

$k_e$= Reliability Modifier, table 6-5, pg. 337

$k_f$= Miscellaneous Modifier

The equations are then applied to the drive shaft:

Material: AISI 12L14 steel

$S_{ut}$ = 540 MPa

$S_y$ = 415 MPa

$$S_e' = 0.5(540) = 270\ MPa$$

$$k_a = a\ {S_{ut}}^b = 1.58(540)^{-0.085} = 0.926$$

$$k_b = 0.879d^{-0.107} = 0.879(0.25\ inch)^{-0.107} = 1.02$$

$k_c = 1$ for bending

$k_d = 1$ for room temperature

$k_e = 0.897$ for 90% reliability

$k_f = 1$ no misc. factors

The endurance limit is then calculated using all of the factors found

$$S_e = (270)(0.926)(1.02)(1)(1)(0.897)(1) = \boxed{228.8\ MPa}$$

After the endurance limit is found, it is necessary to find the stresses on the drive shaft in order to calculate the safety factor against fatigue failure. To calculate the stresses, the driveshaft is treated as a simply supported beam with two loads: the mass of the shaft (as a distributed load), and the mass of the disk, as shown in Figure 46.

First, shear and moment diagrams are created to calculate the maximum shear and moment forces on the driveshaft. For the properties of the driveshaft presented in the resonance calculations, the shear and moment diagrams are presented in Figure 47.

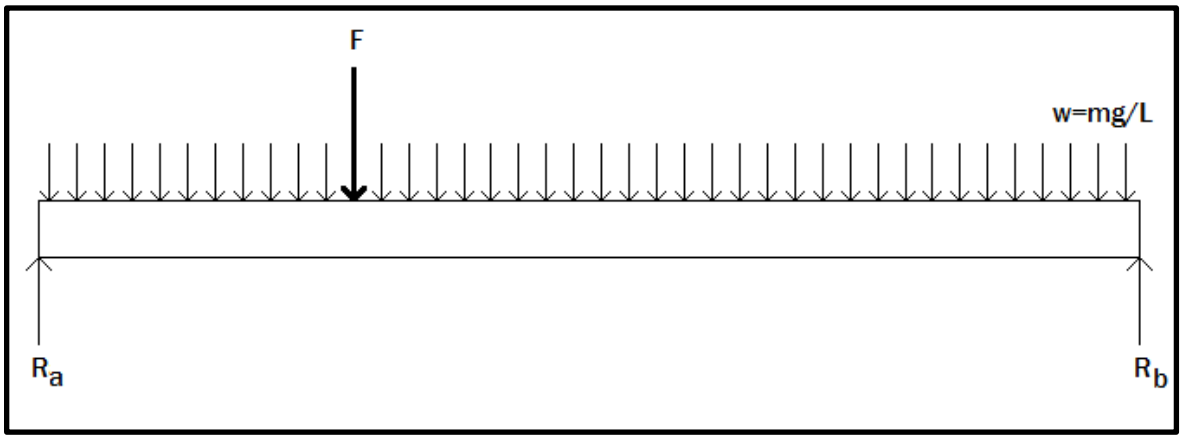


Figure 46 – Driveshaft as a simply supported beam.

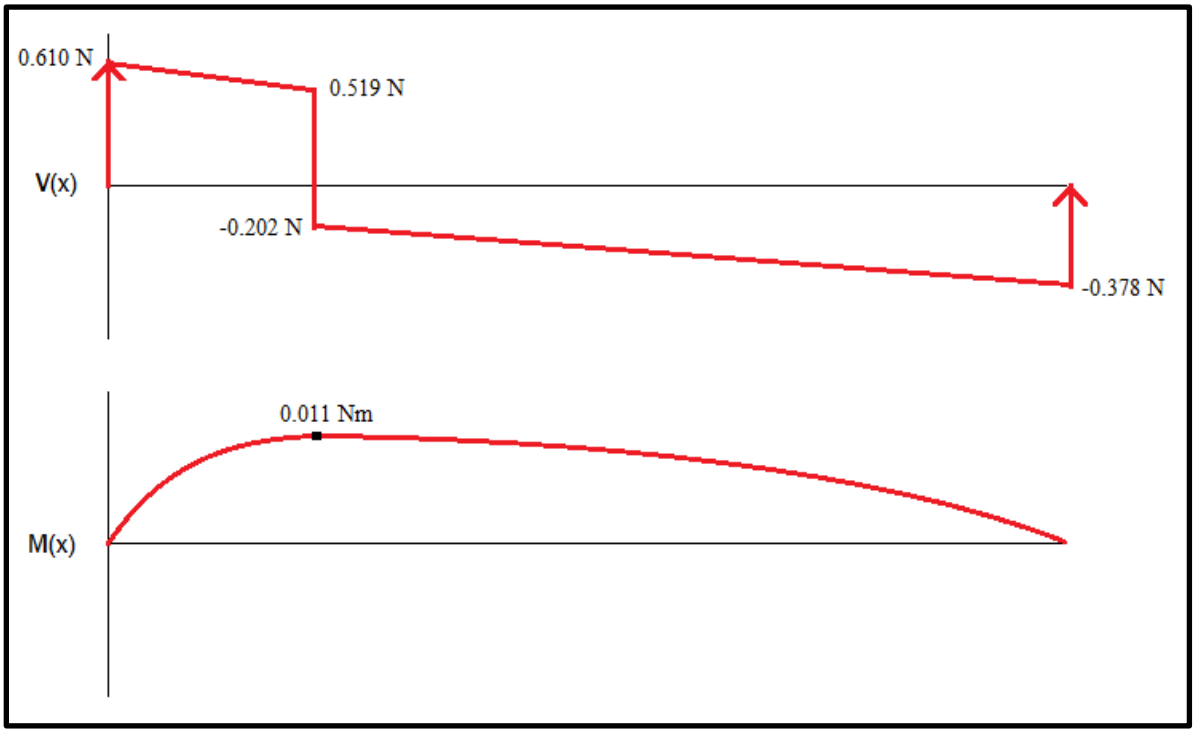


Figure 47 – Shear and Moment diagrams for driveshaft.

After inspection of the shear and moment diagrams, it is determined that the area of the driveshaft which experiences the most fluctuating stress is a stress element on the bottom; right under the disk (under the force F in Figure 13). Figure 48 shows the stress element, B:

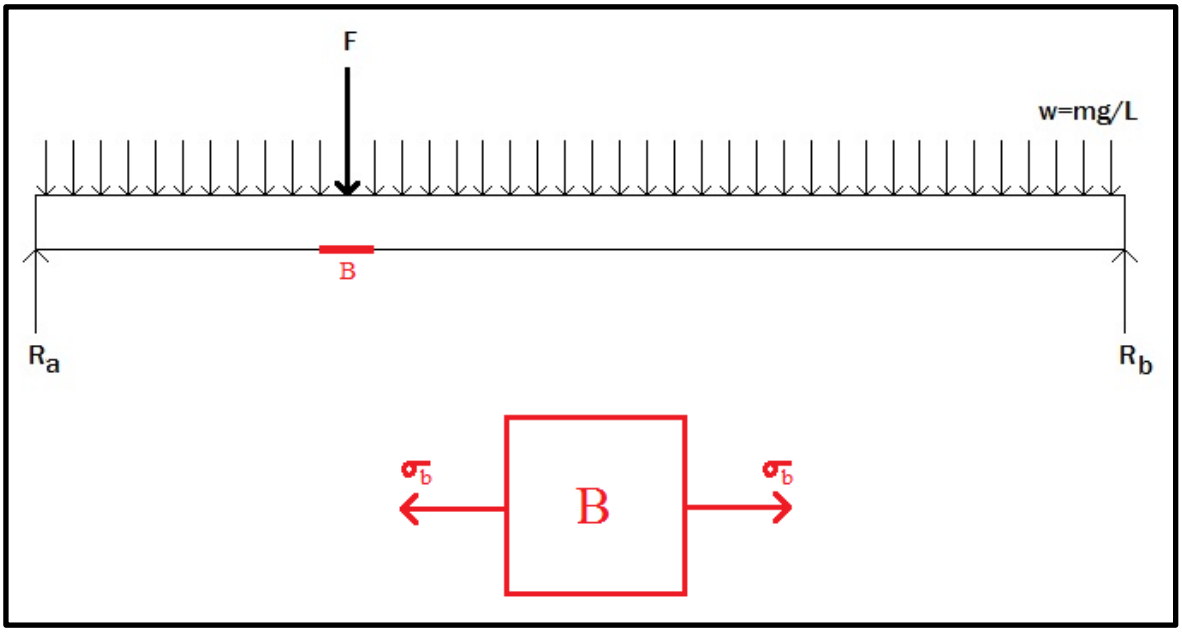


Figure 48 – Stress element B.

To calculate the bending stress, $\sigma_b$, equation 3-24 from Shigley is used, reproduced below (Budynas & Nisbett, 2008, p. 86):

$$\sigma_b = \frac{My}{I}$$

where $M$ = Maximum bending moment,

$y$ = distance from neutral axis to point of interest, (For a round rod, the maximum distance is d/2), and

$I$ = Moment of inertia.

Applying the equation, using the maximum bending moment from Figure 47:

$$\sigma_b = \frac{(0.011)\left(\frac{0.00635}{2}\right)}{7.98x10^{-11}} = \boxed{0.437\ MPa}$$

Since the stress element is in pure bending, the maximum normal stress acting on it is also the maximum principal stress. After the maximum stress is found, the mean and alternating stresses are then calculated. These values allow the use of the failure criterion later on in the calculations. To determine the mean and alternating stresses, equation 6-36 in Shigley are used and reproduced below (Budynas & Nisbett, 2008, p. 293):

$$\sigma_m = \frac{\sigma_{max} + \sigma_{min}}{2}$$

$$\sigma_a = \left|\frac{\sigma_{max} - \sigma_{min}}{2}\right|$$

Since the stress element is rotating, it experiences maximum tension when it is facing down, and maximum compression when it is facing up. Thus, $\sigma_{max}$ is the maximum bending stress previously calculated, 0.437 MPa, and $\sigma_{min}$ is be the negative value of the bending stress, -0.437 MPa. Thus the mean and alternating stresses are:

$$\sigma_m = \frac{0.437 + -0.437}{2} = 0\ MPa$$

$$\sigma_a = \left|\frac{0.437 - -0.437}{2}\right| = 0.874\ MPa$$

Now that all of the components are calculated, the failure criterion can be calculated. Two criteria were used to get a better idea of the safety factor, the Soderberg and the modified Goodman. The equations can be found in Shigley and are reproduced below (Budynas & Nisbett, 2008, p. 298):

$$\frac{\sigma_a}{S_e} + \frac{\sigma_m}{S_y} = \frac{1}{n} \qquad Soderberg$$

$$\frac{\sigma_a}{S_e} + \frac{\sigma_m}{S_{ut}} = \frac{1}{n} \qquad Modified\ Goodman$$

Thus for Soderberg:

$$\frac{0.874}{228.8} + \frac{0}{415} = \frac{1}{n}$$

$$\boxed{n = 261}$$

And for the modified Goodman:

$$\frac{0.874}{228.8} + \frac{0}{540} = \frac{1}{n}$$

$$\boxed{n = 261}$$

Using the two criteria, the safety factor against failure of the shaft due to fatigue is 261.

#### *4.3.2.4 Design Embodiment and Prototype Development*

After the design was developed using CAD and the calculations completed, parts were ordered from different vendors online and locally. Since the dynamometer required a lot of custom parts, aluminum stock was purchased in order to machine those parts. Aluminum was chosen for its ability to be machined relatively easily, and its strength proved sufficient to deal with the imposed stresses.

In order to keep the cost of the dynamometer down, the parts were machined by the author. The result is a completed dynamometer and an embodiment of the concept design as seen in the previous CAD models. The finished dynamometer can be seen in Figure 49 below. Refer to Section 6.1.3 for assessment of the performance of the dynamometer.

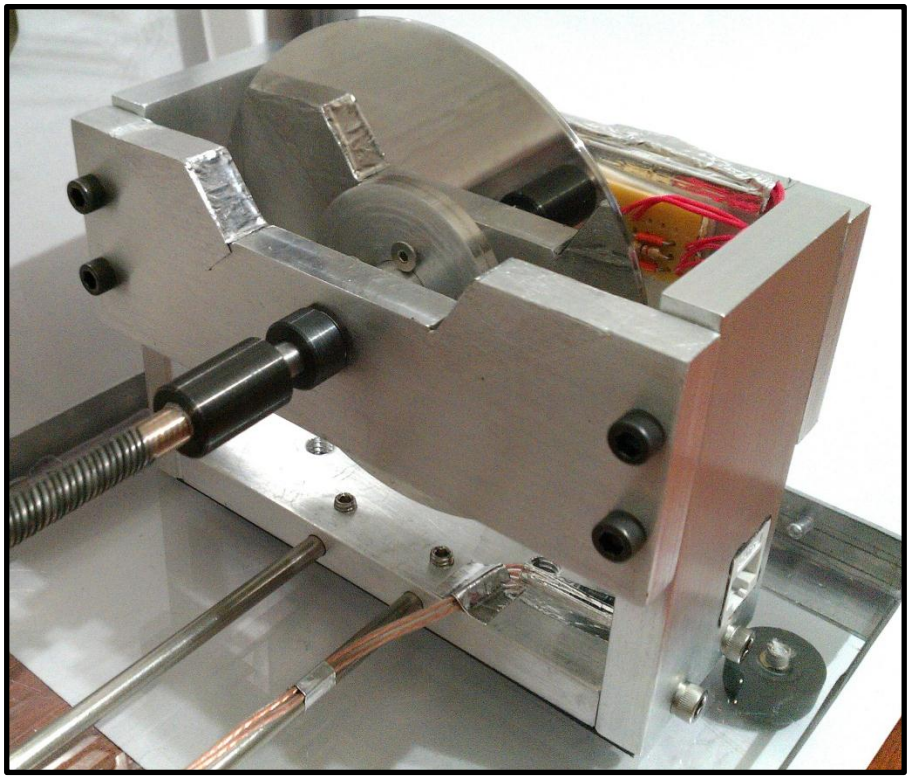

Figure 49 – Completed dynamometer.

A completed bill of materials for the dynamometer can be found in Appendix D. In addition to the dynamometer itself, support equipment was also designed and fabricated, which included a motor stand, protective case, and two controllers (shown in Figures 50 and 51. For detailed descriptions and operation instructions, refer to Appendix E.


Figure 50 – Standalone controller (left), NI myDAQ (right).

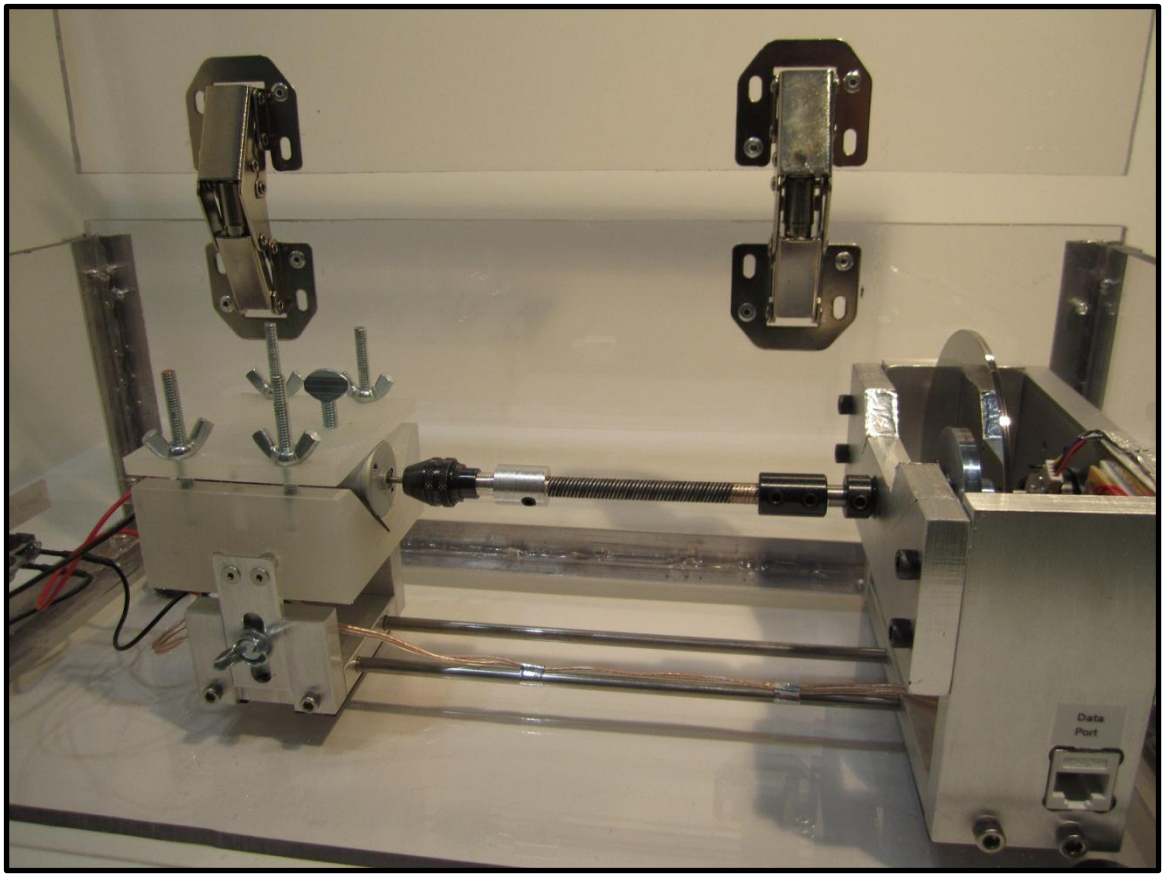


Figure 51 – Complete dynamometer assembly with motor stand and case.

# Chapter 5: Case Studies

## 5.1 Introduction

This Chapter aims to assess the effectiveness of the reverse engineering toolbox created in Chapter 4 by dissecting and quantifying two common household products. These two products were chosen to encompass measurable metrics as well as some dissection methodology. Section 5.3 discusses the results of the case studies.

After searching through archived products, the two items chosen were an air purifier and a toy gun. From a quick inspection, these two products appeared to encompass a fair number of metrics and thus provided a good test for the toolbox. The toy gun is a simple product, and was used mainly for a geometric exercise, while the air purifier has relatively more metrics to measure, which the dissection focused on.

## 5.2 Air Purifier

The first product dissected is an air purifier that filters and ionizes the air, made by Duracraft, model DA-1020 (Figure 52). Little information was found on the product, most likely since it was manufactured in 1995 and has been in storage since then. However, this was of no concern since the goal was to reverse engineer the appliance.

The unit operates by selecting one of three fan speeds: Super, High, and Quiet. The unit also includes the option to turn the "ionizer" feature on and off. This feature supposedly uses high voltage to ionize the air flowing through the machine. Since the air contains dust particles, those dust particles get ionized as well. When the air flows past the filter, the dust electrostatically adheres to the filter, thus cleaning the air (ClearFlite Air Purifiers, 2012).


Figure 52 – The Duracraft air purifier.

Table 12 lists the tools used for dissection and measurement for this product:

| Tool | Purpose |
|---|---|
| Phillips Head Screwdriver | To remove six Phillips head screws |
| Flat head screwdriver | To pry open plastic tabs |
| Wind Vane Anemometer | To measure air flow rate |
| Sound Level Meter | To measure noise level |
| Tachometer | To measure fan speed |
| Ruler | To measure geometric dimensions |
| Digital Scale | To measure mass |
| Accelerometer | To measure vibration |
| Watt Meter | To measure power consumption |

Table 12 – Tools used during dissection of air filtering appliance.

The dissection process began with measurements of geometric data, mass, air flow rate, sound level, vibration and power consumption. These were taken before the product was dissected in order to quantify the product in its initial state. Geometric data was acquired using a ruler with 1/8" resolution, and mass was simply measured using a digital scale. The air flow rate was measured using a handheld anemometer, taken at both the inlet of the machine (where the filter resides) and the outlet. The anemometer gives the air speed, which when multiplied by the inlet and outlet cross sectional area, gives the volumetric flow rate.

Next, the sound level of the machine was tested, to quantify how quiet the machine is during operation. This consisted of holding the sound level meter 30 cm away from the machine, and recording the values at the three different speed settings. The meter used C scale filtering, and thus measured the sound level in dBC.

Afterwards, the accelerometer was used in conjunction with an oscilloscope to measure any vibration of the machine (alternatively, it could have been used with a DAQ card as well). The accelerometer was attached to the outer casing of the machine, near the motor where the highest source of vibration is. However, after multiple measurements, no discernible vibration was produced by the machine or measured by the accelerometer.

Finally, power consumption of the appliance was measured using a watt meter, which plugged in between the appliance and the wall outlet. The meter is easy to use and displays the current power consumption in Watts on its LCD screen.

After the first set of measurements was taken, the outer casing was disassembled to expose the innards of the machine. The disassembly was relatively simple, and consisted of unfastening six Phillips head screws on the bottom, and then prying open three plastic tabs using a flat head screwdriver. On the inside is a simple AC motor with a centrifugal fan blade attached to it. The motor is controlled by the three-position switch,

with a capacitor in line to smooth the voltage. The ionizer is controlled by a simple single pole, single throw (SPST) switch, which feeds the AC voltage directly into three needles; positioned in the path of the outflowing air.

The stripped down machine was then tested using the handheld tachometer to measure the fan speed at different settings. A small piece of reflective tape was attached to one of the fan blades, and then the unit was turned on. The handheld tachometer was aimed at the tape and measurements were recorded.

A table of the accrued measurements is presented in Table 13. Some of the measurements followed behavior that an engineer would expect; however, some of the measurements followed interesting trends. This can be seen when looking at the motor speed data: the motor seems to speed up when the filter is introduced, which also raises the sound level as well. It is beyond the scope of this case study to analyze the fluid dynamics of this phenomenon; however, speculating from previous knowledge, it is most likely caused by a low pressure zone after the filter (caused by the restrictive filter), which then lowers the resistance on the motor allowing it to speed up. In addition, the inlet and outlet volumetric flow rates are mismatched. This is most likely due to leakages in the machine and measurement errors.

Another interesting result is the power consumption, which when taken at face value seems to indicate that the machine uses less power with the filter installed; this is contrary to what an engineer might speculate. However, when a simple calculation of specific power consumption – power consumed per meter cubed of air per second – is performed, the results become much clearer (Table 14). The machine uses less power when the restrictive filter is removed, which is in line with what an engineer with a fluids background expects.

| With Filter | | | | | | | |
|---|---|---|---|---|---|---|---|
| **Speed** | **Air Speed (m/s)** | | **Flow Rate (m^3/s)** | **Fan Speed (RPM)** | **Sound Level (dBC @ 30 cm)** | **Ionizer Setting** | **Power Consumption (Watts)** |
| Super | Inlet | 2.97 | 0.072 | 1776 | 53 | Off | 41.4 |
| | Outlet | 6.34 | 0.057 | | | On | 42.2 |
| High | Inlet | 2.22 | 0.054 | 1418 | 60 | Off | 35.8 |
| | Outlet | 4.62 | 0.042 | | | On | 36.9 |
| Quiet | Inlet | 1.55 | 0.037 | 984 | 66 | Off | 31.2 |
| | Outlet | 3.35 | 0.030 | | | On | 31.6 |

| Without Filter | | | | | | | |
|---|---|---|---|---|---|---|---|
| **Speed** | **Air Speed (m/s)** | | **Flow Rate (m^3/s)** | **Fan Speed (RPM)** | **Sound Level (dBC @ 30 cm)** | **Ionizer Setting** | **Power Consumption (Watts)** |
| Super | Inlet | 2.52 | 0.061 | 1248 | 50 | Off | 43.7 |
| | Outlet | 7.78 | 0.070 | | | On | 44.7 |
| High | Inlet | 1.99 | 0.048 | 998 | 53 | Off | 37.3 |
| | Outlet | 5.95 | 0.054 | | | On | 38.4 |
| Quiet | Inlet | 1.39 | 0.034 | 663 | 58 | Off | 31.5 |
| | Outlet | 3.98 | 0.036 | | | On | 31.8 |

| Geometry (m) | |
|---|---|
| Length | 0.377 |
| Width | 0.18 |
| Height | 0.207 |

| | |
|---|---|
| Mass (kg) | 3.04 |

Table 13 – Measurements taken during the dissection of the air purifier.

| With Filter | | |
|---|---|---|
| **Speed** | **Ionizer Setting** | **Specific Consumption (W/m^3/s)** |
| Super | Off | 722.96 |
| | On | 736.93 |
| High | Off | 857.92 |
| | On | 884.28 |
| Quiet | Off | 1031.13 |
| | On | 1044.35 |

| Without Filter | | |
|---|---|---|
| **Speed** | **Ionizer Setting** | **Specific Consumption (W/m^3/s)** |
| Super | Off | 621.88 |
| | On | 636.11 |
| High | Off | 694.06 |
| | On | 714.53 |
| Quiet | Off | 876.26 |
| | On | 884.60 |

Table 14 – Specific power consumption calculations.

### 5.3 NERF TOY GUN

The second product dissected is a Nerf toy gun that shoots foam projectiles, made by Hasbro (Figure 53). The gun is designed to mimic a crossbow using a plastic bow that attaches to the front (not shown in the figure). This is strictly for aesthetic purposes, and does not aid or hamper the projectile in any way. The gun operates by pulling back the blue handle embedded in the stock, loading the projectile over the barrel, and pulling the trigger to fire. Table 15 lists the tools used for the dissection:


Figure 53 – Nerf toy gun with projectile shown underneath.

| Tool | Purpose |
|---|---|
| Phillips Head Screwdriver | To Remove 11 Phillips head screws |
| Digital Camera W/Laptop | To measure velocity of projectile |
| Tape Measure | To act as distance scale for velocity analysis |
| Digital Hanging Scale | To measure pulling force of blue handle |
| Digital Caliper | To measure geometric data |
| Digital Tabletop Scale | To measure mass |
| Ruler | To measure rough geometric data |

Table 15 – Tools used for dissection of Nerf gun.

The dissection began with rough geometric data and mass measurements. Afterwards, using the digital hanging scale, one end was attached to the handle, and a pulling force was applied to the other end of the scale. The maximum force measured right before the handle locked in position was determined to be the maximum pulling force of the handle.

Afterwards, the tape measure was secured to the edge of a long table to serve as a distance marker for the velocity analysis (shown in Figure 54). A digital camera was set up to capture the motion of the projectile when fired. The projectile was then held as close to the tape as possible (to prevent perspective effects from introducing inaccuracies), and then the gun was fired. The resulting footage was played back frame-by-frame, taking note how many frames the projectile needed to cross a certain distance. Since the camera has a set and constant frame rate, the time between frames can be calculated, and thus, the velocity as well. Table 16 summarizes the gathered data:

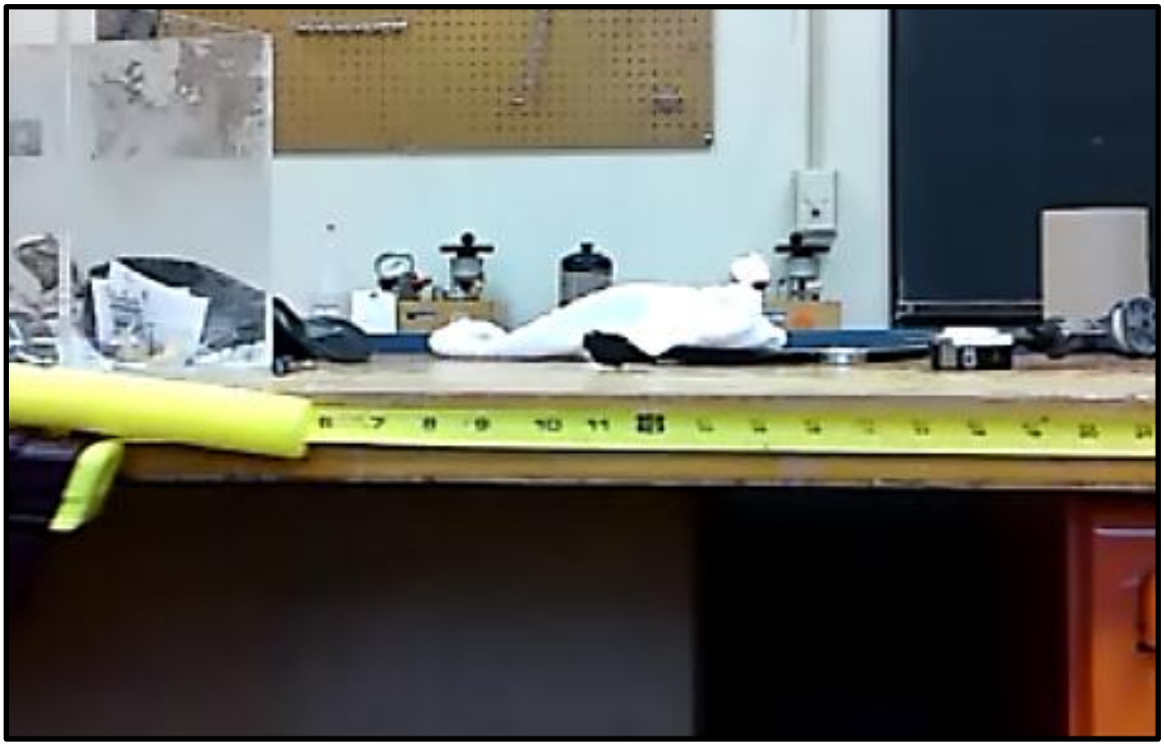

Figure 54 – lab setup for velocity measurement.

| | |
|---|---|
| **velocity** | 32 ft/s (9.75 m/s) |

| | |
|---|---|
| **force** | 19.4 lb (86.3 N) |

| | |
|---|---|
| **mass (kg)** | 0.5 |

| | |
|---|---|
| **rough geometry (m)** | 0.546 (Length) |
| | 0.203 (Width) |
| | 0.038 (Thickness) |

Table 16 – Measurements taken during dissection of toy gun.

Unfortunately, the frame rate of the camera available for the velocity analysis, which was 29 frames per second, was not fast enough to comfortably determine the velocity. This would not be an issue with the camera from the toolbox, which operates at 120 frames per second. However, the camera used was good enough for a rough estimate when viewed over a larger distance scale. This has one disadvantage in that it gives the average velocity of the projectile, instead of the barrel velocity.

After the velocity measurements, the gun was then dissected in order to learn more about its methods of operation. The gun has an air piston that occupies the majority of the gun's internal cavity, connected to the barrel by means of a flexible hose. The piston is actuated by a spring loaded handle, which locks when pulled back to its maximum travel. The trigger is then used to release the handle, and by means of the spring, rapidly compresses the air inside the piston, shooting the projectile out of the barrel.

In order to demonstrate the toolbox's geometric gathering capabilities, one of the internal components, the yellow trigger, was chosen to be reverse engineered and modeled using SolidWorks® CAD software. Once such a model is developed, the engineer can redesign or analyze the part using various software packages.

The geometric properties were gathered using a digital caliper with 0.001 inch resolution. The resulting data was then used to recreate the part using the CAD software. The original trigger and the CAD developed trigger are shown in Figure 56:

Figure 55 – Dissected view of Nerf gun.

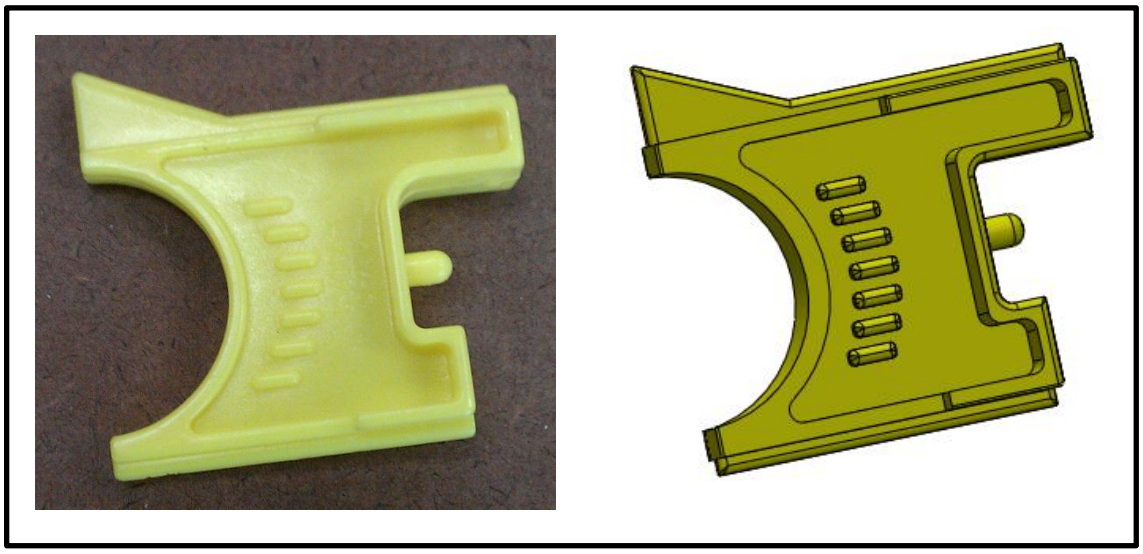

Figure 56 – Original trigger (left), computer model (right).

As can be seen from the figure, using the digital caliper, the trigger was reproduced with great accuracy, down to the aesthetic design features. Of course, the digital caliper is not the sole tool needed to accomplish this task; a working knowledge of using CAD software is needed as well.

## 5.4 Results and Conclusions

As a result of the two case studies performed, some valuable insight was gained on the usefulness and utility of the toolbox. Granted, the toolbox was not used entirely; however, it was still enough to give a good indication of how the toolbox will perform.

A tool is only as good as its user, and the reverse engineering toolbox is no different. The first step to utilizing the reverse engineering toolbox correctly is to determine which metrics are to be measured. The different possibilities and combinations are abundant for any given product, and thus the engineer must choose the ones that will aid in the analysis. For the two case studies, the metrics were chosen according to what a customer might look for when using the item. In the first case, the air purifier, the customer will most likely be concerned about how much power it consumes, how much air gets filtered per hour, and how loud the unit is. These considerations prompted the measurement of air flow rate, power consumption, and sound level, as a start. A customer might also be concerned with how big the unit is and how much it weighs, for aesthetic and ergonomic purposes, prompting measurements of geometry and mass.

For the second case study, with the Nerf toy gun, the most important metric a customer will most likely care about is the velocity, and consequently, the maximum shooting distance. Also of likely importance are the size, weight, and the ease of use of the gun. These considerations prompted the measurement of geometry, mass, and the pulling force of the handle. A geometry exercise was added to the toy gun to demonstrate a case where the engineer needs to replicate a specific part or parts from a machine without access to any blueprints or design specifications. This situation can arise if the part breaks and is no longer manufactured, or for use when analyzing the competition. Using digital calipers, the part was replicated to about two digits of accuracy. For a more accurate model, a 3D laser scanner could have been used as well.

More advanced customer needs analysis techniques could have been used, coupled with functional modeling, to create a better list of metrics; however, for the purposes of these case studies, the needs measured above were sufficient.

One cannot forget to discuss the accuracy of such measurements. However, given the nature of the toolbox, the tools included can vary, since they are made by different manufacturers to different specifications. This leads to variations in tool accuracy, and thus the engineer will have to be aware of the tools he or she is using when conducting the analysis.

As far as dissection goes, the toolbox performed as expected. The products chosen turned out to be very simple in construction, and only needed two types of screwdrivers to dissect completely. Similar to the situation with quantification tools, it is important to have the appropriate tool for the specific task. For example, when prying apart a plastic casing held by tabs, it is important to understand how the tabs fit together. Instead of prying apart the two halves with a crow bar, a simple screwdriver placed in the right spot will release the casing with almost no effort. The aim of the toolbox is then to provide a selection of tools that cover as many situations as possible.

# Chapter 6: Conclusion and Future Work

## 6.1 CONCLUSIONS

The purpose of this research was to create a comprehensive toolbox that can be used for reverse engineering projects by students, and with further expansion, professionals. The goals for the development included low cost, ease of use, and implementation of commercial off the shelf products as much as possible. The development of a portable dynamometer is also documented in this thesis, the goal of which is to provide a more accessible and inexpensive tool to measure power output of miniature DC and AC motors.

### 6.1.1 Assessment of toolbox development and performance

The development of the toolbox involved using basic data gathering techniques to create a list of metrics most likely to be measured by a reverse engineering student. However, even though this thesis is targeted towards use in academia, the list of metrics and tools presented in Chapter 3 can also be expanded for use by professionals or anybody desiring to have reverse engineering capabilities.

To assess whether the toolbox met its goals, the analysis first begins with the cost. An absolute figure cannot be placed on the tools; this is due to the fact that tools can be purchased through a variety of avenues, including locally and online, with and without bulk discounts and corporate deals. However, through the research in this thesis, the prices for the tools presented were obtained from online sources, and are prices that the average consumer expects to pay. The total cost for the toolbox, including dissection and quantification tools (but excluding the dynamometer) is around $1549. This is a very reasonable price for mid to high level tools, even for the average consumer in a non-academic setting. Compared to the closest competitor for this toolbox, the system from

Vernier, which costs over $1700 for less than half of the tools, the toolbox meets the low cost goal.

The second goal set for the toolbox is its usefulness. It would be foolish to claim complete compatibility with every product on the market; consumer products are constantly evolving and it is only a matter of time until manufacturers start using new manufacturing techniques. However, from the data gathered from the case studies performed in Chapter 5, the toolbox developed proved sufficient to properly dissect and quantify the two household products, and from that analysis, should prove sufficient to dissect the majority of household products consisting of purely mechanical or electromechanical constituents.

The final goal for the toolbox is its availability. Given the flexibility in tool selection of the toolbox, many of the tools can be found off the shelf in major hardware and electronics stores. Some of the tools are specialized and will be harder to come by; for example, the miniature dynamometer. For these tools, lower cost and more portable versions were explored in Chapter 3, or as in the case of the dynamometer a more accessible version was created.

However, the most important development from this research, as a whole, is not the physical toolbox. Instead, it is a consolidated and concise list of metrics and appropriate tools that any engineer will need to properly outfit a reverse engineering facility. Using this list, many different and unique toolboxes can be created, each with a different combination of tools to suit the needs of the user. The toolbox presented in this thesis is just one of many versions; this version was chosen to meet the goals of low cost, usefulness, and availability, most appropriate for an academic setting. A professional user with significantly more resources will most likely be able to afford high quality and sophisticated tools, and thus create a more advanced toolbox.

### 6.1.2 Assessment of dynamometer development

The goal for creating the portable dynamometer was to try to explore another method of creating a tool for measuring the power output of fractional horsepower DC and AC motors. The tools available on the market are scarce, bulky, and no doubt, very expensive. Thus, the goals for the dynamometer were for it to be low cost (around $200), easy to use, and made from commonly available parts and materials.

The development of the dynamometer was a very complicated experience that puts the entire design and development process in perspective. Beginning with the design portion, many iterations were performed, with each step making the dynamometer simpler and easier to manufacture, while reducing part count and features that would introduce measurement errors and failure points. This was done after many consultations with the machine shop staff, whose experience proved valuable in honing the design. This is in line with the concept of "Design for Manufacture (DFM)," an art practiced by many engineers in the field to reduce manufacturing costs and boost productivity.

### 6.1.3 Assessment of dynamometer performance

The performance of the dynamometer was evaluated using the criteria of accuracy, ease of use, cost, portability, and robustness.

#### *6.1.3.1 Accuracy*

The accuracy of the dynamometer was assessed by performing tests against known power curves for two DC motors. The two motors tested were manufactured by Mabuchi Motor Co., an electronics company based in Japan, and are designated as RK-370CA and RK-385PH (Mabuchi Motor Co., 2012a) (Mabuchi Motor Co., 2012b). The most straightforward method would be to research the datasheets for the motors through the company, then compare the calibrated dynamometer to the data sheets. However,

Mabuchi Motor Co. produces a wide portfolio of DC motors, and to differentiate between the applications, they are grouped by series. Datasheets are only available for these series, and not for the specific motor. This presented a problem since the motors in the series vary widely and do not share many common characteristics. Refer to Appendix F for the data sheets.

To remedy the problem, an estimated power curve was gathered experimentally by measuring the two most important data points on a torque vs. speed curve: stall torque and no-load speed (shown in Figure 57). The stall torque was measured by attaching a lever arm of known length to the motor, with the end terminating at a fine point. The end was then placed over a very sensitive jeweler's scale to measure the force exerted. The motor was then powered and the value on the scale noted. To measure no-load speed, the motor was allowed to run freely with only a small piece of reflective tape attached to the shaft. A handheld, no contact, tachometer was then used to measure the speed. The two data points were then graphed and the resulting line became the target torque vs. speed curve.

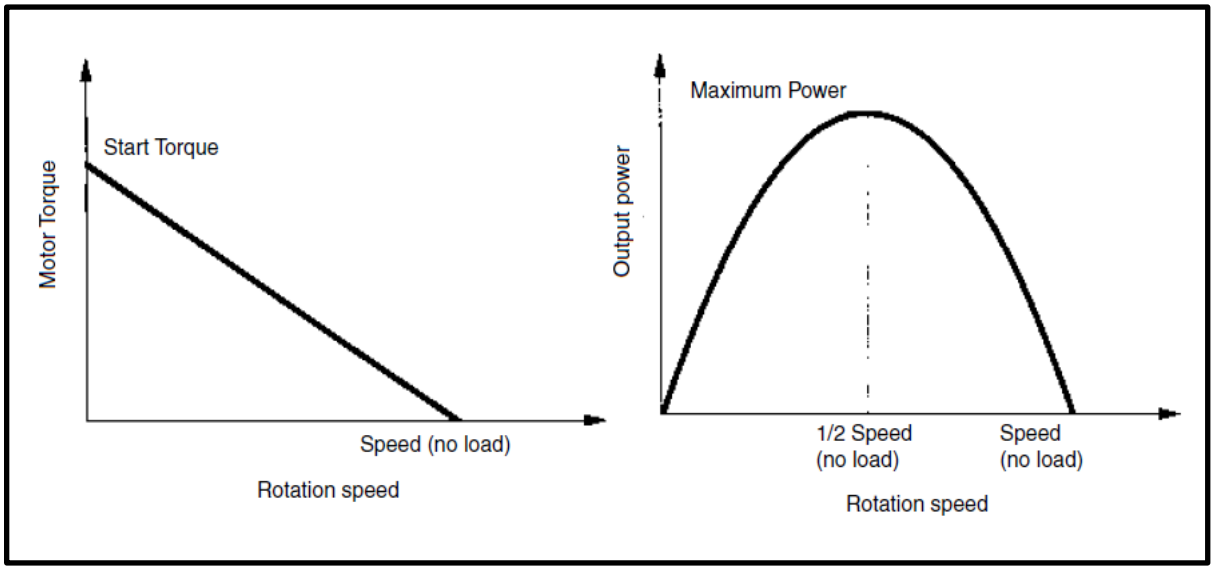


Figure 57 – Torque and Power vs speed for a typical DC motor (Crouzet Automatismes SAS, 2012).

Testing consisted of three runs for each motor, measuring both toque vs. speed and power output vs. speed. The results were compared with each other and analyzed for patterns. The compiled results are shown in Figures 58 through 61. The curves labeled "Experimental Data" are the results from the hand measurements, and thus serve as the target curves.

Looking at the results, there exists a discrepancy between the no load speed of the motor and the full speed of the dynamometer. This was suspected to be the result of both viscous bearing friction and air drag on the rotating disk. To verify this theory, a rough simulation of the dynamic behavior of a DC motor was created using the bond graph method. The bond graph is shown in Figure 62:

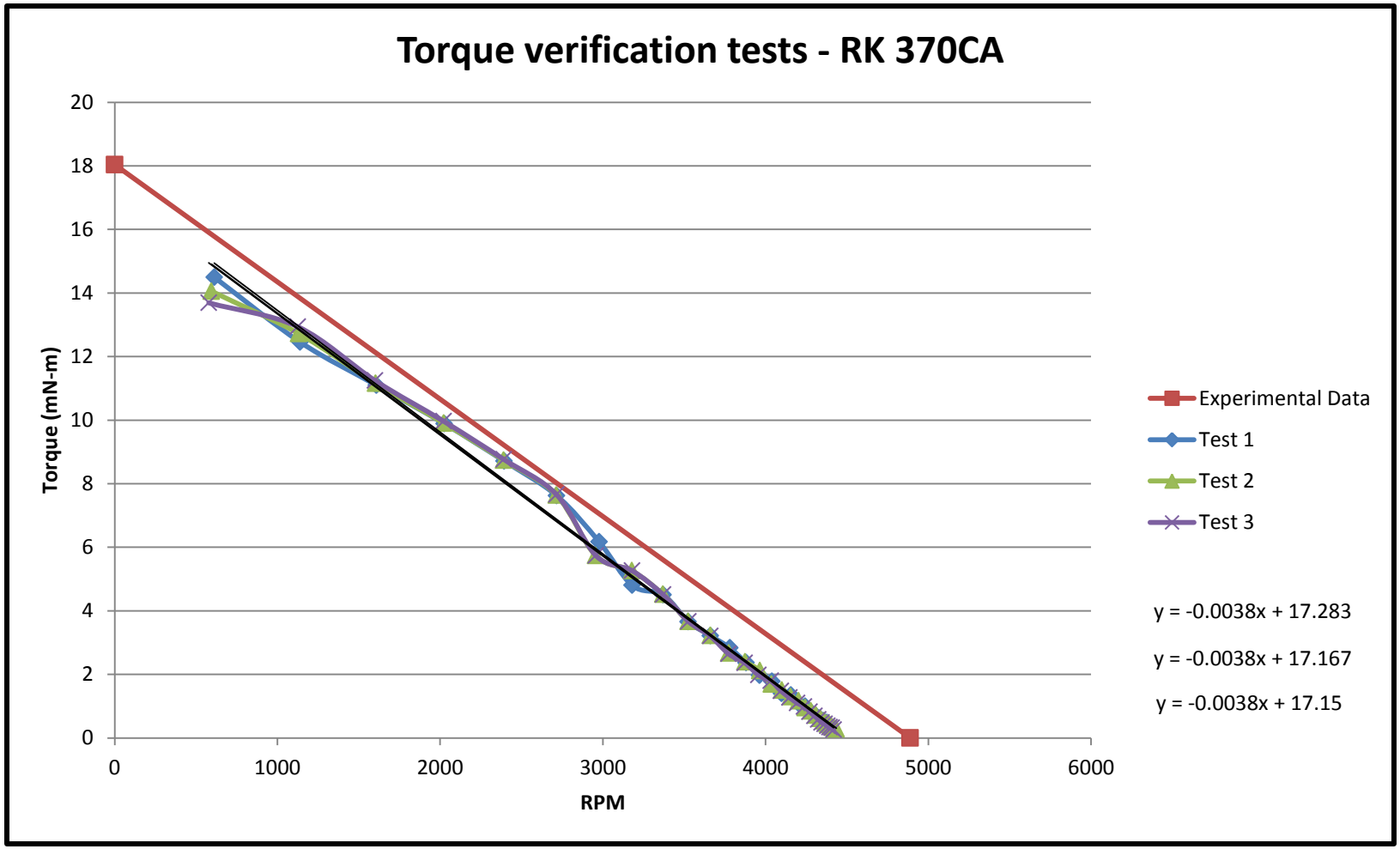


Figure 58 – Torque test data for the first of the DC motors.

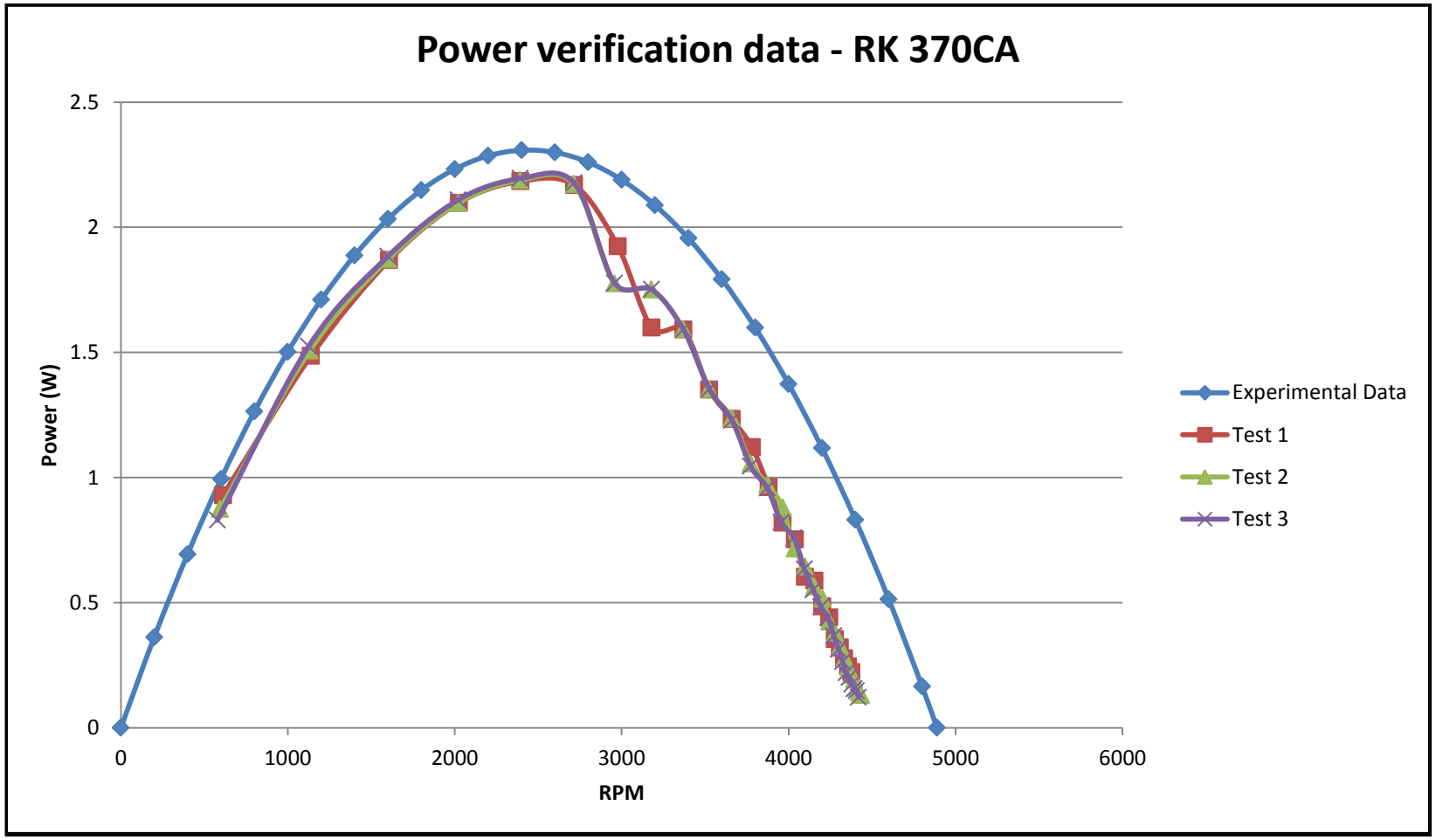


Figure 59 – Power test data for the first of the DC motors.

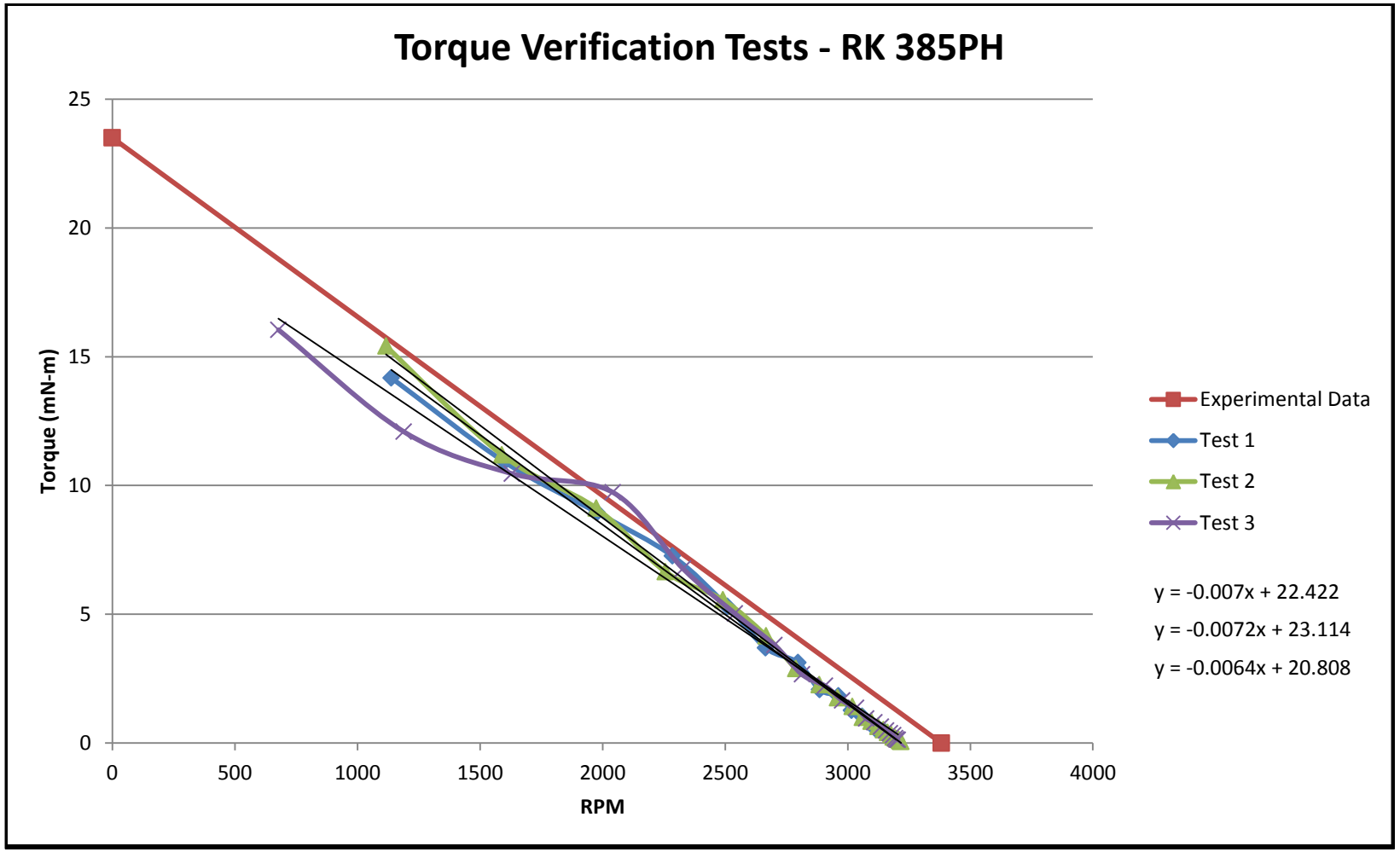


Figure 60 - Torque test data for the second of the DC motors.

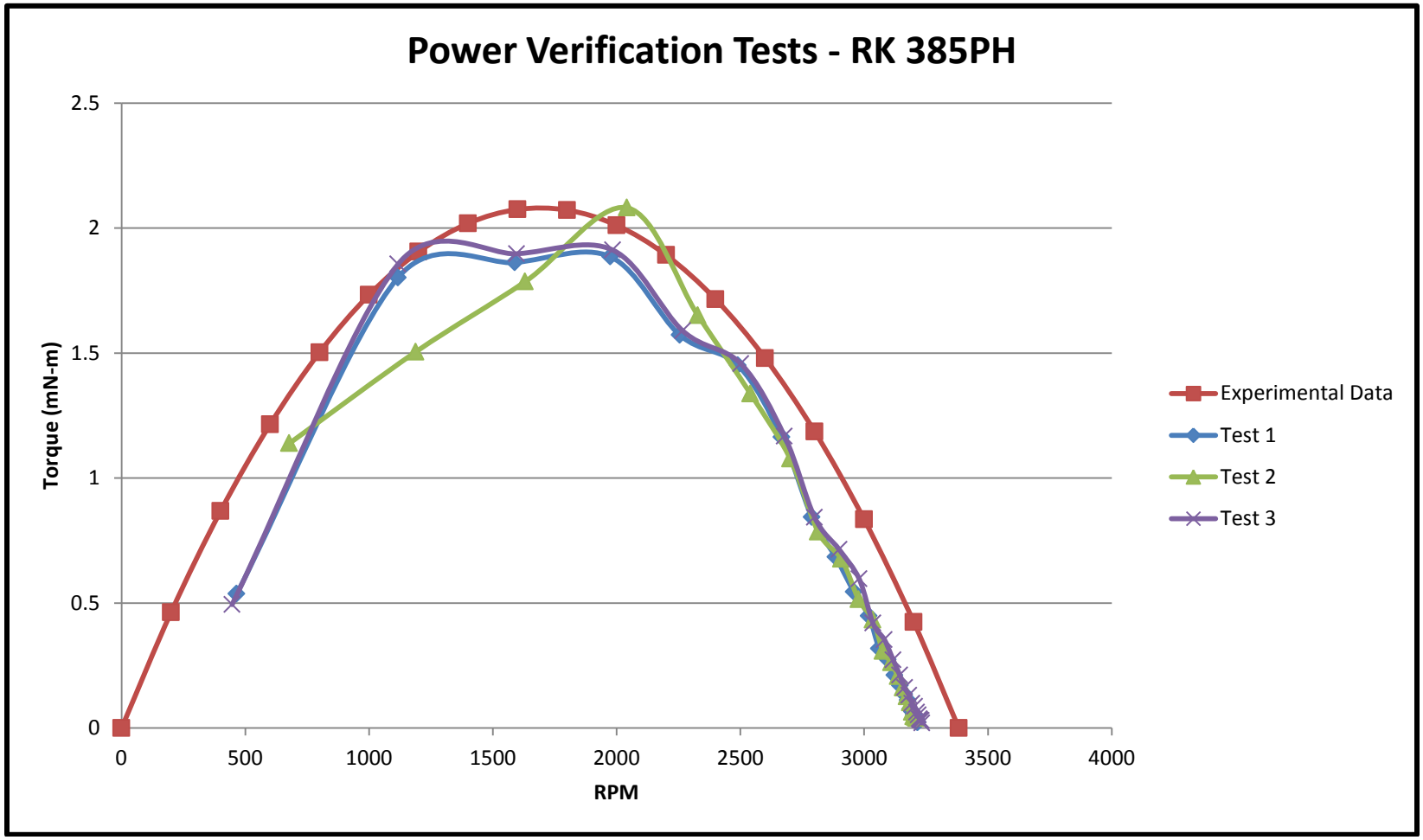


Figure 61 - Power test data for the second of the DC motors.

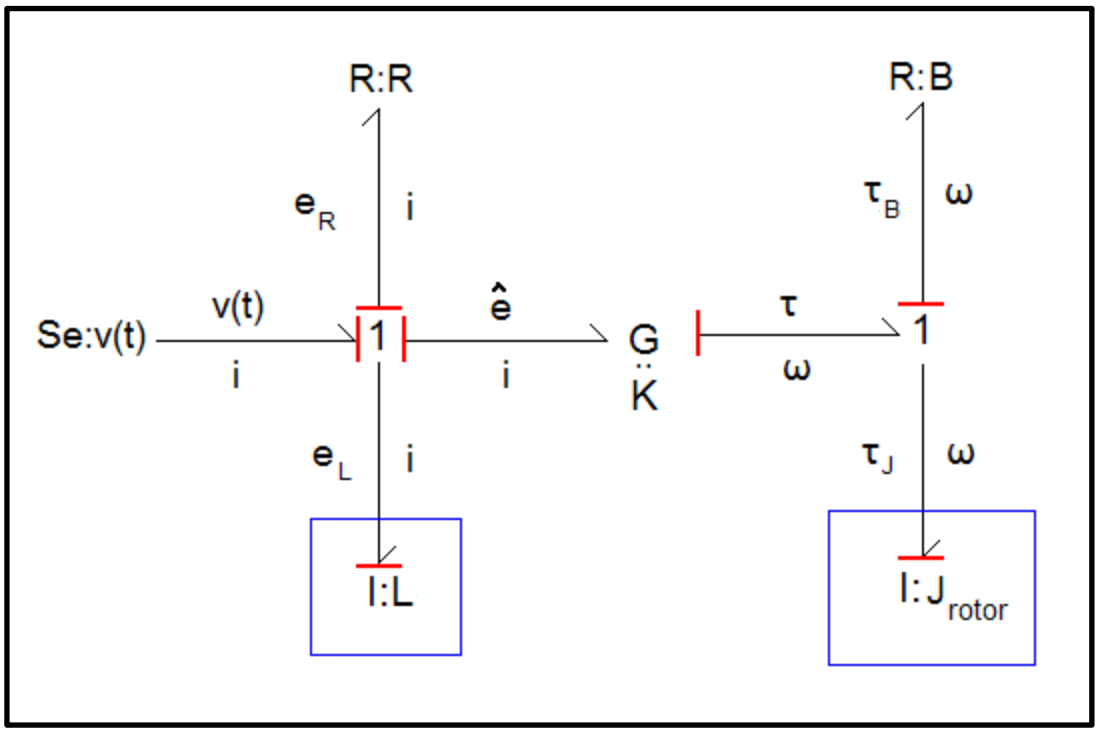


Figure 62 – Bond graph of a series DC motor.

The independent elements are shown in blue boxes. Deriving the state equations results in:

$$\frac{dh}{dt} = \frac{\lambda}{L}K - \frac{h}{J}B$$

$$\frac{d\lambda}{dt} = v(t) - \frac{\lambda}{L}R - \frac{h}{J}K$$

Since the behavior, rather than the accuracy, of the model is of importance, arbitrary but realistic values were used for the physical constants. The simulation was then run in MATLAB using a Runge-Kutta numerical integration method. The resulting angular velocity profile was used to calculate torque and power for a base case with no

friction, and three additional cases where the friction constant, B, was increased by a factor of ten for each run. The results are shown in Figures 63 and 64:

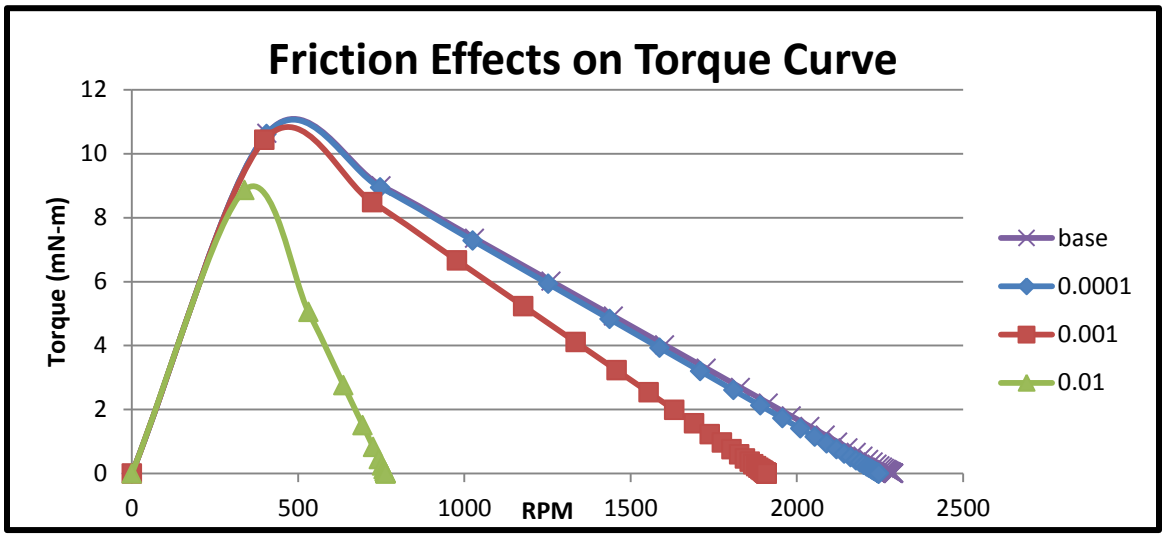


Figure 63 – Friction effects on torque output

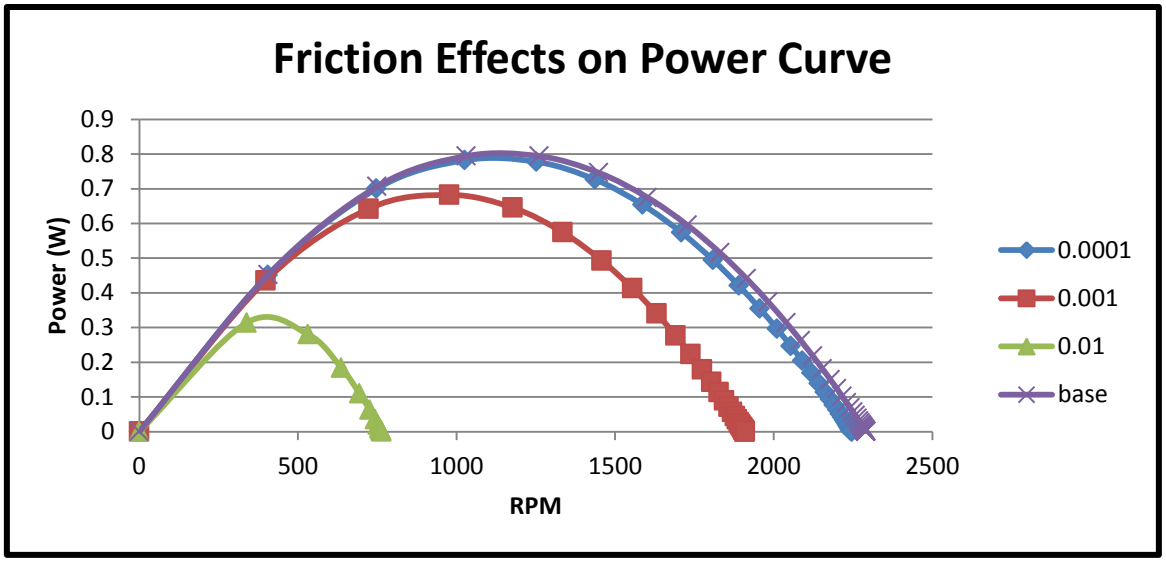


Figure 64 – Friction effects on power output.

As predicted, the motor's maximum angular speed was reduced with increasing friction, thus explaining the discrepancy between the measured and experimental data. The same effect can be seen with the power curve as well.

As for the accuracy of the torque values, a simple mean and percent error can be determined by performing a curve fit and taking the y-intercept of the resulting lines. The RK-370CA resulted in a mean of 17.2 mN-m with a total error of 4.6% from the measured value of 18.04 mN-m. Concurrently, a similar analysis for the RK-385PH results in a mean of 22.10 mN-m with a total error of 5.9% from the measured value of 23.5 mN-m.

It was observed that the starting behavior of the torque curve measured by the dynamometer exhibited some of the "peaking" behavior shown in Figure 63. This can be due to the fact that different types of DC motors exhibit different behavior depending on the internal circuitry (series, shunt, etc). To find the "predicted" stall torque using a curve fit, the first two data points were eliminated, keeping the linear portion of the measured torque curve instead.

Even though hard numbers for measurement error were not set for assessment of accuracy, an error of roughly 5% can be deemed acceptable for a less expensive alternative to commercial dynamometers. This can be improved in future iterations, discussed more in Section 6.2.

#### *6.1.3.2 Ease of Use*

The ease of use metric can be interpreted in several ways, including ergonomics and complexity of the product. The dynamometer fulfills the ease of use metric by incorporating several user friendly features:

1) Plug and play controllers that connect through a standard Ethernet port. Easily switch between the two depending on preference: a customizable, computer based DAQ system; or a portable, stand-alone model with on-board data storage.
2) Breakout screw terminal to attach external power supply easily, which accepts any form of low current DC and AC power.
3) Motor stand has integrated alligator clips to easily connect power to the motor, and a motor control relay to simplify the testing procedure by allowing software based motor control.
4) Controllers have easy-to-use user interfaces and built in instructions for on-the-go reference.
5) Only six steps to start a measurement session:
    a. Secure motor to motor stand
    b. Attach power supply cables to motor
    c. Connect motor to dynamometer
    d. Connect power supply to screw terminals
    e. Connect controller of choice
    f. Start test
6) Modular system layout: any of the components (dynamometer, motor stand, and controller) can be disconnected from the overall system and reconfigured or used separately.
7) Sturdy acrylic case to protect the user against any rotating assembly failure, as well as mute any motor noise.

#### *6.1.3.3 Cost*

The initial cost goals for the dynamometer were not met very well. Numerous mistakes and oversight created a budgetary deficit and required more monetary resources to be spent. What is shown in the bill of materials in Appendix D is the final part count; however, the development process went through many iterations of those parts, increasing the total final cost. One can argue that this is just the research and development phase, and once a working prototype is created, subsequent versions will be cheaper and easier to make.

All in all, the cost for the finalized parts in the dynamometer totaled to $130, which includes the rotating assembly, housing, and tachometer. This figure does not include the controller or accessory features such as the motor stand and protective casing, since these can be highly customizable and made from many different materials. This figure does not include machining costs either. Depending on the skill of the engineer, a professional machine shop might be required, significantly driving up the cost of the dynamometer.

Since an inertial dynamometer is conceptually simple, the design can be replicated with less expensive materials quite easily. The example documented in this thesis was created using medium to high grade quality parts for reliability reasons; for applications not requiring such characteristics, less expensive parts can be used.

#### *6.1.3.4 Portability*

The dynamometer measurement system consists of two main parts: the dynamometer assembly, which includes the dynamometer and motor stand; and the controller. Depending on which controller the user chooses, a computer might also be required. Finally, the last requirement is an external power supply; however, due to the

various power options that fractional horsepower motors can use, this remains to be provided by the user. A higher level system layout is provided in Figure 65.

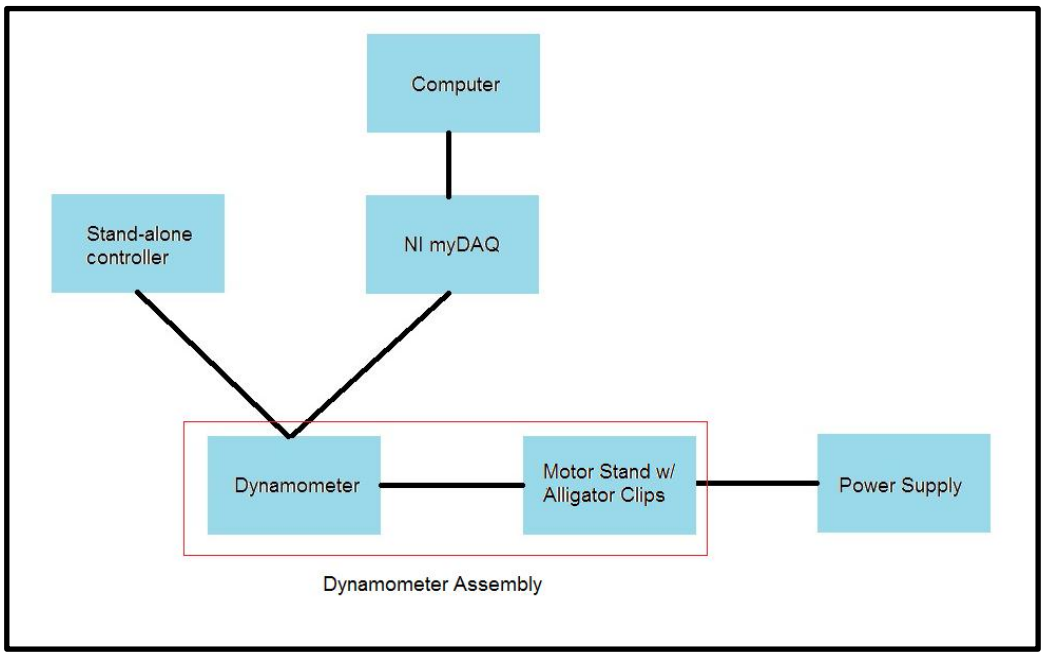


Figure 65 – Dynamometer measurement system layout, shown with all possible constituents.

The dynamometer assembly consists of the acrylic case shown in Figure 50, which includes the dynamometer itself and the motor stand. The assembly weighs 3.5 kg (7.8 lb), about the weight of a large laptop, and measures 15” L x 6.5” W x 5” H (38.1 cm x 16.5 cm x 12.7 cm), which gives the test assembly a small footprint that can be placed on a typical tabletop.

The controllers, as mentioned previously, consist of one standalone model, and one “tethered” DAQ model that needs a separate computer. In terms of portability, the standalone model is the most convenient, offering built in memory card data logging,

which can be transferred and viewed on a computer later, as well as rechargeable battery for portable power.

Excluding the external power supply for the motor (which can also be a portable battery), the dynamometer measurement system can be operated with only two small, portable components, greatly enhancing its portability and successfully meeting another design objective.

#### *6.1.3.5 Robustness*

The robustness of the dynamometer is fulfilled through several features. Since the inertial dynamometer consists of a very minimal amount of parts, the assembly has few modes of failure. These include catastrophic failure of the disk, bearing seizure, and failure of parts due to resonance and vibrational effects.

The assembly is protected with a tough, aluminum-reinforced acrylic case, which serves the purpose of protecting the assembly, as well as shielding the user from any accidental shrapnel caused by catastrophic failure. The dynamometer itself is also protected by its thick aluminum frame.

The controllers have fail safe modes built in, including the normally open motor control relay. In case of a failed measurement session or an unresponsive controller, the user needs to only turn off or unplug the unit, automatically shutting off the motor from a safe distance.

Aside from physical robustness, the dynamometer's method of operation is also very simple, and can be replicated and diagnosed easily, since it consists of one rotating disk and one measurement system. This offers an advantage over a more complex dynamometer type, which can introduce compounding of error due to multiple sensors and moving parts.

## 6.2 FUTURE WORK

The first candidate for further development is the quantification of dissection techniques and methods. Since the toolbox developed in this research provides the tools necessary for dissection, it is important to know how to use the tools properly, and which tool to use depending on the specific situation. A "guide" can be created that documents the different types of fasteners, adhesives, tabs, etc., and how the user can go about removing such objects in order to dissect the machine as non-destructively as possible. This list, in conjunction with the list of tools presented in this thesis, will create a database of useful knowledge that any engineer can refer to when reverse engineering machines.

The second avenue for future development is the dynamometer. This thesis presented one attempt at development by building an inertial dynamometer and attempting to calibrate the controllers. Future development can include potential redesign of some of the parts, as well as a more accurate and statistically significant calibration procedure. This can include the elimination of erratic behavior during the startup sequence, as well as algorithms to eliminate noise from the measurements. Also, the spinning disk needs a better method of balancing, which will increase the rated design speed to accommodate faster motors.

One of the controllers implemented a Virtual Instrument created using LabVIEW. Future development can include an expansion of this VI to include automatic write-to-file capability and generation of summary reports. Also, the accuracy and repeatability of the measurements can be improved by implementing signal filters, and also rapidly sampling each data point several times during every interval, recording the average instead. Technical details and calibration procedures are outlined more in Appendix E.

# Appendix A: ME 366J Product Dissection Survey

1. What type of product did you dissect? (choose the best description)

   Mainly Electrical (i.e. TV Remote Control)
   Mainly Mechanical (i.e. Fishing Reel)
   Mainly Pneumatic (i.e. Vacuum)
   Mechatronic (i.e. Power tools)

2. What is the product?

3. How difficult would you say it was to dissect?

   Easy (simple tools needed, no cutting or drilling)
   Medium (slightly complex tools needed, some prying of parts required)
   Difficult (special tools required i.e. Safety Torx, Cutting or drilling of fasteners or housing required)

4. What was the hardest part of the dissection?

   Fasteners
   Outer casing
   Removing the different parts inside (motor, switch, etc)Other (please specify)

5. How long would you estimate the dissection process took?

   0-1 hr
   2-4 hrs
   5-7 hrs
   8-10 hrs
   >10 hrs

6. What tools did you use? (Select all that apply)

   Screwdriver (Flathead)
   Screwdriver (Phillips)
   Screwdriver (Torx)
   Hex Keys
   Pliers
   Vice Grip
   Open ended wrench

Socket wrench
Drill
Power Saw
Manual Saw
Knife (Xacto or regular)
Other (please specify)

7. During the dissection process, which of these metrics did you measure before, during, and after the product was disassembled? (Select all that apply)

Geometry
Weight
Torque (of either a powered motor or mechanical parts)
Force (of either a powered motor of mechanical parts)
Voltage
Current
Temperature
Light intensity
Surface Roughness
Material Hardness
Material properties (tensile/compressive strength, yield strength, young's modulus)
Air speed
pressure (air)
pressure (liquid)
Sound intensityOther (please specify)

8. What tools did you use to measure these metrics?

scale
Force gauge
Torque gauge
ruler
caliper
tape measure
laser range finder
Thermometer (mercury or digital)
thermocouple
laser thermometer
IR camera
Hardness Tester
Tensile/compressive tester
Light intensity meter
Surface roughness meter

Decibel meter
Wind speed gauge
hot wire anemometer
Pressure gauge
manometer
Multimeter (voltage, resistance, current, capacitance)
Other (please specify)

9. Please state any recommended tools you would like to see in a reverse engineering toolbox for use in ME 366J

# Appendix B: Compiled Results from the House of Quality Matrices

Pre 2011 Pool

**Total Matrices:** 24

| | | | | | | | | | | | | | | | | | | | | | | | | | |
|---|---|---|---|---|---|---|---|---|---|---|---|---|---|---|---|---|---|---|---|---|---|---|---|---|---|
| Geometry | 23 | 96% | x | x | x | x | x | x | x | x | x | x | x | x | x | x | | x | x | x | x | x | x | x | x |
| Time | 17 | 71% | x | x | x | | | x | x | x | x | x | x | | x | | | x | | x | x | x | x | x | x | |
| Sound level | 18 | 75% | x | x | x | x | x | x | x | | | | x | x | | x | x | x | x | | x | x | | x | x | x |
| Mass | 18 | 75% | x | x | x | x | x | | | x | x | | | x | x | x | | x | x | x | x | x | | x | x | x |
| Temperature | 11 | 46% | x | | | | | | x | | | x | | x | | x | x | x | | x | | | x | | x | x |
| Elec. Prop. | 15 | 63% | | x | x | x | | x | | x | | x | x | | | | x | x | x | x | | x | x | | x | x |
| Torque | 9 | 38% | | x | x | x | x | | | | | x | x | | | | | x | | | | | | x | x | |
| Force | 7 | 29% | | | | x | | x | | | | | x | x | x | | x | x | | | | | | | | |
| Angular velocity | 7 | 29% | x | x | x | | | | | x | | | x | | | x | | | | | x | | | | | |
| Pressure | 4 | 17% | | | x | | | | | | | | | | x | | | | x | | | | | | x | |
| Flow rate | 6 | 25% | x | | | | | | x | x | | | | | | x | | | | | | x | | | x | |
| Material prop. | 7 | 29% | | | | | | | | x | | x | x | x | x | x | | x | | | | | | | | |
| Light intensity | 3 | 13% | x | | | | x | | | | | | | | | | | x | | | | | | | | |
| Linear velocity | 2 | 8% | | | | | | | | | x | | | | | | | | | x | | | | | | |
| Vibration | 1 | 4% | | x | | | | | | | | | | | | | | | | | | | | | | |
| Friction | 2 | 8% | | | | | x | | | | | | | x | | | | | | | | | | | | |

2011 Pool

**Total Matrices:** 16

| | | | | | | | | | | | | | | | | | | |
|---|---|---|---|---|---|---|---|---|---|---|---|---|---|---|---|---|---|---|
| Geometry | 15 | 94% | x | x | x | x | x | x | | x | x | x | x | x | x | x | x | x |
| Time | 9 | 56% | x | | | | x | | x | x | | x | x | x | x | | | x |
| Sound level | 6 | 38% | | x | | x | | x | | | | | | | x | | x | x |
| Mass | 13 | 81% | x | x | x | x | x | x | x | x | x | | | x | x | x | x | |
| Temperature | 4 | 25% | | | x | | | | | x | x | | | | | | | x |
| Elec. Prop. | 4 | 25% | x | | x | | | | | x | x | | | | | | | |
| Torque | 5 | 31% | | | | x | x | x | | | | | | x | | x | | |
| Force | 5 | 31% | | | | | x | | x | | x | x | | x | | | | |
| Angular velocity | 9 | 56% | | | x | x | x | x | | | | x | | x | x | x | x | |
| Pressure | 2 | 13% | | | x | | | | | x | | | | | | | | |
| Flow rate | 3 | 19% | | | x | | x | | | x | | | | | | | | |
| Material prop. | 6 | 38% | | | x | | | x | x | | | | | | x | x | | x |
| Light intensity | 0 | 0% | | | | | | | | | | | | | | | | |
| Linear velocity | 3 | 19% | x | | | | x | | | | | | x | | | | | |
| Vibration | 1 | 6% | | | | | | | | x | | | | | | | | |
| Friction | 4 | 25% | | x | x | x | | | | | | | x | | | | | |

# Appendix C: Compiled Results of ME 366J Student Survey

Unmodified Data: Total Responses = 17

**1. What type of product did you dissect? (choose the best description)**

| | | |
|---|---|---|
| Mainly Electrical (i.e. TV Remote Control) | 0 | 0% |
| Mainly Mechanical (i.e. Fishing Reel) | 7 | 41% |
| Mainly Pneumatic (i.e. Vacuum) | 2 | 12% |
| Mechatronic (i.e. Power tools) | 8 | 47% |

**2. What is the product?**

| |
|---|
| Lil' Sew and Sew hand stitcher |
| Shark HH vacuum |
| Nerf gun |
| A rotating tie rack |
| Handheld sewing machine |
| Rotato Express |
| Traveling Tractor Sprinkler |
| The Claw (personal version of the claw arcade game) |
| Automatic Peeler |
| Automatic tennis ball launcher for dogs made by Go Dog Go |
| automatic hose reel (water powered) |
| iPong robot |
| A ping pong robot |
| A handheld sewing machine |
| NERF Vortex Gun |
| Garden Groom (hedge trimmer) |
| Tennis ball launcher |

**3. How difficult would you say it was to dissect?**

| | | |
|---|---|---|
| Easy | 11 | 65% |
| Medium | 4 | 24% |
| Difficult | 2 | 12% |

**4. What was the hardest part of the dissection?**

| | | |
|---|---|---|
| Fasteners | 5 | 29% |
| Outer casing | 2 | 12% |
| Removing the different parts inside (motor, switch, etc) | 10 | 59% |

**5. How long would you estimate the dissection process took?**

| | | |
|---|---|---|
| 0-1 hr | 6 | 35% |
| 2-4 hrs | 11 | 65% |
| 5-7 hrs | 0 | 0% |
| 8-10 hrs | 0 | 0% |
| >10 hrs | 0 | 0% |

**6. What tools did you use? (Select all that apply)**

| | | |
|---|---|---|
| Screwdriver (Phillips) | 17 | 100% |
| Screwdriver (Flathead) | 11 | 65% |
| Pliers | 10 | 59% |
| Drill | 2 | 12% |
| Hex Keys | 1 | 6% |
| Knife (Xacto or regular) | 1 | 6% |
| Manual Saw | 1 | 6% |
| Open ended wrench | 1 | 6% |
| Screwdriver (Torx) | 1 | 6% |
| Soldering iron | 1 | 6% |
| Wire Cutter | 1 | 6% |
| Power Saw | 0 | 0% |
| Socket wrench | 0 | 0% |
| Vice Grip | 0 | 0% |

**7. During the dissection process, which of these metrics did you measure before, during, and after the product was disassembled? (Select all that apply)**

| | | |
|---|---|---|
| Geometry | 13 | 76% |
| Weight | 8 | 47% |
| Torque (of either a powered motor or mechanical parts) | 2 | 12% |
| Force (of either a powered motor of mechanical parts) | 2 | 12% |
| Elect. Properties | 2 | 12% |
| Material properties (tensile/compressive strength, yield strength, young's modulus) | 1 | 6% |
| Temperature | 0 | 0% |

| | | |
|---|---|---|
| Light intensity | 0 | 0% |
| Surface Roughness | 0 | 0% |
| Material Hardness | 0 | 0% |
| Air speed | 0 | 0% |
| pressure (air) | 0 | 0% |
| pressure (liquid) | 0 | 0% |
| Sound intensity | 0 | 0% |

**8. What tools did you use to measure these metrics?**

| | | |
|---|---|---|
| caliper | 10 | 59% |
| scale | 6 | 35% |
| ruler | 6 | 35% |
| tape measure | 5 | 29% |
| Force gauge | 2 | 12% |
| Multimeter (voltage, resistance, current, capacitance) | 2 | 12% |
| Torque gauge | 1 | 6% |
| laser range finder | 0 | 0% |
| Thermometer (mercury or digital) | 0 | 0% |
| thermocouple | 0 | 0% |
| laser thermometer | 0 | 0% |
| IR camera | 0 | 0% |
| Hardness Tester | 0 | 0% |
| Tensile/compressive tester | 0 | 0% |
| Light intensity meter | 0 | 0% |
| Surface roughness meter | 0 | 0% |
| Decibel meter | 0 | 0% |
| Wind speed gauge | 0 | 0% |
| hot wire anemometer | 0 | 0% |
| Pressure gauge | 0 | 0% |
| manometer | 0 | 0% |

**9. Please state any recommended tools you would like to see in a reverse engineering toolbox for use in ME 366J**

| |
|---|
| More scales |
| Just basic stuff, like screwdrivers. Our disassembly was very easy, so maybe I'm biased. |

| |
|---|
| Please make the tools more accessible (scale was locked in a closet and we had to wait for our TA to be available to get it out). Accessible calipers would also be nice. And mainly, it needs some serious organization. A real tool chest would be great. That room is a mess and there's no telling where you will find what. |
| More sets of calipers. Fishing line. Exacto knife that stays open (does not automatically spring shut) |
| metal hammer, calipers, chisel, band saw |
| More assortment of screwdrivers. |

Modified Data: Total Responses = 11

**1. What type of product did you dissect? (choose the best description)**

| | | |
|---|---|---|
| Mainly Electrical (i.e. TV Remote Control) | 0 | 0% |
| Mainly Mechanical (i.e. Fishing Reel) | 5 | 45% |
| Mainly Pneumatic (i.e. Vacuum) | 1 | 9% |
| Mechatronic (i.e. Power tools) | 5 | 45% |

**3. How difficult would you say it was to dissect?**

| | | |
|---|---|---|
| Easy | 7 | 64% |
| Medium | 2 | 18% |
| Difficult | 2 | 18% |

**4. What was the hardest part of the dissection?**

| | | |
|---|---|---|
| Fasteners | 2 | 18% |
| Outer casing | 2 | 18% |
| Removing the different parts inside (motor, switch, etc) | 7 | 64% |

**5. How long would you estimate the dissection process took?**

| | | |
|---|---|---|
| 0-1 hr | 4 | 36% |
| 2-4 hrs | 7 | 64% |
| 5-7 hrs | 0 | 0% |
| 8-10 hrs | 0 | 0% |
| >10 hrs | 0 | 0% |

**6. What tools did you use? (Select all that apply)**

| | | |
|---|---|---|
| Screwdriver (Phillips) | 11 | 100% |
| Screwdriver (Flathead) | 8 | 73% |
| Pliers | 7 | 64% |
| Drill | 1 | 9% |
| Hex Keys | 1 | 9% |
| Knife (Xacto or regular) | 1 | 9% |
| Manual Saw | 1 | 9% |
| Open ended wrench | 1 | 9% |
| Screwdriver (Torx) | 1 | 9% |
| Soldering iron | 1 | 9% |
| Wire Cutter | 1 | 9% |
| Power Saw | 0 | 0% |

| | | |
|---|---|---|
| Socket wrench | 0 | 0% |
| Vice Grip | 0 | 0% |

**7. During the dissection process, which of these metrics did you measure before, during, and after the product was disassembled? (Select all that apply)**

| | | |
|---|---|---|
| Geometry | 8 | 73% |
| Weight | 5 | 45% |
| Force | 2 | 18% |
| Elec. Properties | 2 | 18% |
| Torque | 1 | 9% |
| Material properties | 1 | 9% |
| Temperature | 0 | 0% |
| Light intensity | 0 | 0% |
| Surface Roughness | 0 | 0% |
| Material Hardness | 0 | 0% |
| Flow Rate | 0 | 0% |
| pressure | 0 | 0% |
| Sound intensity | 0 | 0% |

**8. What tools did you use to measure these metrics?**

| | | |
|---|---|---|
| caliper | 6 | 55% |
| scale | 4 | 36% |
| ruler | 3 | 27% |
| tape measure | 3 | 27% |
| Multimeter (voltage, resistance, current, capacitance) | 2 | 18% |
| Force gauge | 1 | 9% |
| Torque gauge | 1 | 9% |
| laser range finder | 0 | 0% |
| Thermometer (mercury or digital) | 0 | 0% |
| thermocouple | 0 | 0% |
| laser thermometer | 0 | 0% |
| IR camera | 0 | 0% |
| Hardness Tester | 0 | 0% |
| Tensile/compressive tester | 0 | 0% |
| Light intensity meter | 0 | 0% |
| Surface roughness meter | 0 | 0% |
| Decibel meter | 0 | 0% |

| | | |
|---|---|---|
| Wind speed gauge | 0 | 0% |
| hot wire anemometer | 0 | 0% |
| Pressure gauge | 0 | 0% |
| manometer | 0 | 0% |

# Appendix D: Bill of Materials for Dynamometer

| Part Number | Man. Number | Part Name | Description | Supplier | Price ea. | Quantity | Subtotal |
|---|---|---|---|---|---|---|---|
| 9 | 5G108-RW5 | Ethernet Jack | Connect dyno to controller | Mouser | $ 6.99 | 1 | $ 6.99 |
| 13 | - | Index Wheel | To reflect IR beam to sensor | US Digital | $ - | 1 | $ - |
| 14 | E4P | IR TX/RX | To register revolutions | US Digital | $ 35.10 | 1 | $ 35.10 |
| 12 | - | Hard Drive Platter | Use as rotor | Discount Electronics | $ 20.00 | 1 | $ 20.00 |
| 1 | - | Dremel Chuck | Mini chuck for Dremel Tool | Home Depot | $ 10.98 | 1 | $ 10.98 |
| - | - | 8-32 x 5/8" Screw | - | Home Depot | $ 0.60 | 8 | $ 4.80 |
| - | - | 8-32 X 0.75" Screw | - | Home Depot | $ 0.55 | 4 | $ 2.20 |
| - | - | 6-32 X 0.5" Screw | - | Home Depot | $ 0.35 | 8 | $ 2.80 |
| - | - | 4-40 x 3/8" Screw | - | Home Depot | $ 0.33 | 6 | $ 1.98 |
| 6 | 1327k115 | Drive Shaft | 0.25" OD 12L14 | McMaster-Carr | $ 3.78 | 1 | $ 3.78 |
| 3 | 57155K336 | Shaft Bearings | 1/4" ID, 3/8" OD, 56,000 RPM | McMaster-Carr | $ 7.00 | 2 | $ 14.00 |
| 10 | 91125a493 | Threaded Spacer | 2" long, 8-32 Threading | McMaster-Carr | $ 2.98 | 4 | $ 11.92 |
| 16 | 9414t6 | Shaft Collar | 1/4" ID, Secure drive shaft | McMaster-Carr | $ 0.60 | 2 | $ 1.20 |
| 11 | - | 1.625" Aluminum Cyl. | Use to make Spindle | Online Metals | $ 4.38 | 1 | $ 4.38 |
| 4,5,7,8,15 | - | 1.75" x 0.375" Aluminum Bar | Use to make Housing panels | Online Metals | $ 7.96 | 1 | $ 7.96 |
| 2 | - | 0.5" Aluminum Cyl. | Use to make chuck adapter | Online Metals | $ 1.10 | 1 | $ 1.10 |
| | | | | | | **Total** | $ 129.19 |

# Appendix E: Dynamometer Operating Instructions

PLEASE READ ALL WARNINGS AND PRECAUTIONS. AUTHOR IS NOT RESPONSIBLE FOR INJURY CAUSED BY MISUSE OF PRODUCT

The dynamometer uses a spinning disk that can reach speeds up to 10,000 RPM. Even though every care has been taken to design a safe and robust machine, accidents can happen. Spinning flywheels can store a tremendous amount of kinetic energy, and if they rupture, the resulting shrapnel can cause serious damage. NEVER OPERATE THE DYNAMOMETER WITH THE COVER OPEN! The acrylic case has been built to protect against and slow down any accidental rupture of the disk. This is not a fool proof system, and because of that, ALWAYS USE SAFETY GLASSES!

The system has been designed for 10,000 RPM maximum, but it is recommended to stay under 7,000 RPM to account for any misalignments between the motor and the chuck.

# Introduction

The TorkBlock dynamometer system was built to allow the user to measure the power output of fractional horsepower DC and AC motors. This is a helpful tool to aid in quantification during reverse engineering.

The TorkBlock is based on an inertial dynamometer: the motor spins a disk of known mass, and the acceleration of the disk is measured. These acceleration values are then converted to torque using the relation

$$Torque = angular\ acceleration * moment\ of\ inertia$$

The torque is then plotted against the angular velocity values to obtain the torque-speed curve for the motor. In addition, the power output of the motor can be found using the relation

$$Power = torque * angular\ velocity$$

The dynamometer was designed and built to be as accurate and robust as possible. However, keep in mind that this is a prototype and that it is not a perfect tool; therefore, measurements cannot be guaranteed 100%, but rather should be taken as an approximate value.

# System Description

The dynamometer measurement system consists of two major components: the dynamometer assembly and the controller. The assembly is shown in detail below:

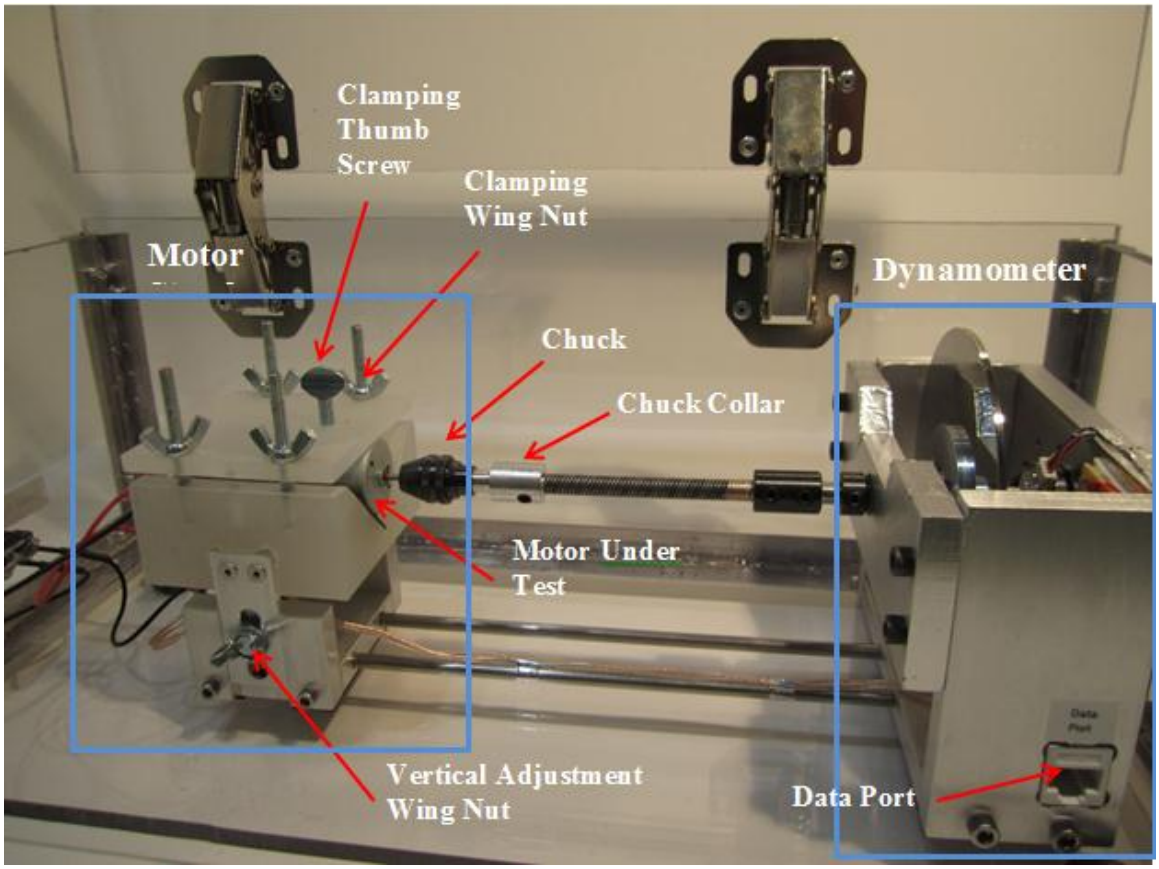


The motor stand, shown on the left, is used to secure the motor under test. The clamping wing nuts are used to clamp down on the motor using the flat adjustable clamp above the motor. The clamping thumb screw is used in cases where the motor is smaller than the "V" shape of the block, where it can reach down and secure the motor.

The Vertical adjustment wing nuts (one on each side) are used to set the height of the motor stand in order to line up the motor shaft and the chuck. The chuck is then used to tighten onto the shaft of the motor, resulting in a secure connection to the dynamometer.

The dynamometer, shown on the right, consists of the rotating assembly and tachometer used to measure the power output of the motor. It interfaces with the controllers using a single data port.

The two different controllers are shown below:


The standalone controller, shown on the left, is battery powered, and stores the gathered data on board using an SD memory card. Two buttons are used to input user commands, and a single LCD screen communicates with the user. It interfaces with the dynamometer using the yellow cable.

The tethered controller, a National Instruments myDAQ system, is a data acquisition module designed to be used with LabView. The user interface is taken care of by means of a Virtual Instrument (VI), discussed more in detail below. The myDAQ also interfaces with the dynamometer using the yellow cable.

## Standalone Controller

The standalone controller, as its name implies, does not need a separate computer to gather data. It does, however, need a computer to read the stored data on the memory card. It is shown in detail below:

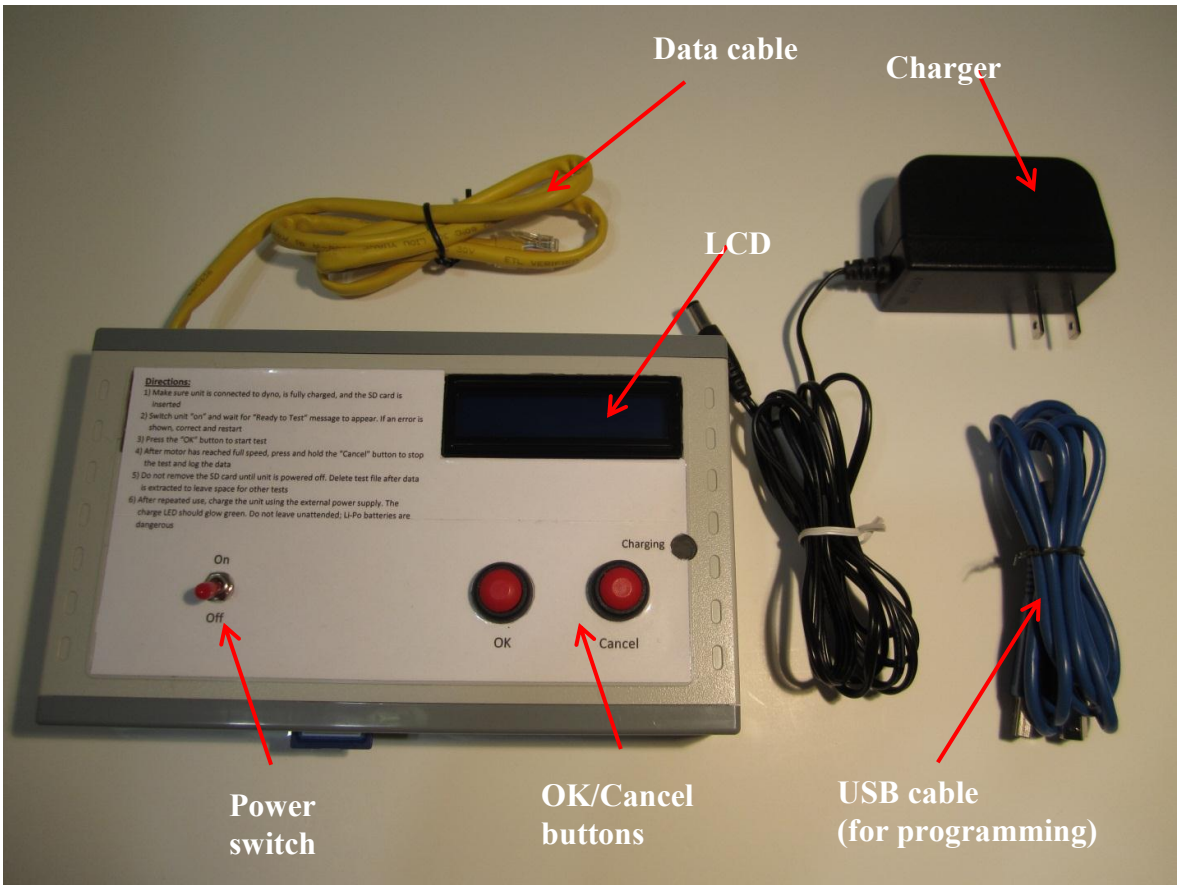

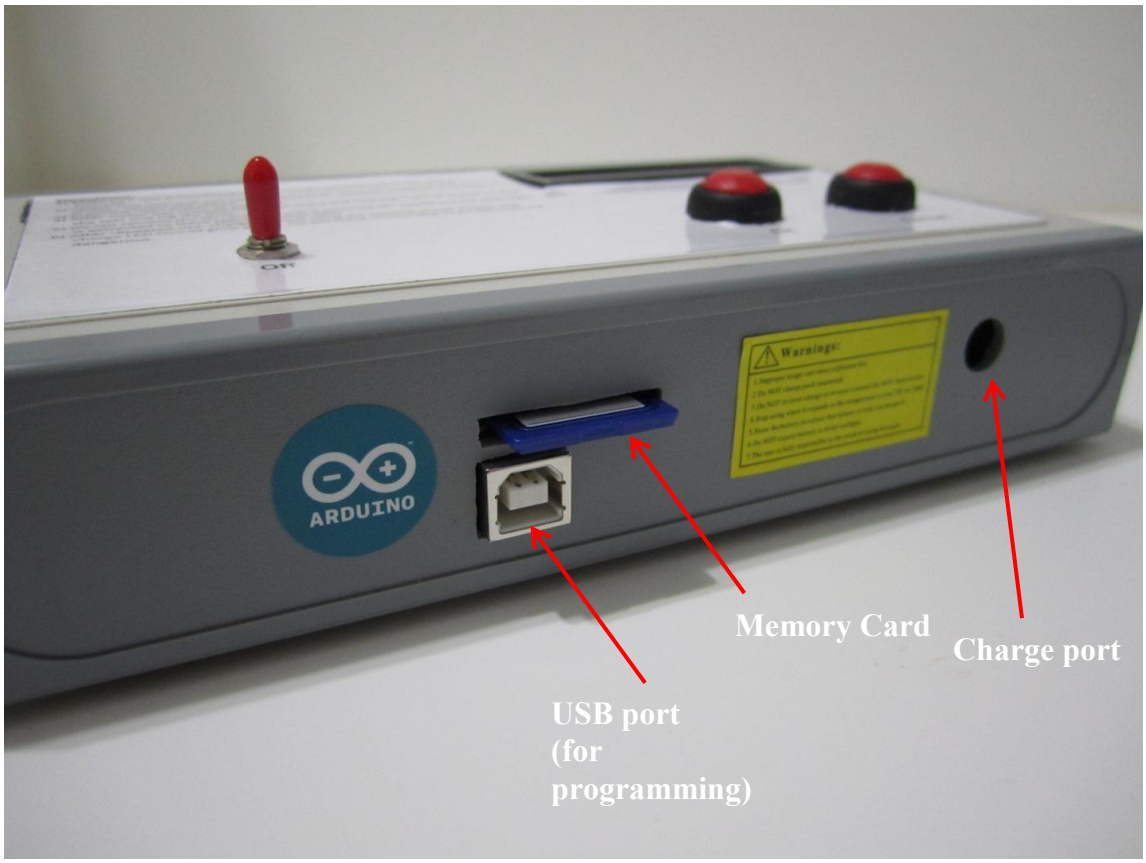
ARDUINO
Memory Card
Charge port
USB port
(for
programming)

## NI myDAQ

The myDAQ module is the other controller able to interface with the dynamometer. It is not an independent controller; it is rather dependent on a computer running NI's LabView software. It is shown below:

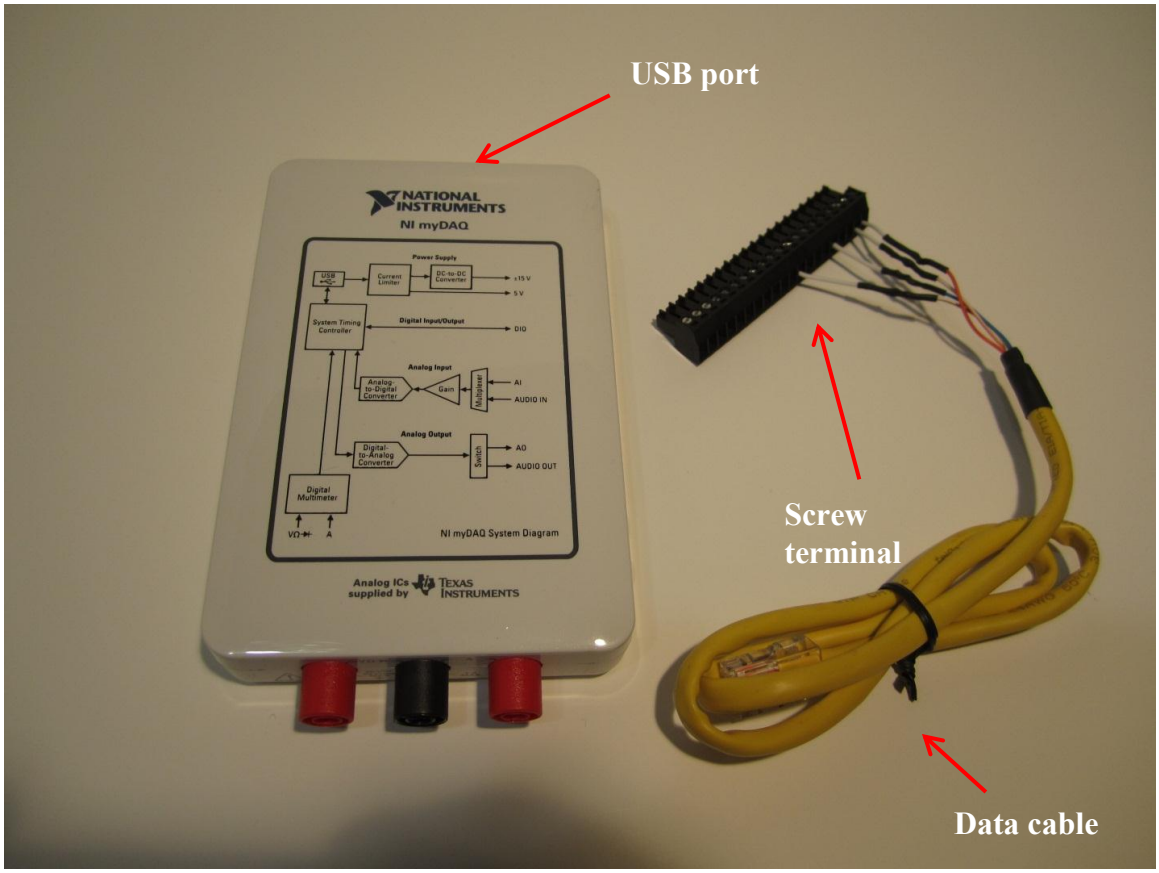

# Taking Measurements

The TorkBlock dynamometer system has been designed to be as user friendly as possible. Taking a measurement consists of six steps, outlined below:

a. Attach power supply cables to motor
b. Secure motor to motor stand
c. Connect motor to dynamometer
d. Connect power supply to screw terminals
e. Connect controller of choice
f. Start test

**a) Attach power supply cables to motor**

Use the built in alligator clips and attach to the motor's power terminals. Make sure the clips are insulated properly and are not touching each other.

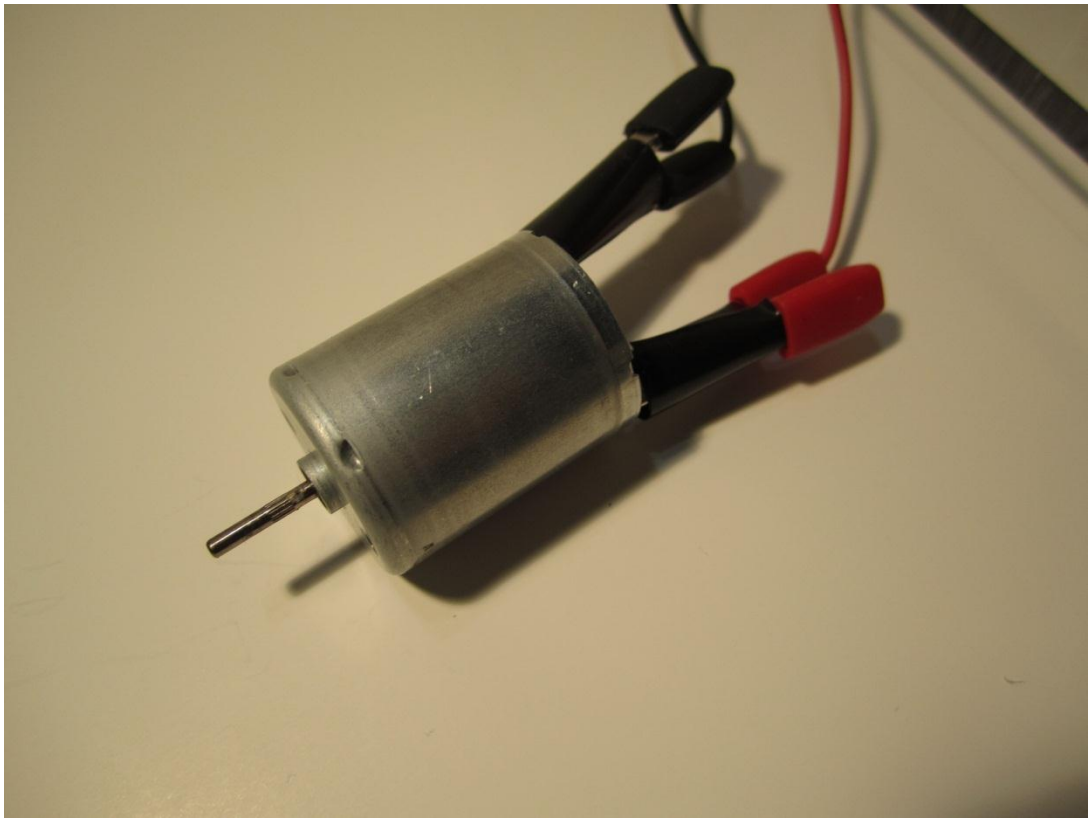

**b) Secure motor to motor stand**

This is an important step, since an improperly motor will move about during the test, possibly causing damage and injury.

Slide the motor stand backwards to clear the chuck. Slide the motor into the V block and use the four wing nuts on top to clamp down onto the motor. If the motor is too small for the V block, use the thumb screw in the middle to clamp down onto it.

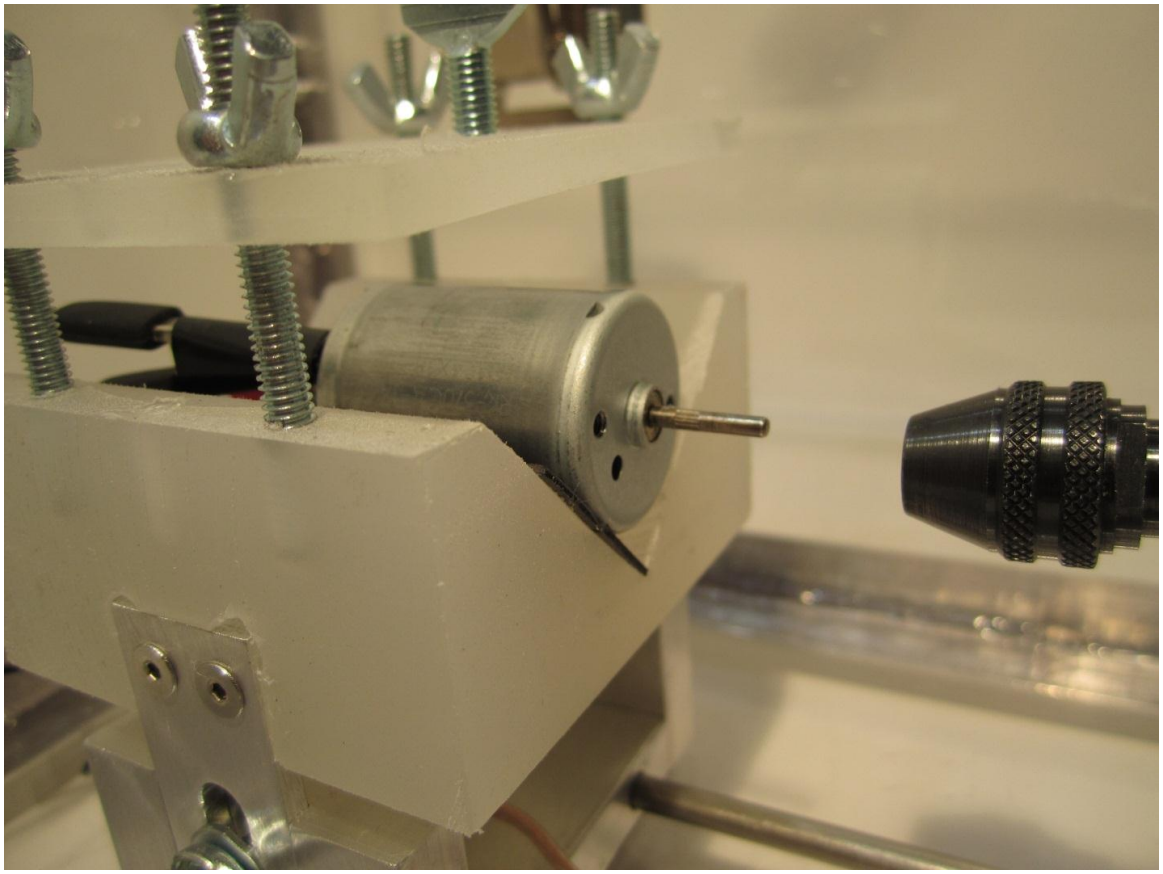

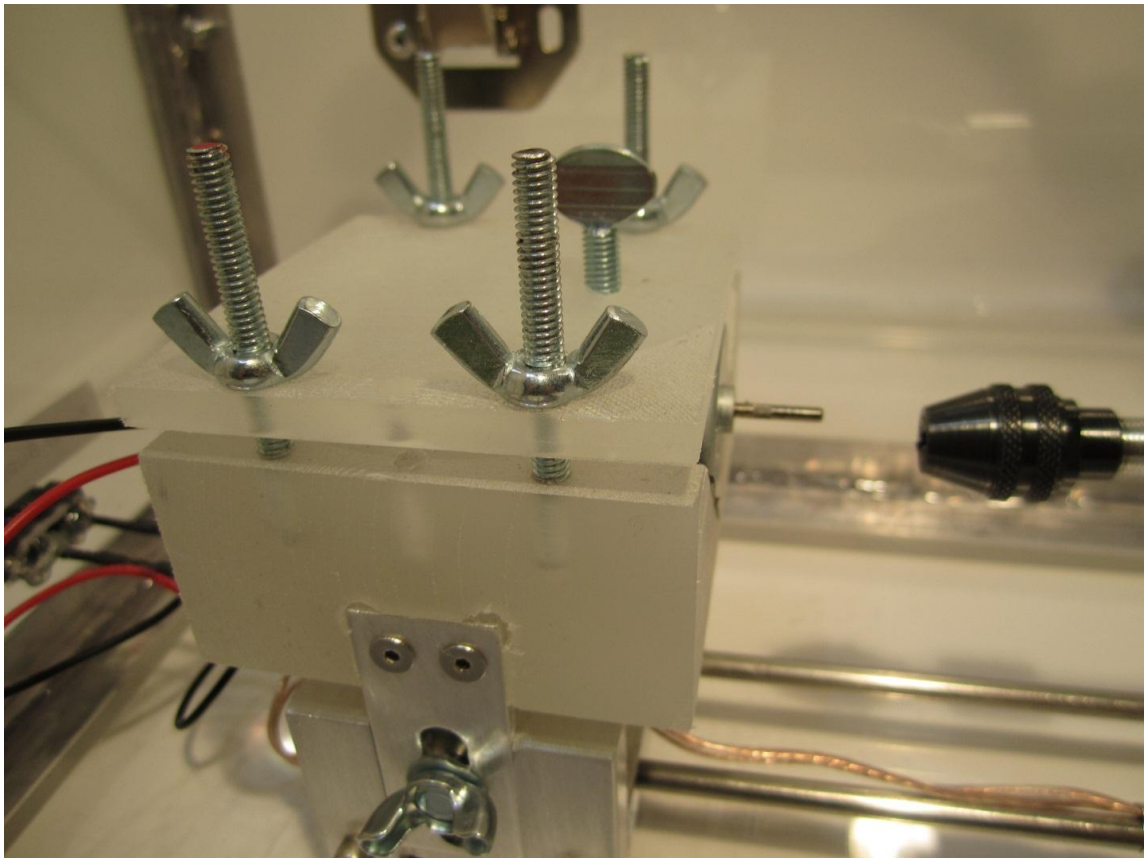

**c) Attach motor to dynamometer**

This is the most sensetive step in the preperation procedure, and should be performed CAREFULLY. Double check your work before proceeding.

Loosen the vertical adjustment wing nuts and adjust the heigh of the motor stand until it is somewhere close to the height of the chuck, then tighten temporarily. Slide the motor stand forward, inserting the shaft into the chuck. With one hand holding the collar, and the other holding the chuck, tighten the chuck clockwise until it is secured to the shaft.

Loosen the wing nuts again, this time adjusting the height so that the flexible shaft is as level as can possible be. Even though the flexible shaft is designed to account for minor misalignments, the closer it is to straight, the better the measurements will be. When you are done, tighten the wing nuts securely.

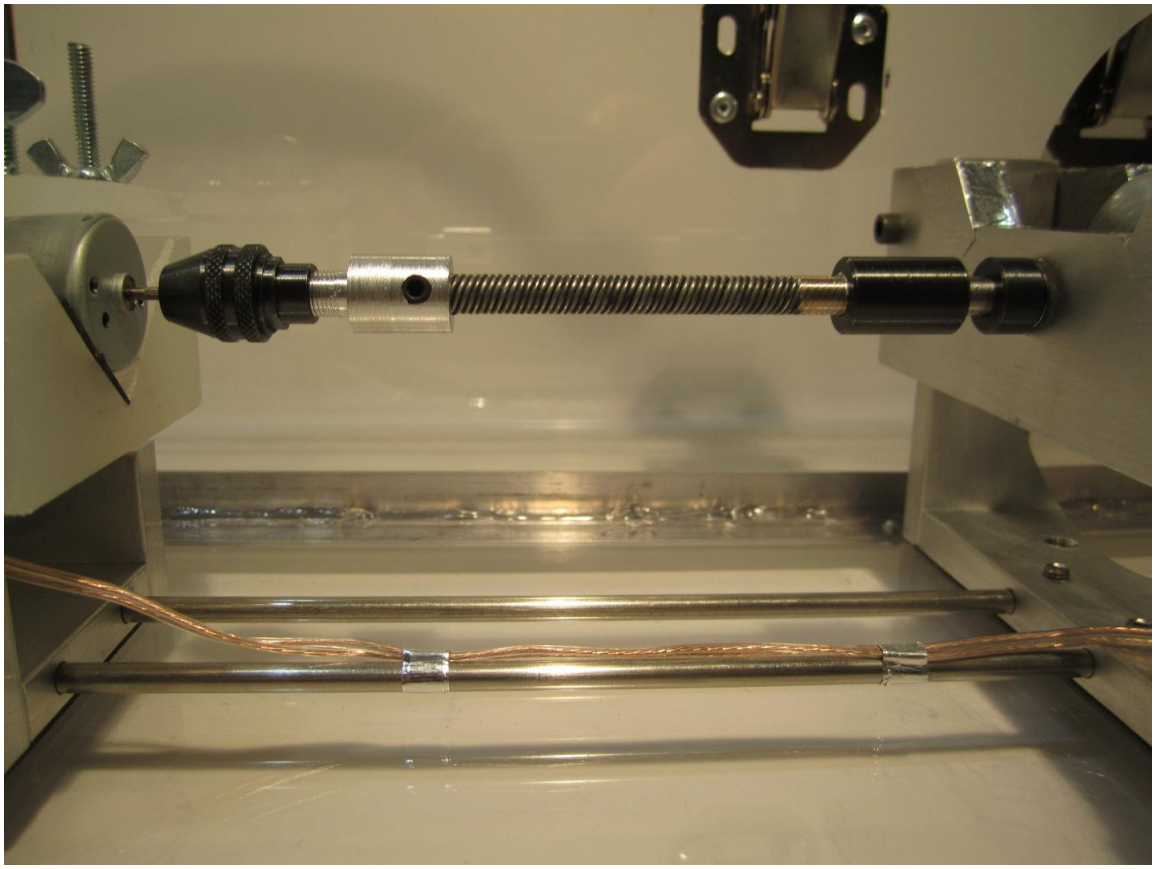

**d) Connect power supply to screw terminals**

Use the screw terminals located on the case to supply power to the motor. The power system accepts both DC and AC voltage, depending on the motor being tested. Insert the two leads into the two OUTERMOST terminals and tighten securely.

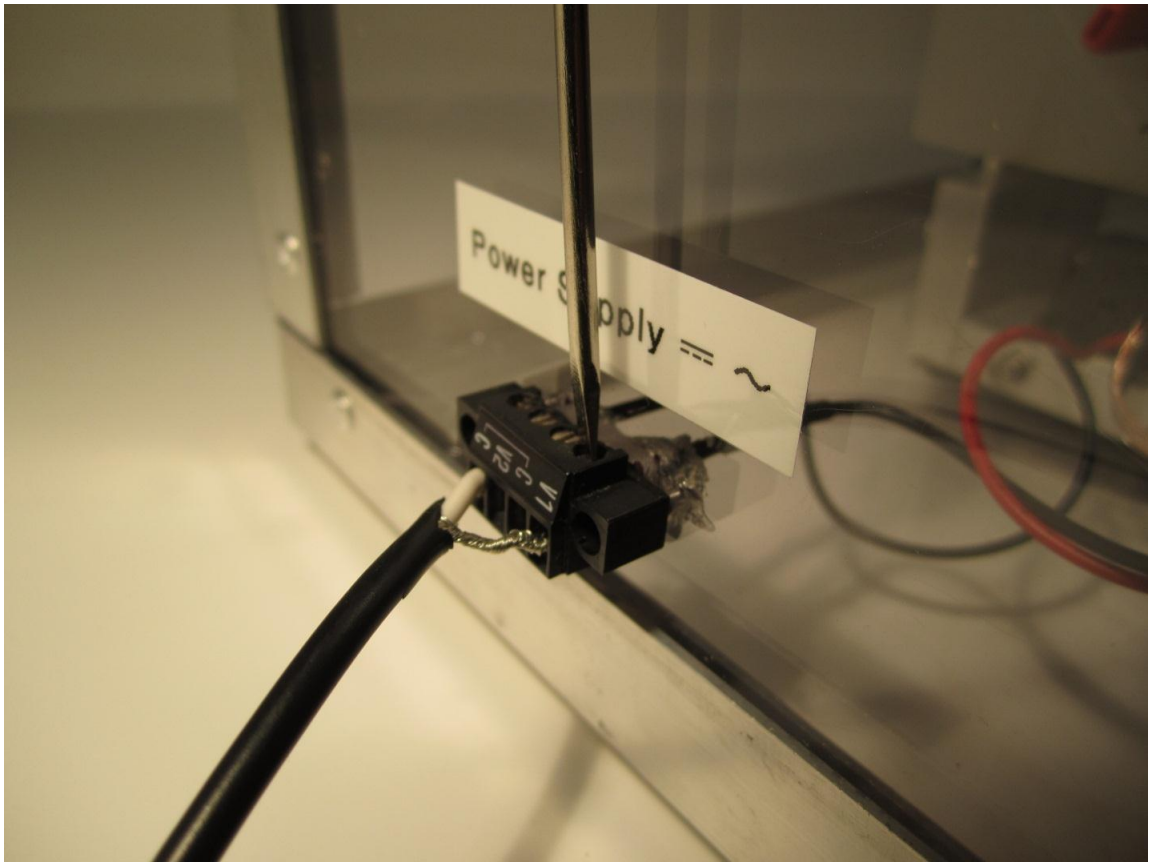

**e) Connect controller of choice**

Simply slide the data cable connector into the data port.

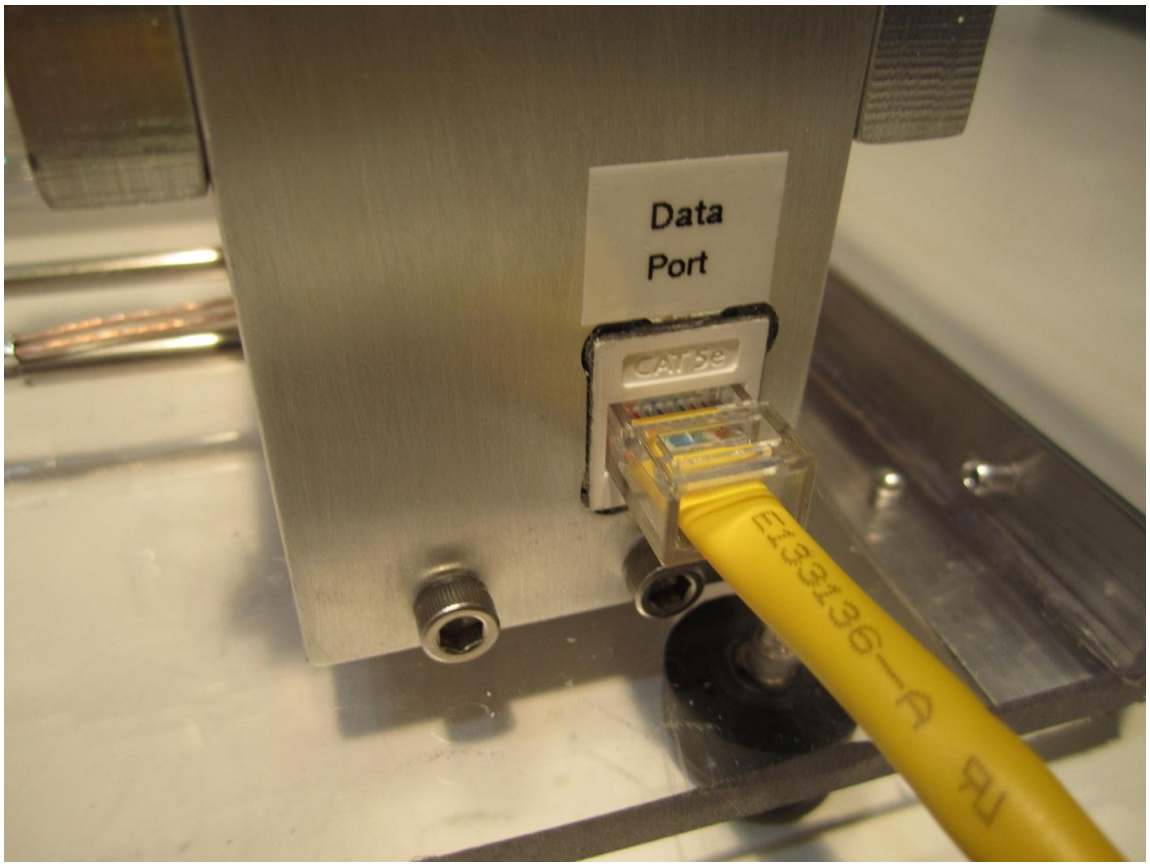

**f) Start test**

**IMPORTANT: Make sure the lid is closed before proceeding. Running the dynamometer with case open exposes you to danger if any components fail. ALWAYS WEAR YOUR SAFETY GLASSES!**

Depending on the controller used, the method differs slightly. Both methods are outlined below:

Standalone controller

To start a measurement session with the standalone controller, turn the unit on and wait for the "Ready to test" message to appear on the LCD. If any error appears, refer to the troubleshooting section.

Press the OK button to start the test. The relay will switch on and power will be supplied to the motor. The motor will then accelerate until it reaches full speed. When that happens, press and hold the CANCEL button until the relay switches off, and the LCD shows "Test Complete!"

The controller then writes the data to file, and prompts the user to turn off the controller. Remove the memory card from the unit and insert into the computer. The memory card will contain an excel files of the data measured.

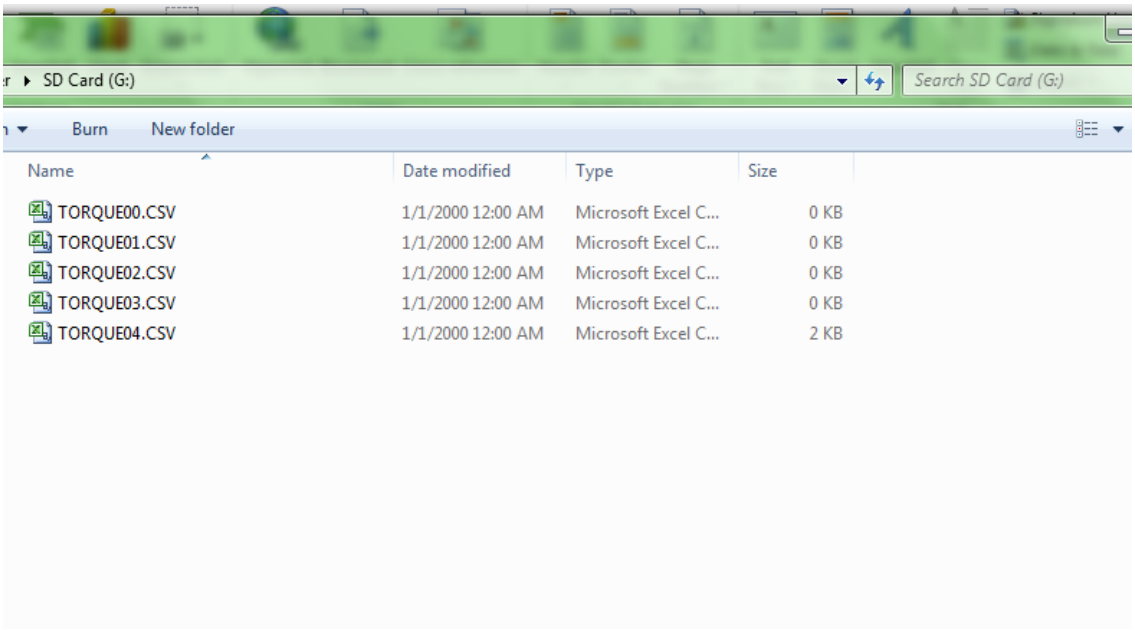

The files are labeled in the order of testing. Once the file is opened, a table with three columns should be present: angular speed, torque, and power. Notice the top of the file includes a timestamp for future reference. If the time stamp shows an error instead, refer to the troubleshooting section.

Insert a XY scatter graph, at which point the torque speed curve and the power curve can be analyzed. Refer to the "Interpreting Data" section for more information on how to read the results.

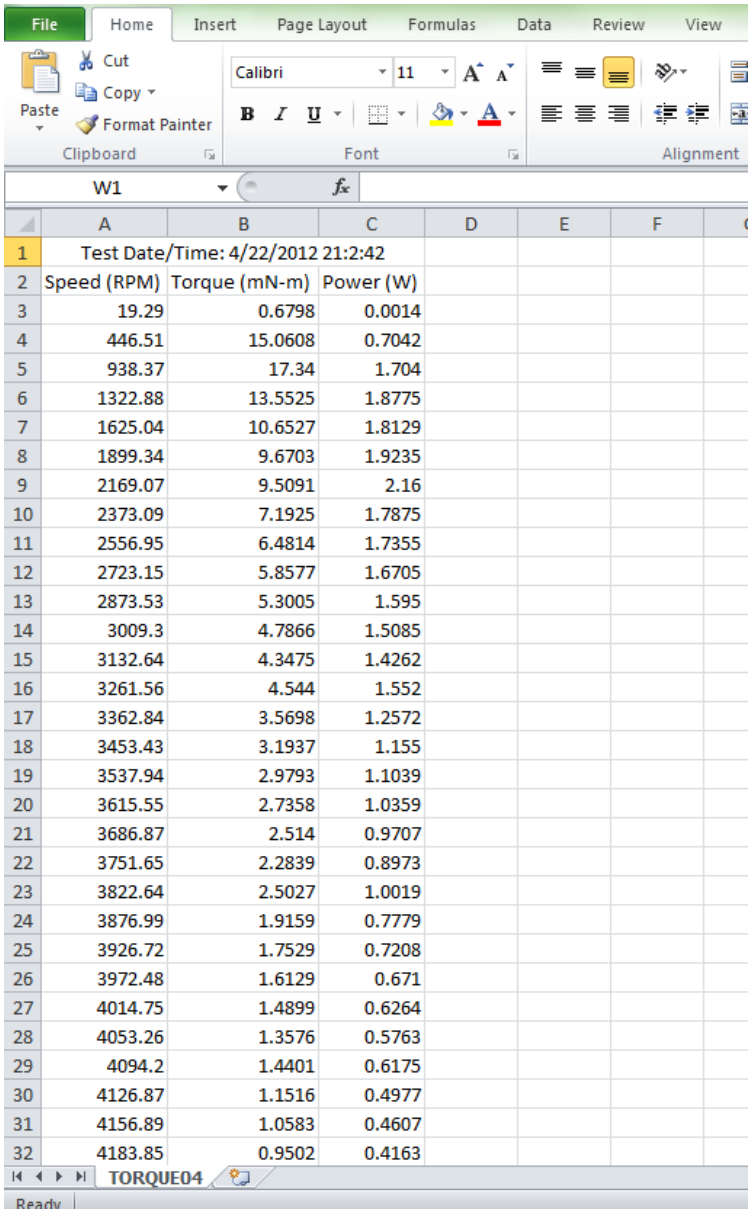


| | A | B | C | D | E | F |
|---|---|---|---|---|---|---|
| 1 | Test Date/Time: 4/22/2012 21:2:42 | | | | | |
| 2 | Speed (RPM) | Torque (mN-m) | Power (W) | | | |
| 3 | 19.29 | 0.6798 | 0.0014 | | | |
| 4 | 446.51 | 15.0608 | 0.7042 | | | |
| 5 | 938.37 | 17.34 | 1.704 | | | |
| 6 | 1322.88 | 13.5525 | 1.8775 | | | |
| 7 | 1625.04 | 10.6527 | 1.8129 | | | |
| 8 | 1899.34 | 9.6703 | 1.9235 | | | |
| 9 | 2169.07 | 9.5091 | 2.16 | | | |
| 10 | 2373.09 | 7.1925 | 1.7875 | | | |
| 11 | 2556.95 | 6.4814 | 1.7355 | | | |
| 12 | 2723.15 | 5.8577 | 1.6705 | | | |
| 13 | 2873.53 | 5.3005 | 1.595 | | | |
| 14 | 3009.3 | 4.7866 | 1.5085 | | | |
| 15 | 3132.64 | 4.3475 | 1.4262 | | | |
| 16 | 3261.56 | 4.544 | 1.552 | | | |
| 17 | 3362.84 | 3.5698 | 1.2572 | | | |
| 18 | 3453.43 | 3.1937 | 1.155 | | | |
| 19 | 3537.94 | 2.9793 | 1.1039 | | | |
| 20 | 3615.55 | 2.7358 | 1.0359 | | | |
| 21 | 3686.87 | 2.514 | 0.9707 | | | |
| 22 | 3751.65 | 2.2839 | 0.8973 | | | |
| 23 | 3822.64 | 2.5027 | 1.0019 | | | |
| 24 | 3876.99 | 1.9159 | 0.7779 | | | |
| 25 | 3926.72 | 1.7529 | 0.7208 | | | |
| 26 | 3972.48 | 1.6129 | 0.671 | | | |
| 27 | 4014.75 | 1.4899 | 0.6264 | | | |
| 28 | 4053.26 | 1.3576 | 0.5763 | | | |
| 29 | 4094.2 | 1.4401 | 0.6175 | | | |
| 30 | 4126.87 | 1.1516 | 0.4977 | | | |
| 31 | 4156.89 | 1.0583 | 0.4607 | | | |
| 32 | 4183.85 | 0.9502 | 0.4163 | | | |

NI myDAQ

Plug the USB cable into the computer running LabView. Open the VI labeled "TorkBlock.vi" or "TorkBlock_filter.vi," the difference being that the second VI includes an adjustable moving average filter to smooth out the data.

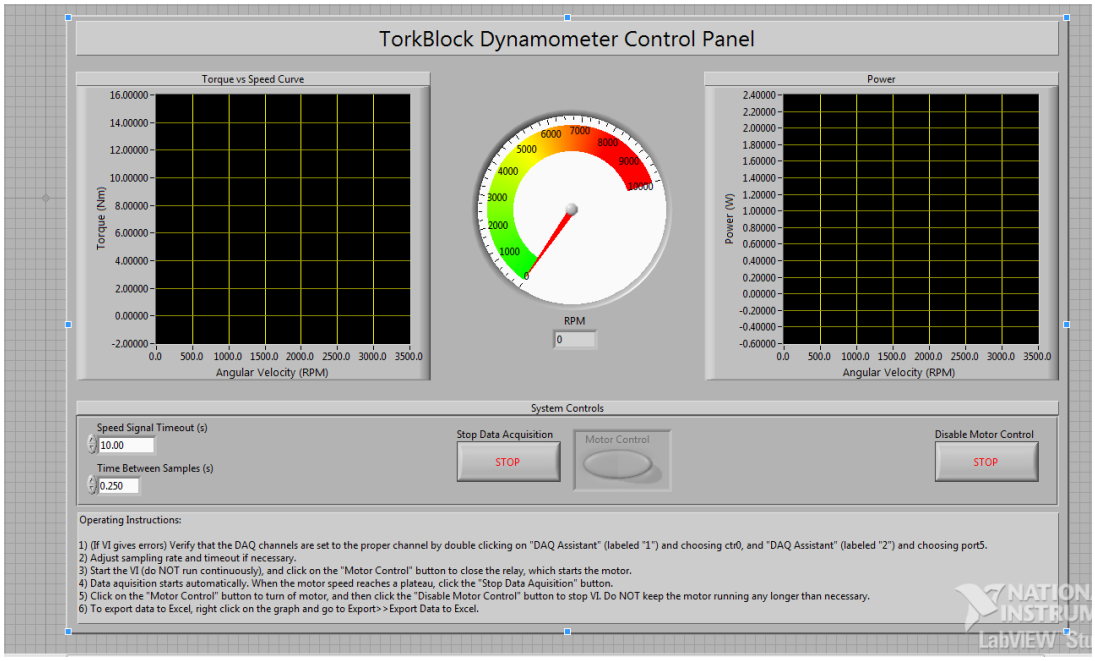


When ready, start the VI by clicking on the arrow on the top. Do NOT choose the "run continuously" button. Press the "Motor Control" button to start the motor. The motor will accelerate and reach full speed. Data is displayed live on the graphs.

When the motor reaches full speed, press the "Stop Data Acquisition" button to stop data logging. It is important that this step be done first, or else the data will be corrupted from deceleration of the motor.

Afterwards, press the "Motor Control" button to stop the motor. Finally, press the "Disable Motor Control" to stop the VI.

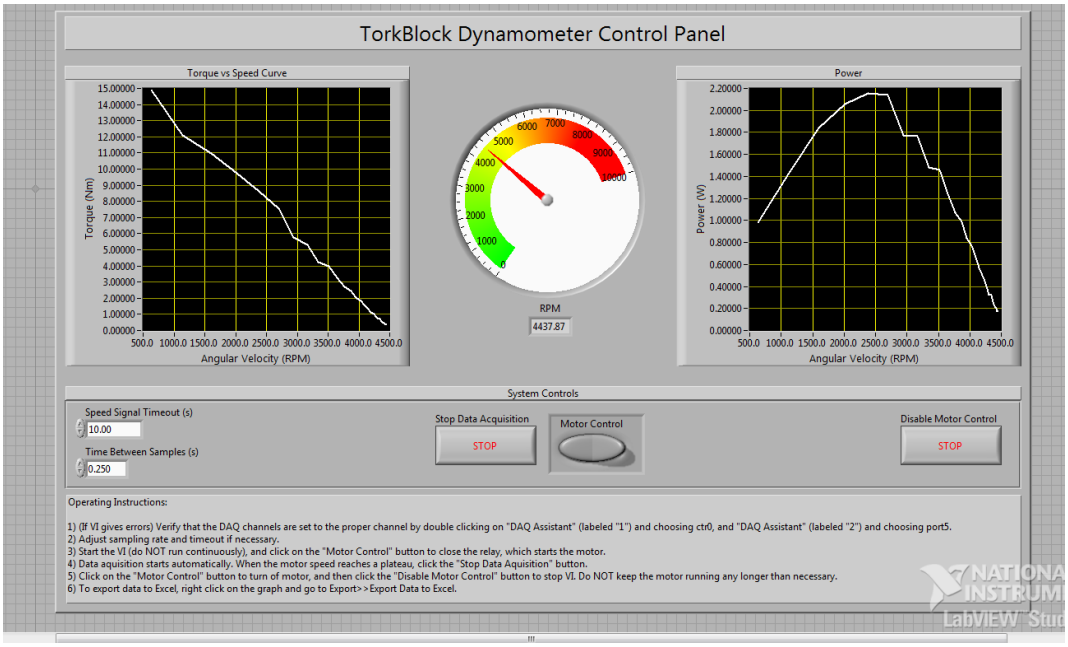


The data can be exported to Excel by right clicking on either the Torque or Power graphs, then selecting Export>>Export Data to Excel. Refer to the "Interpreting Data" section for more information on how to read the results.

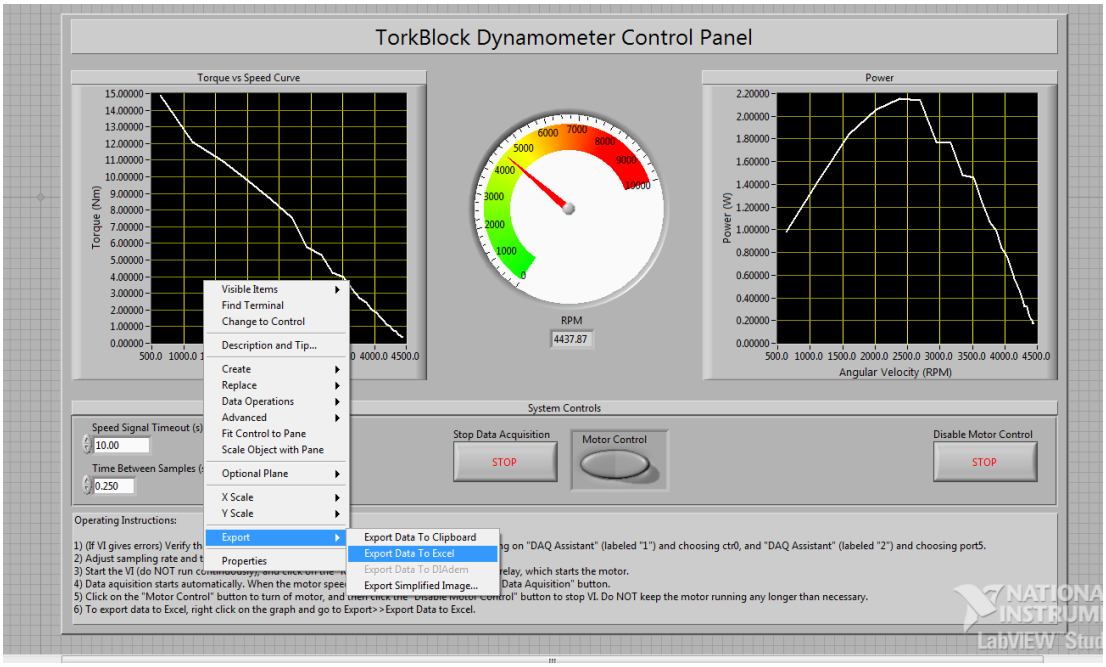

# Interpreting Data

An example torque data set from the NI myDAQ is seen below, after being exported to Excel:

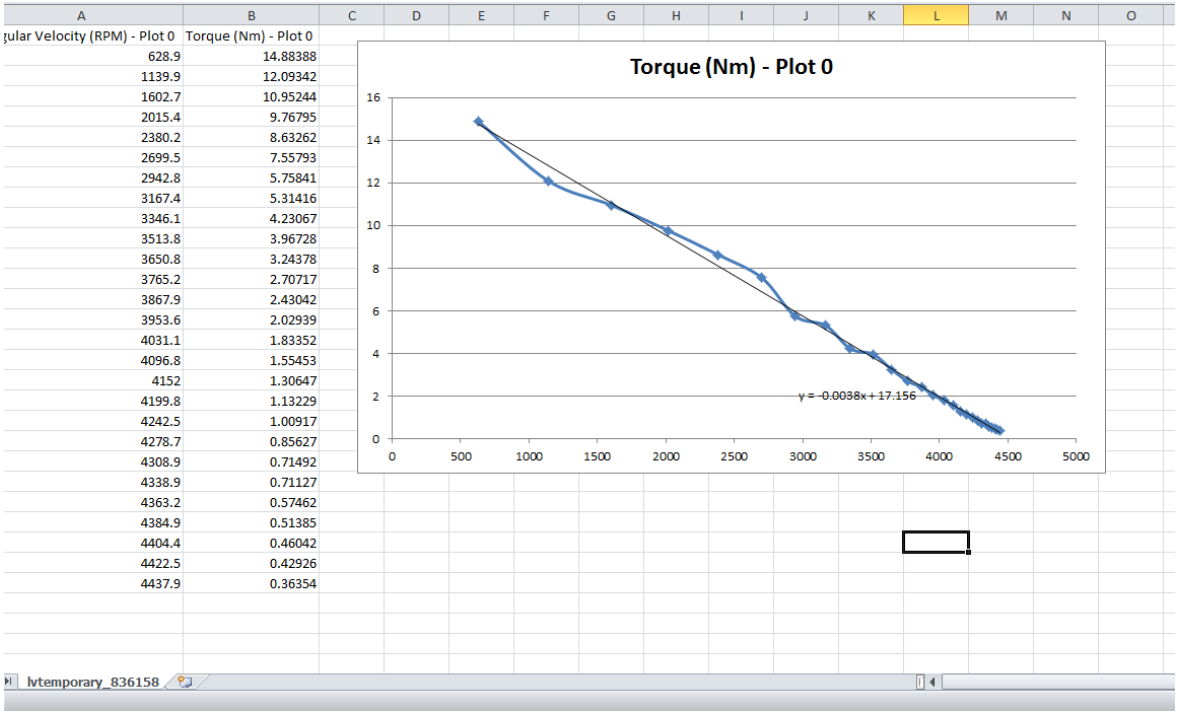


The dataset was then graphed using a XY scatter plot: torque on the Y-axis, angular velocity on the X-axis. A linear curve fit was then performed. The Y-intercept, as shown in the equation below the graph, is the stall torque. This is the maximum amount of torque a DC motor can make, which occurs when the motor is not rotating. The X-intercept is the no-load speed; the maximum speed the motor can accelerate to, which occurs when there is no load on the motor. These are the two most important characteristics of a DC motor, which then allow the user to get an idea of how the motor will behave.

Due to calibration errors, signal noise, and unforeseen variables, the measured data is rarely perfect. As a result, some data manipulation and analysis must be done to interpret what the motor's characteristics truly are.

The power curve of a motor can vary from a perfect linear relationship, depending on the type of motor it is. However, for most DC motors, it generally follows a linear trend. Sometimes, artifacts due to starting conditions can be present in the data, shown below:

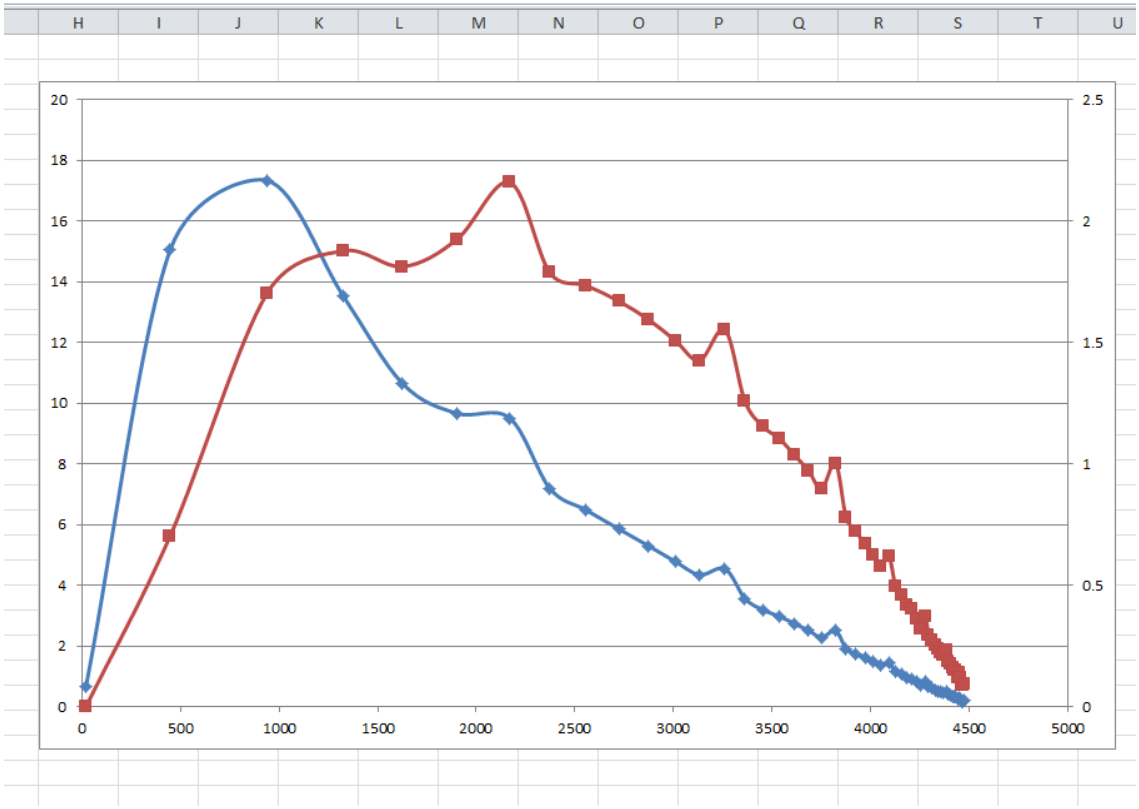


A peak can be seen in the torque curve (blue), at which it then follows a linear trend downwards to no-load speed. This condition does not allow the direct measurement of the stall torque, since the graph does not intersect the Y axis cleanly. In addition, if a linear curve fit is performed on the raw data, the Y-intercept will be skewed by the data points leading up to the peak.

To remedy the situation, the first few data points are eliminated, leaving the linear portion with which a linear curve fit can be performed, shown below:

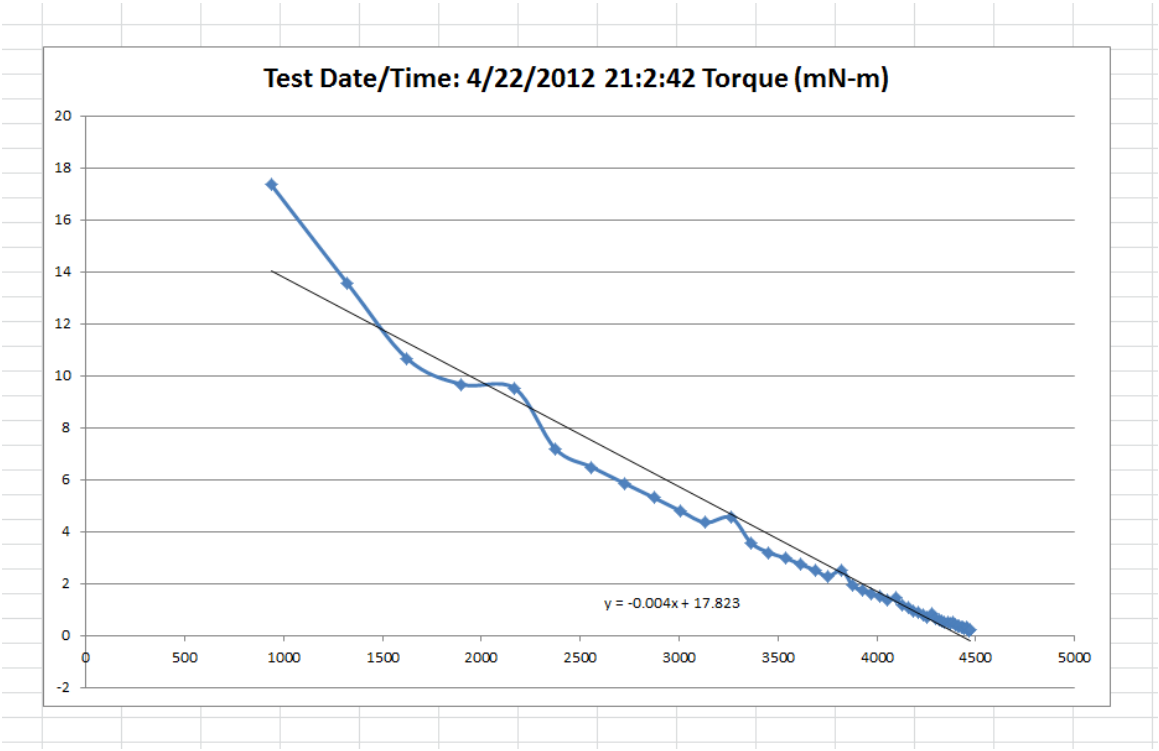


The resulting graph then allows the user to extract the stall torque, as well as the no-load speed.

Similarly, the data set can exhibit other behavior; it is up to the user to recognize any trends that do not make sense, and correct the data accordingly.

# Troubleshooting

| Problem | Solution |
|---|---|
| Motor does not start | Check power supply is attached securely to the two OUTERMOST terminals |
| | Check alligator clips are attached securely to the motor |
| | Listen for the relay's click. If absent, check and make sure a signal is being output to the relay's coil by verifying voltage on pin 5 relative to ground on pin 8 (See "Design Reference" section). If voltage is present, relay might be damaged. Replace with a SPDT relay with a 5V coil.<br>If voltage is absent, check controller is functioning properly. |
| | If problem cannot be resolved, power motor manually. |
| Excessive vibration | Make sure shaft is as straight as possible. |
| | Make sure motor sits level and centered in the motor stand (use shims if necessary). A motor that is inclined induces misalignment in the shaft |
| | make sure disk is free of any debris that might cause imbalance |
| No speed signal | Make sure data cable is attached securely. |
| | If using NI myDAQ, make sure "DAQ assistant" is initialized to the proper channel. |
| | If problem cannot be resolved, Tachometer might be damaged. Replace with appropriate encoder. The existing model is a US digital E4P Optical Encoder Kit. Use the existing index wheel. |
| **Standalone Controller** | |
| Error: Cannot Open File | When using standalone controller, this error indicates that there are more than 100 files on the SD card. Delete files and try again |
| Error: No card detected | Insert SD card into unit |
| Error: Real Time Clock Failed | When present in log file, this error indicates that the Real Time Chip onboard the standalone controller is not functioning. This can be due to a dead coin cell battery. Open controller and replace with appropriate battery. See "Advanced Operations" section. |
| Date and time incorrect in log file | This is due to a dead coin cell battery. Open controller and replace with appropriate battery. See "Advanced Operations" section. |
| **NI myDAQ** | |
| Error: wrong channels | Make sure the DAQ assistant channels are set appropriately as described in the VI instructions |
| Error: Speed Signal Timeout | The timeout stops the VI when the appropriate amount of time has passed with the disk at a standstill. If the timeout occurs too often, increase the timeout interval. |

# Advanced Operations

This section is intended for use to modify or repair the dynamometer system, in the event that unsatisfactory performance is observed or an improvement is to be made.

## Customizing the Controllers

This section describes the method of operation of each controller, as well as documents how to go about customizing their operation. This is needed in order to re-calibrate the controllers to improve measurement accuracy. **Advanced programming knowledge and electronic theory is required.**

Standalone controller

The standalone controller is based on an Arduino Uno board running an ATMega328 microprocessor. The microprocessor runs a C program that controls all of the inputs and outputs. The data is logged using a data logging shield with an SD card reader. The data logging shield also includes a Real Time Clock chip that keeps track of the date and time even when the power is turned off. It does this by using a small coin cell battery that has a life of about 5 years. When this battery runs out, the RTC module loses time and will not function until the battery is replaced, resulting in a "Real Time Clock Failed" message or incorrect time and date in the log file. However, the rest of the controller will still function as normal.

To replace the battery, pop open both gray ends on the controller and the two white halves will then separate. Locate the coin cell battery and replace. Reassemble the controller in reverse.

You are not done yet, as the RTC will still need to be programmed. Refer to "Design Reference" section for the reprogramming code.

To reprogram the controller, you need to download and install the Arduino IDE from their website: http://www.arduino.cc/. Also on the website are instructions to install the drivers.

Use the blue USB cable provided with the controller to connect to the computer and upload the appropriate code.

CAUTION! ONCE THE NEW CODE IS UPLOADED, THE OLD ONE IS LOST! BE ABSOLUTELY SURE YOU KNOW WHAT YOU ARE DOING!

NI myDAQ

The myDAQ is a lot simpler to modify, since all of the programming is run on the computer through a LabView VI. The only software needed to do this is LabView and any support software for the myDAQ (which should be present for the controller to work in the first place).

## Calibration Procedure

Every effort was made to ensure that the dynamometer controllers were calibrated properly against known measurements; however, there is always room for improvement. This section shows how to modify each controller's programming in order to change the calibration.

There are two major changes that can be performed: changing the calibration factor, which in the case of this dynamometer, is the moment of inertia term; and changing or implementing a data filter.

Standalone Controller

Changes to the standalone controller are more difficult to make than the myDAQ, since they involve dealing with uploading code and potentially, rewriting parts of the code. To upload new C code, or modify the existing one, follow the instructions outlined in the "Customizing the Controllers" section and the "Design Reference" section. It would be wasteful and time consuming to reproduce all of the knowledge needed to make changes and upload new code, since a wealth of information is available on the web for the Arduino. Visit Arduino's website, www.arduino.cc, for in depth instructions, examples, and support.

To change the calibration factor, which happens to be the moment of inertia, you will have to change the variable "I," shown below in the code snippet:

```
.
.
.
File logfile;

volatile long long now=0;
volatile long long later=0;
float RPM1=0.0;
float RPM2=0.0;
float A=0.0;
float I=0.0505;
float torque=0.0;
long g=0;
long calcint=150000;
long long calctime=0;
long long totes=0;
long long totestotal=0;
float delta=0.0;
float power=0.0;

int OK = 0;
.
.
.
```

Increasing "I" will increase the torque value that the program outputs, and vice versa. After the "I" value is updated, the new code will have to be uploaded using the Arduino IDE.

NI myDAQ

Modifying the VI that controls the myDAQ requires knowledge of LabView. The calibration factor, "I," is located below in the block diagram:

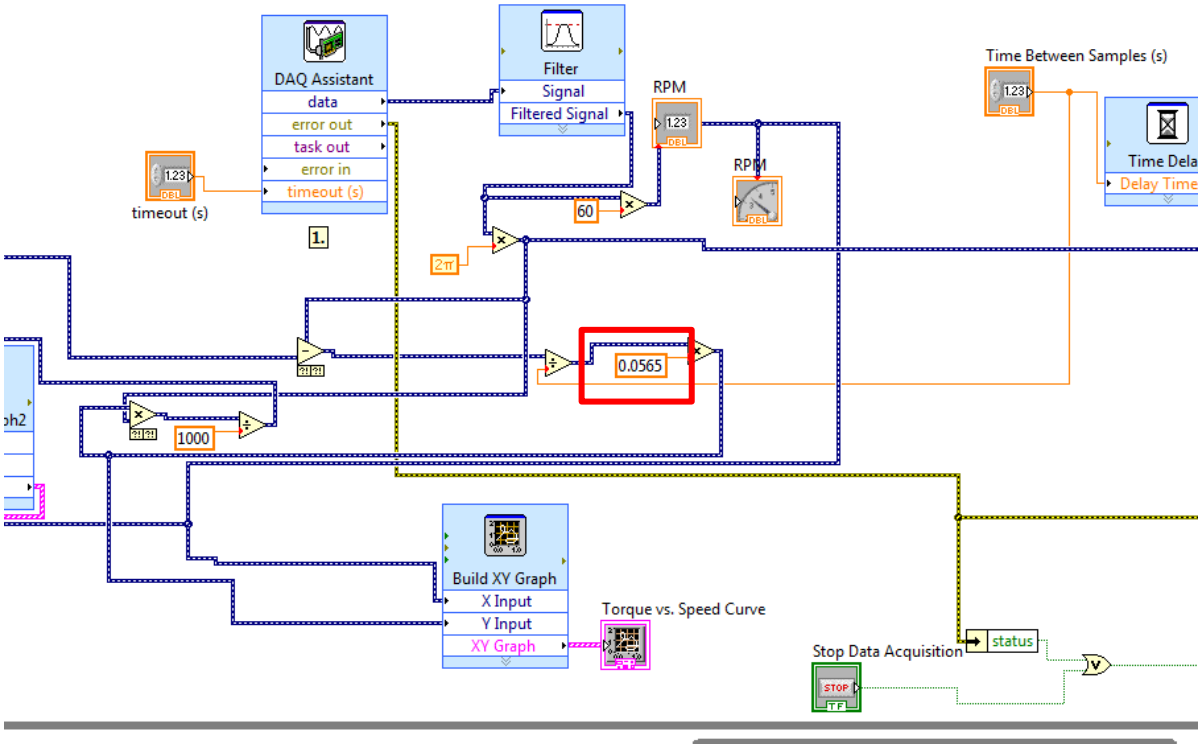


To change the filter, double click on the "Filter" subVI, and change the appropriate settings. You can also add extra filters and data conditioning modules as seems fit.

Procedure

The actual procedure followed when calibrating the dynamometer involved testing two DC motors with known stall torque values. These were then compared to the stall torque measured by the dynamometer. The percent difference between the two values was computed and applied to the "I" term, and tested again. The process was repeated until the results were within a satisfactory error range. For this dynamometer, it was roughly 5%.

## Design Reference

Controller pin out (applies to both controllers):

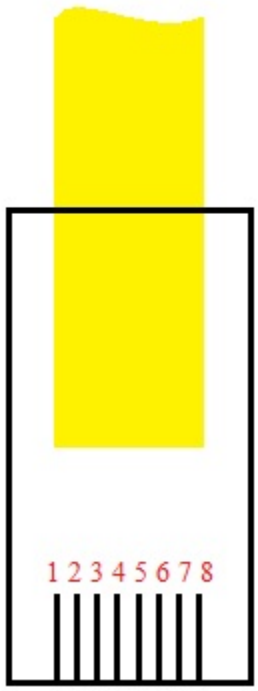


Pin 1: Encoder Channel A (Input)
Pin 2: Encoder Channel B (Input)
Pin 3: Unused
Pin 4: Unused
Pin 5: Relay Coil (Output)
Pin 6: Unused
Pin 7: 5V
Pin 8: Ground

Relay Wiring Diagram:

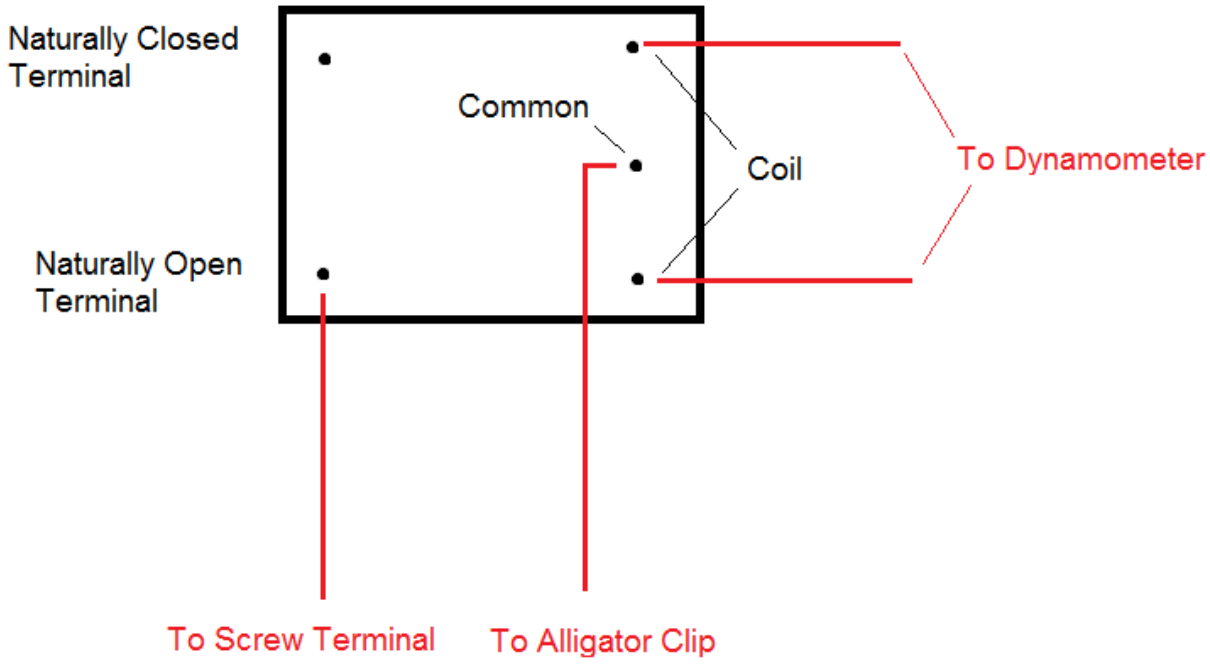

C codes for Arduino IDE

These programs can be used to modify and reprogram parts of the microcontroller. To upload these programs, you need to download and install the Arduino IDE from the arduino website, as well as the appropriate libraries listed after the "include" commands (for example, SD library, Wire library, RTClib library, LiquidCrystal library, etc…). Some of them come with the IDE download, and other have to be searched for online.

C code for controller user interface

```
#include <SD.h>
#include <Wire.h>
#include <RTClib.h>
#include <LiquidCrystal.h>

RTC_DS1307 RTC;

const int chipSelect = 10;
LiquidCrystal lcd(9,8,A3,A2,A1,A0);
File logfile;

volatile long long now=0;
volatile long long later=0;
float RPM1=0.0;
float RPM2=0.0;
float A=0.0;
float I=0.0505;
float torque=0.0;
long g=0;
long calcint=150000;
long long calctime=0;
long long totes=0;
long long totestotal=0;
float delta=0.0;
float power=0.0;

int OK = 0;
int Cancel = 0;
int OK_button = 4;
int Cancel_button = 3;
int relay = 5;

void setup()
{
  pinMode(A0,OUTPUT);
  pinMode(A1,OUTPUT);
  pinMode(A2,OUTPUT);
  pinMode(A3,OUTPUT);
  pinMode(8,OUTPUT);
  pinMode(9,OUTPUT);
  pinMode(relay, OUTPUT);
  /*
  Serial.begin(115200);
  Serial.println("Debug Mode");
  */
  lcd.begin(16,2);

  lcd.clear();
  lcd.setCursor(2,0);
  lcd.print("TorkBlock UI");
  lcd.setCursor(3,1);
  lcd.print("by Roy Eid");
```

```
delay(1500);

if (!SD.begin(chipSelect))
{
  error("No Card Detected");
}

char filename[] = "TORQUE00.CSV";
for (uint8_t i = 0; i < 100; i++)
{
  filename[6] = i/10 + '0';
  filename[7] = i%10 + '0';
  if (! SD.exists(filename))
  {
    logfile = SD.open(filename, FILE_WRITE);
    break;
  }
}

if (! logfile)
{
  error("Cannot Open File");
}

Wire.begin();
if (!RTC.begin())
{
  logfile.println("Real Time Clock failed");
}

lcd.clear();
lcd.setCursor(0,0);
lcd.print("Ready to Test");
lcd.setCursor(0,1);
lcd.print("OK        Cancel");

while (OK != 1)
{
  OK = digitalRead(OK_button);
  Cancel = digitalRead(Cancel_button);
  if (Cancel == 1)
  {
    Test_cancel();
  }
  delay(50);
}

logfile.print("Test Date/Time: ");

DateTime now;
now = RTC.now();

logfile.print(now.month(), DEC);
logfile.print("/");
logfile.print(now.day(), DEC);
logfile.print("/");
logfile.print(now.year(), DEC);
logfile.print(" ");
logfile.print(now.hour(), DEC);
logfile.print(":");
logfile.print(now.minute(), DEC);
logfile.print(":");
logfile.println(now.second(), DEC);

logfile.println("Speed (RPM),Torque (mN-m),Power (W)");
```

```
  lcd.clear();
  lcd.setCursor(0,0);
  lcd.print("Test in Progress");
  lcd.setCursor(0,1);
  lcd.print("            Stop");

  digitalWrite(relay,HIGH);

  attachInterrupt(0, count, RISING);

  calctime=micros();
}

void loop()
{
    totes=now-later;
    totestotal=totestotal+totes;
    g++;

    if (g >= 500)
    {
      totes=totestotal/g;
      RPM2=6283000.00/float(totes);
      g=0;
      totestotal=0;
    }

    delta=micros()-calctime;

    if (delta>calcint)
    {
      detachInterrupt(0);

      A=(RPM2-RPM1)/(delta/1000000);
      torque=A*I;
      power=torque*RPM2/1000;
      /*
      Serial.print(RPM2*9.549,2);
      Serial.print(", ");
      Serial.print(torque,4);
      Serial.print(", ");
      Serial.println(power,4);
      */
      logfile.print(RPM2*9.549,2);
      logfile.print(",");
      logfile.print(torque,4);
      logfile.print(",");
      logfile.print(power,4);
      logfile.println();

      RPM1=RPM2;

      Cancel=digitalRead(Cancel_button);
      if (Cancel == 1)
      {
        Test_complete();
      }

      calctime=micros();

      attachInterrupt(0, count, RISING);
    }
}

void count()
{
```

```
  later=now;
  now=micros();
}

void error(char *str)
{
  lcd.clear();
  lcd.setCursor(0,0);
  lcd.print("Error:");
  lcd.setCursor(0,1);
  lcd.print(str);
  while(1);
}

void Write_File()
{
  lcd.clear();
  lcd.setCursor(0,0);
  lcd.print("Writing File....");
  logfile.flush();
  delay(1000);
}

void Test_complete()
{
  digitalWrite(relay,LOW);

  Write_File();

  lcd.clear();
  lcd.setCursor(0,0);
  lcd.print("Test Complete!");
  delay(1000);
  lcd.clear();
  lcd.setCursor(0,0);
  lcd.print("Turn Off System");
  lcd.setCursor(0,1);
  lcd.print("and Remove Card");
  while(1)
  {}
}

void Test_cancel()
{
  lcd.clear();
  lcd.setCursor(0,0);
  lcd.print("Test Cancelled");
  delay(2000);
  lcd.clear();
  lcd.setCursor(0,0);
  lcd.print("Restart sys. to");
  lcd.setCursor(0,1);
  lcd.print("begin new test");
  while(1)
  {}
}
```

C code to reprogram RTC chip (http://www.ladyada.net/make/logshield/rtc.html) you have to load the user interface code above after this step is complete!

```
// Date and time functions using a DS1307 RTC connected via I2C and Wire lib

#include <Wire.h>
#include "RTClib.h"

RTC_DS1307 RTC;

void setup () {
    Serial.begin(57600);
    Wire.begin();
    RTC.begin();

  if (! RTC.isrunning()) {
    Serial.println("RTC is NOT running!");
    // following line sets the RTC to the date & time this sketch was compiled
    RTC.adjust(DateTime(__DATE__, __TIME__));
  }
}

void loop () {
    DateTime now = RTC.now();

    Serial.print(now.year(), DEC);
    Serial.print('/');
    Serial.print(now.month(), DEC);
    Serial.print('/');
    Serial.print(now.day(), DEC);
    Serial.print(' ');
    Serial.print(now.hour(), DEC);
    Serial.print(':');
    Serial.print(now.minute(), DEC);
    Serial.print(':');
    Serial.print(now.second(), DEC);
    Serial.println();

    Serial.print(" since midnight 1/1/1970 = ");
    Serial.print(now.unixtime());
    Serial.print("s = ");
    Serial.print(now.unixtime() / 86400L);
    Serial.println("d");

    // calculate a date which is 7 days and 30 seconds into the future
    DateTime future (now.unixtime() + 7 * 86400L + 30);

    Serial.print(" now + 7d + 30s: ");
    Serial.print(future.year(), DEC);
    Serial.print('/');
    Serial.print(future.month(), DEC);
    Serial.print('/');
    Serial.print(future.day(), DEC);
    Serial.print(' ');
    Serial.print(future.hour(), DEC);
    Serial.print(':');
    Serial.print(future.minute(), DEC);
    Serial.print(':');
    Serial.print(future.second(), DEC);
    Serial.println();

    Serial.println();
    delay(3000);
}
```

# Appendix F: Datasheets for DC Motors

# RK-370CA

MABUCHI MOTOR
Carbon-brush motors

**OUTPUT : 0.5W~24W (APPROX)**

WEIGHT : 51g (APPROX)

Typical Applications Home Appliances
Precision Instruments : Printer / Copy Machine / Laser Printer / Vending Machine

| MODEL | VOLTAGE | | NO LOAD | | AT MAXIMUM EFFICIENCY | | | | | STALL | | |
|---|---|---|---|---|---|---|---|---|---|---|---|---|
| | OPERATING RANGE | NOMINAL | SPEED | CURRENT | SPEED | CURRENT | TORQUE | | OUTPUT | TORQUE | | CURRENT |
| | | | r/min | A | r/min | A | mN·m | g·cm | W | mN·m | g·cm | A |
| RK-370CA-10800 | 12~30 | 24V CONSTANT | 5100 | 0.015 | 4310 | 0.082 | 2.58 | 26.3 | 1.16 | 16.7 | 170 | 0.45 |
| RK-370CA-15370 | 12~24 | 12V CONSTANT | 5500 | 0.032 | 4690 | 0.19 | 2.71 | 27.7 | 1.33 | 18.4 | 188 | 1.07 |
| RK-370CA-081050 | 12~30 | 24V CONSTANT | 3900 | 0.010 | 3210 | 0.047 | 1.90 | 19.3 | 0.64 | 10.8 | 110 | 0.22 |

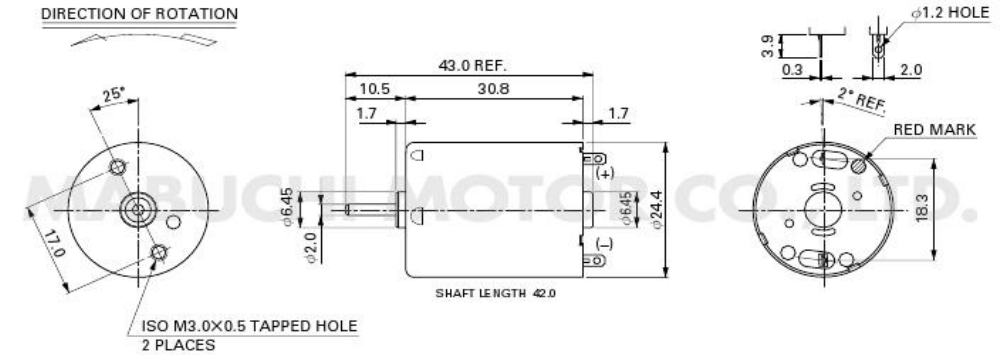


Usable machine screw length 2.0 max. from motor mounting surface.

UNIT: MILLIMETERS

**RK-370CA-10800** 24.0V

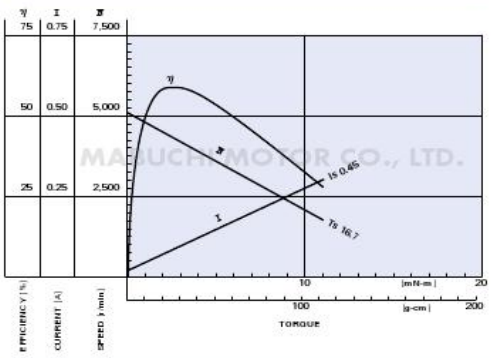


**RK-370CA-15370** 12.0V

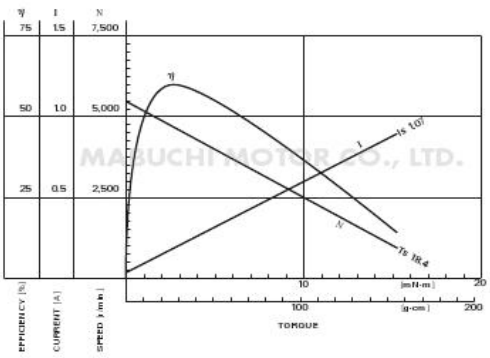


**MABUCHI MOTOR CO.,LTD.** Headquarters 430 Matsuhidai, Matsudo City, Chiba, 270-2280 Japan. Tel:81-47-710-1177 Fax:81-47-710-1132 (Sales Dept.)

# RS-385PH

MABUCHI MOTOR
Carbon-brush motors

**OUTPUT : 0.9W~40W (APPROX)**

WEIGHT : 82g (APPROX)

Typical Applications: Automotive Products
Home Appliances
Precision Instruments : Printer / Copy Machine / Laser Printer

| MODEL | | VOLTAGE | | NO LOAD | | AT MAXIMUM EFFICIENCY | | | | | STALL | | |
|---|---|---|---|---|---|---|---|---|---|---|---|---|---|
| | | OPERATING RANGE | NOMINAL | SPEED | CURRENT | SPEED | CURRENT | TORQUE | | OUTPUT | TORQUE | | CURRENT |
| | | | | r/min | A | r/min | A | mN·m | g·cm | W | mN·m | g·cm | A |
| RS-385PH-16140 | (*1) | 12~30 | 24V CONSTANT | 8700 | 0.070 | 7420 | 0.41 | 8.30 | 84.6 | 6.44 | 56.4 | 575 | 2.35 |
| RS-385PH-17120 | (*2) | 8~35 | 23.5V CONSTANT | 8600 | 0.076 | 7430 | 0.48 | 10.1 | 103 | 7.82 | 73.8 | 752 | 3.05 |

(*1) Thickness of flux yoke: 0.6t
(*2) Thickness of flux yoke: 1.0t

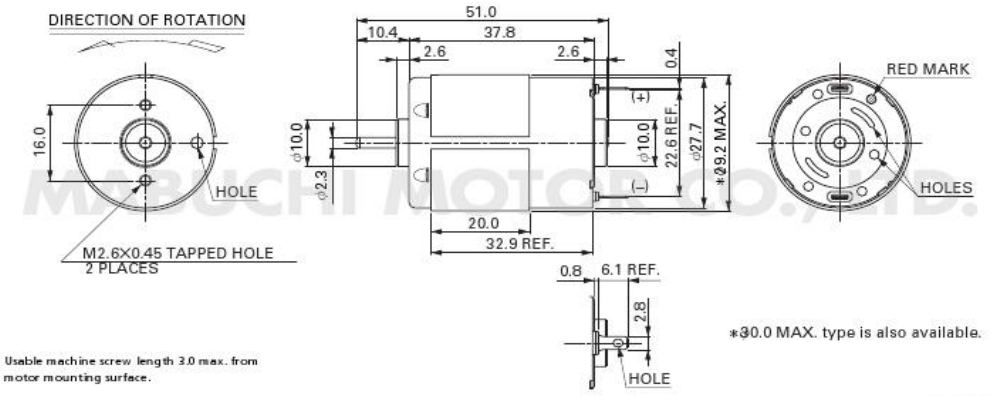


Usable machine screw length 3.0 max. from motor mounting surface.

UNIT: MILLIMETERS

## RS-385PH-16140 24.0V

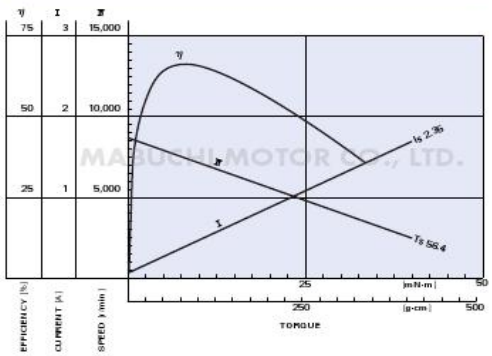


## RS-385PH-17120 23.5V

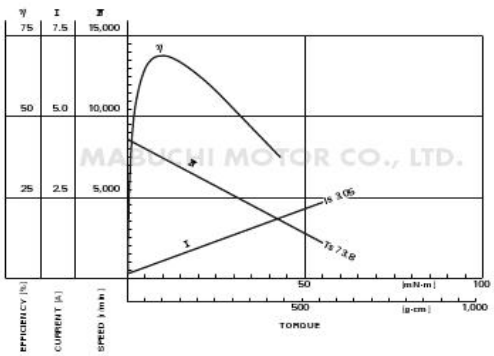


**MABUCHI MOTOR CO.,LTD.** Headquarters 430 Matsuhidai, Matsudo City, Chiba, 270-2280 Japan. Tel:81-47-710-1177 Fax:81-47-710-1132 (Sales Dept.)

# Bibliography


3D digital corp. (2010, July 11). *3D Laser Scanner*. Retrieved 2012, from http://www.3ddigitalcorp.com/laser-scanner.html

Agilent Technologies. (2012). *Agilent 3458A Multimeter* [Brochure]. Retrieved from http://cp.literature.agilent.com///E.pdf

Amazon.com, Inc. (2012a). *Neiko 20713A Professional Digital Laser Photo Non-Contact Tachometer*. Retrieved March 14, 2012, from http://www.amazon.com/A-Professional-Non-Contact-Measurement//I5LDVC

Amazon.com, Inc. (2012b). *Mastech Digital Illuminance/Light Meter LX1330B*. Retrieved March 14, 2012, from http://www.amazon.com/Digital-Illuminance-Light-LX1330B//S19W3W

Amazon.com, Inc. (2012b). *Staedtler Protractor 6“ 360 Degrees*. Retrieved March 14, 2012, from http://www.amazon.com/Protractor-360-Degrees-56880-15BK//XWTNZ8

Amazon.com, Inc. (2012c). *Neiko 01407A Stanless Steel 6-Inch Digital Caliper*. Retrieved March 14, 2012, from http://www.amazon.com/A-Extra-Large-SAE-Metric-Conversion//GSLKIW/=sr_1_1?ie=UTF8&qid=1331781418&sr=8-1

American Weigh. (2011a). *American Weigh TL-330 Industrial Hanging Scale*. Retrieved March 14, 2012, from http://www.americanweigh.com/_info.php?cPath=46&products_id=813

American Weigh. (2011b). *American Weigh SR-1KG Digital Hanging Scale*. Retrieved March 14, 2012, from http://www.americanweigh.com/_info.php?cPath=46&products_id=2170

Analog Devices, Inc. (2010). *ADXL335*. Retrieved March 14, 2012, from http://www.analog.com//files/_sheets/.pdf

Balmac. (n.d.). *Model 200 Vibration Meter*. Retrieved February 29, 2012, from http://www.balmacinc.com//.pdf

Barr, R., Schmidt, P., Krueger, T., & Twu, C.-Y. (2000, October). An Introduction to Engineering Through an Integrated Reverse Engineering and Design Graphics Project. In *Journal of Engineering Education*.

Bell, S., & Morse, S. (2003). *Measuring Sustainability : Learning By Doing*. Earthscan Ltd.

Bosch. (n.d.). *Digital Laser Rangefinder Kit DLR165K*. Retrieved January 31, 2012, from http://www.boschtools.com////.aspx?pid=DLR165K#specs

Brain, M. (n.d.). *How Thermometers Work*. Retrieved February 18, 2012, from http://home.howstuffworks.com/.htm

Budynas, R. G., & Nisbett, J. K. (2008). *Shigley's Mechanical Engineering Design*. New York: McGraw Hill.

ClearFlite Air Purifiers. (2012). *Negative Ion Air Purifiers*. Retrieved March 22, 2012, from http://www.airpurifiers.com//ion.htm

Crouzet Automatismes SAS. (2012). *Some principles of direct current (D.C.) motors*. Retrieved April 8, 2012, from http://datasheet.seekic.com///_8285000201491.pdf

Dille, J. (n.d.). *Torque Wrenches- How Good Are They?* Retrieved February 27, 2012, from http://home.jtan.com/~joe//_3.htm

Dillon. (2012). *Mechanical Force Gauges* [Brochure]. Retrieved from http://www.dillon-force.com//_force_gauges_L_08595-0012.pdf

Dortch, G. (2012). *Instrumentation Engineering*. New Delhi: World Technologies.

Dwyer, D. (2012). *How Quartz Watches Work*. Retrieved February 14, 2012, from http://electronics.howstuffworks.com//watches/watch2.htm

Dwyer Instruments, Inc. (2012). *Series 1221/1222/1223 Flex-Tube® U-Tube Manometer*. Retrieved March 14, 2012, from http://www.dwyer-inst.com/////-1222-1223/

*Explorer® Analytical and Precision Balances*. (2012). Retrieved February 13, 2012, from Ohaus website: http://us.ohaus.com/////families/US.aspx

Extech. (2012). *SDL600: Sound Level Meter/Datalogger*. Retrieved February 15, 2012, from http://www.extech.com//.asp?catid=18&prodid=680

Extech. (2012b). *461895: Combination Contact/Photo Tachometer*. Retrieved March 6, 2012, from http://www.extech.com////_461995data.pdf

Extech. (2012c). *EX330: 12 Function Mini MultiMeter + Non-Contact Voltage Detector*. Retrieved March 14, 2012, from http://www.extech.com//.asp?catid=48&prodid=277

Extech. (2012d). *Water Resistant Stopwatch/Clock*. Retrieved March 14, 2012, from http://www.extech.com////.pdf

Faro. (n.d.). *An Introduction to Protable CMMS*. Retrieved from http://www.faro.com/.aspx?ct=di&content=pro&item=4

Faro. (2012). *FaroArm*. Retrieved February 15, 2012, from http://www.faro.com/.aspx?ct=di&content=pro&item=2

Flexbar Machine Corporation. (2012). *Hardness Testing File Set*. Retrieved March 14, 2012, from http://www.flexbar.com///TESTING-FILE-SET-26p5383.htm

Fluke Corporation. (2012a). *Fluke 574 Precision Infrared Thermometer*. Retrieved February 27, 2012, from http://www.fluke.com////Thermometers/4-Precision-Infrared-Thermometer.htm?PID=72387

Fluke Corporation. (2012b). *Fluke 289 True-rms Industrial Logging Multimeter with TrendCapture*. Retrieved February 27, 2012, from http://www.fluke.com///Multimeters/Multimeters/luke-289.htm?PID=56061

Fox Electronics. (2008). *Theory of Operation*. Retrieved February 29, 2012, from http://www.foxonline.com/.htm

Franceschini, F. (2002). *Advanced Quality Function Deployment*. Boca Raton, FL: St. Lucie Press.

Fred V. Fowler Company, Inc. (n.d.). *Hardness Tester File Set*. Retrieved March 12, 2012, from http://www.fvfowler.com///_373.pdf

Gossen. (2011). *Mavolux 5032C Digital USB Lux Meter*. Retrieved March 1, 2012, from hhttp://www.gossen-photo.us/c-digital-usb-digital-footcandle-lux-meter

Hoover Dam Technology. (2011). *Information about luxmeter*. Retrieved February 29, 2012, from http://www.beihan.cn//.pdf

Instron. (2012a). *Tensile Testing*. Retrieved March 4, 2012, from http://www.instron.us///_types//.aspx

Instron. (2012b). *Instron Products*. Retrieved March 4, 2012, from http://www.instron.us///Electromechanical-Systems.aspx

Instron. (2012c). *Pendulum, Drop Weight and Instrumented Impact Testing*. Retrieved March 4, 2012, from http://www.instron.us///_types//_types.aspx

Kern-Sohn. (2009). *HMR Leeb rebound hardness tester*. Retrieved March 11, 2012, from http://www.kern-sohn.com///catalogue-284.html

Knier, G. (2002). *How do Photovoltaics Work?* Retrieved March 1, 2012, from NASA website: http://science.nasa.gov/news/at-nasa///

Komelon USA Corporation. (2011). *25' Self Lock Speed Mark*. Retrieved March 14, 2012, from http://www.komelonusa.com/.asp?dvn=1&cat=3&sct=17&product_id=118

Kompatscher, M. (2004, November 11). *Equotip - Rebound Hardness Testing After D. Leed*. Retrieved from http://www.imeko.org//-2004/TC5-2004-014.pdf

Konica Minolta. (2012). *VIVID 9i 3D Laser Scanner* . Retrieved February 15, 2012, from http://sensing.konicaminolta.us//i-3d-laser-scanner/

Koolance. (2012). *INS-FM17N Coolant Flow Meter*. Retrieved March 14, 2012, from http://www.koolance.com/cooling/_info.php?product_id=740

*La Crosse Technology EA-3010U Hand Held Anemometer*. (n.d.). Retrieved March 14, 2012, from www.crosse-technology.com/u.html

Lomas, C. G. (2011). *Fundamental of Hot Wire Anemometry*. New York: Cambridge University Press.

Mabuchi Motor Co. (2012a). *RK-370CA* [Brochure]. Retrieved from http://www.mabuchi-motor.co.jp/bin//_catalog.cgi?CAT_ID=rk_370ca

Mabuchi Motor Co. (2012b). *RK-385PH* [Brochure]. Retrieved from http://www.mabuchi-motor.co.jp/bin//_catalog.cgi?CAT_ID=rs_385ph

Magtrol Inc. (2012). *Micro Dyne Motor Testing System* [Brochure]. Retrieved from http://www.magtrol.com//.pdf

*Mark-10 Force Gauge Series 5*. (n.d.). Retrieved February 21, 2012, from http://www.mark-10.com///.html

McMaster-Carr. (n.d.). *Pressure Gauges*. Retrieved March 14, 2012, from http://www.mcmaster.com/#38545k162/=gnk823

McMaster Carr. (n.d.,b). *Pro-Value Satin-Chrome Steel Precision Rules*. Retrieved March 14, 2012, from http://www.mcmaster.com/#rule-straightedges/=go12sa

Mitutoyo America Corporation. (2011). *ABSOLUTE Digimatic Caliper Series 500-with Exclusive ABSOLUTE Encode Technology* . Retrieved January 31, 2012, from http://www.mitutoyo.com/.aspx?group=1381

Mitutoyo America Corporation. (2011). *Coolant Proof Micrometer Series 293-with Dust/Water Protection Conforming to IP65 Level* . Retrieved February 19, 2012, from http://www.mitutoyo.com/ndisingGroup.aspx?group=1089

Morris, A. S. (2011). *Measurement and Instrumentation*.

*M-Pact Precision Analytical Balances*. (n.d.). Retrieved February 13, 2012, from Sartorius website: http://www.sartorius-mechatronics.com///Balances/Pact-Precision-%7C-Analytical-Balances/yyk5c/erkugw6/.htm?view=models

National Instruments Corporation. (2012). *NI myDAQ*. Retrieved March 14, 2012, from http://www.ni.com//

Oehler Research, Inc. (2012). *Model 35 Proof Chronograph*. Retrieved March 4, 2012, from http://www.oehler-research.com/.html

Ohaus. (2012). *CS Portable Balances*. Retrieved March 20, 2012, from http://us.ohaus.com/////families/US.aspx

Omega. (2012). *Technical Reference*. Retrieved February 18, 2012, from http://www.omega.com//

Omega. (2012b). *Hot Wire Anemometer*. Retrieved March 6, 2012, from http://www.omega.com//.asp?ref=HHF42&Nav=grec06

Omega. (2012c). *All Plastic Ultra-Low Flow Sensors* [Brochure].

Omega. (2012d). *Digital Rotating Vane Anemometer*. Retrieved March 8, 2012, from http://www.omega.com//.asp?ref=HHF5000&Nav=grec06

Omega. (2012e). *Very High Accuracy Pressure Transducer with 0 to 5 Vdc Output* . Retrieved March 9, 2012, from http://www.omega.com//-5v.html

Optech. (2006). *About Lidar*. Retrieved March 4, 2012, from http://www.optech.ca/.htm

OSHA. (n.d.). *Instruments Used to Conduct a Noise Survey*. Retrieved February 15, 2012, from http://www.osha.gov//////.html

Otto, K., & Wood, K. (2001). *Product Design: Techniques in Reverse Engineering and New Product Development*. Upper Saddle River, NJ: Prentice Hall.

P3 International. (2012). *P3 - Kill A Watt*. Retrieved February 23, 2012, from http://www.p3international.com////-CE.html

Palmer Wahl. (2012). *-35/50°C Partial Immersion Lab Thermometer Model Number 20140M*. Retrieved February 18, 2012, from http://www.palmerwahl.com/_home.php?cat=7&catl=20&line=88&itm=892#

Paulter, N. G., Jr., & Larson, D. R. (2009, April 20). *Reference ballistic chronograph*.

PCE Instruments. (n.d.). *Vibration meter PCE-VT 3000*. Retrieved February 31, 2012, from http://www.industrial-needs.com/data/meter-PCE-VT-3000.htm

Petruso, K. M. (1981). Early Weights and Weighing in Egypt and the Indus Valley. *M Bulletin (Boston Museum of Fine Arts), 79*, 44-51. Retrieved from http://www.jstor.org//

Pyle Audio. (2012). *Sound Level Meter with A and C Frequency Weighting*. Retrieved March 14, 2012, from http://www.pyleaudio.com///Level-Meter-with-A-and-C-Frequency-Weighting

RadarGuns. (2012). *How Radar Guns Work*. Retrieved March 4, 2012, from http://www.radarguns.com/radar-guns-work.html

*Sartorius AZ124, M-POWER Series Analytical Balance*. (2012). Retrieved February 13, 2012, from http://www.itinscales.com//?product_id=25466

Sears. (2012). *Craftsman Tools*. Retrieved March 13, 2012, from http://www.craftsman.com/

Seebeck Effect. (2012). In *Encyclopedia Britannica*. Retrieved from http://www.britannica.com////effect

Shooting Chrony. (2011). *Shooting Chrony® Models & Master Chrony® Models*. Retrieved March 14, 2012, from http://www.shootingchrony.com/ucts_SCMMCM.htm

*Spring Mechanical Scales*. (2012). Retrieved February 13, 2012, from Ohaus website: http://us.ohaus.com/////families/US.aspx

Stalker Radar. (2012). *The Stalker Sport 2*. Retrieved March 4, 2012, from http://www.stalkerradar.com//.html

Starrett. (2011). *Product Detail*. Retrieved January 31, 2012, from http://www.starrett.com//detail?k=C604R-12

Sun-Tec Corporation. (n.d.). *PT portable Tensile Tester*. Retrieved March 11, 2012, from http://www.sunteccorp.com/_features.htm

Svantek. (n.d.). *SVAN 979*. Retrieved February 15, 2012, from http://svantek.com/vibration-analysers/-new-sound-and-vibration-analyser.html

TFT Tools, Inc. (n.d.). *Operation Instruction: Bevel Protractor*. Retrieved February 23, 2012, from http://www.tfttools.com/.pdf

Tohnichi America Corp. (2012). *Digital Torque Gauge BTGE-G Series*. Retrieved February 27, 2012, from http://www.tohnichi.com//watch-gauge-BTGE-g.asp

*Traceable Stopwatch*. (2012). Retrieved February 15, 2012, from Science Lab website: http://www.sciencelab.com/////

Tresna. (2008). *Types of Calipers*. Retrieved January 31, 2012, from http://www.tresnainstrument.com/_of_caliper.html

Vernier Software & Technology. (2012). *Sensors*. Retrieved March 13, 2012, from http://www.vernier.com///

Vidyasagar, S. (2011). *How a digital multimeter works? Block diagram of basic digital multimeter*. Retrieved February 27, 2012, from http://vsagar.com////a-digital-multimeter-works-block-diagram-of-basic-digital-multimeter/

Virdi, S. (2012). Light. In *Construction Science* (pp. 446-479). Retrieved from EBL database.

Wang, W. (2011). *Reverse Engineering: Technology of Reinvention*. Boca Raton, FL: CRC Press.

Wika Instruments, Inc. (2010). *Bourdon Tube Pressure Gauge Stainless Steel Construction Model 21X.5*. Retrieved March 9, 2012, from http://www.wika.us//_PM_21X_53_en_us_15145.pdf

Wilson Hardness. (2012a). *Rockwell Testing*. Retrieved March 4, 2012, from http://www.wilson-hardness.com///.aspx

Wilson Hardness. (2012b). *Rockwell 2000 Series Hardness Testers*. Retrieved March 4, 2012, from http://www.wilson-hardness.com///SeriesHardnessTesters.aspx

Wolfe, J. (n.d.). *dB: What is a decibel?* Retrieved February 15, 2012, from University of New South Wales website: http://www.animations.physics.unsw.edu.au//.htm

Wood, K., Jensen, D., Bezdek, J., & Otto, K. (2001, July). Reverse Engineering and Redesign: Courses to Incrementally and Systematically Teach Design. In *Journal of Engineering Education*.

Woodford, C. (2011, February 12). *Thermochromic color-changing materials*. Retrieved February 18, 2012, from http://www.explainthatstuff.com/materials.html

Woodman Labs, Inc. (2011). *HD HERO2*. Retrieved March 14, 2012, from http://gopro.com/comparison-hd-hero2-hd-hero-cameras/

# Vita

Born and raised in Houston, Texas, Roy Eid was born with a Phillips screwdriver in his hand. After discovering that he had a passion for designing and building machines to make life easier, Roy attended The University of Texas at Austin and received his Bachelor of Science in Mechanical Engineering. He then went on to stay and receive his Master of Science in Design and Manufacturing.

Permanent email: roy.eid@utexas.edu

This thesis was typed by the author